Engineering an Immuno-Isolating Hydrogel-Based Capsule to Restore Ovarian Endocrine Function

by

James Day

A dissertation submitted in partial fulfillment
of the requirements for the degree of
Doctor of Philosophy
(Biomedical Engineering)
in The University of Michigan
2020

Doctoral Committee:

Associate Professor Ariella Shikanov, Chair
Associate Professor Marilia Cascalho
Associate Professor Lonnie Shea
Associate Professor Jan Stegemann

James Day

dayjr@umich.edu

ORCID iD: 0000-0003-1304-0442

This dissertation is dedicated to my parents, Marlene and Dennis Day

ACKNOWLEDGEMENTS

There are many people I would like to thank who have made this dissertation possible. First, I'd like to thank my mentor, Ariella Shikanov. Working in your lab for over 5 years has been a pleasure and the value of your mentorship cannot be overstated in helping me become a better scientist. You taught me what the right questions to ask are and how to design a quality experiment. I'll take the lessons I've learned from you forward for the rest of my scientific career.

I'd also like to thank the rest of my committee members. Dr. Marilia Cascalho, you were like a second mentor to me and I thank you for your willingness to walk me through material pertaining to immunological aspects of this work. Without you and the collaboration with your lab, this work would not be possible. Dr. Lonnie Shea, thank you for being so open to contribute to this work and add invaluable insight through our meetings. Also, thank you for not scoring too many points against me when I guarded you in basketball. Dr. Jan Stegemann, thank you for providing invaluable insight in aspects of biomaterial sciences and thank you for your continued mentorship and accessibility in mentoring all biomaterials students in the BME department.

I would like to thank all the members of the Shikanov Lab during my time here. Working with such ambitious, brilliant, and detail-oriented colleagues made me strive to be a better scientist every day. Thank you for creating such a collaborative, open environment in the Shikanov Lab.

To my friends made during my time in Ann Arbor, thank you for providing a release from the daily grind of doctoral research. I came in not knowing a single person in Michigan and I leave with friends for life. I will always cherish the golf outings, Michigan football games, and weekends in Ann Arbor. To all the grad students in BME, thank you for creating such a collaborative environment throughout the department. It really gives all the students a sense of togetherness and facilitates life-long friendships.

Lastly, I'd like to thank my family for their unwavering support throughout my life and academic career. To my parents, thank you for providing constant love and support and instilling a love of engineering in me. Without you, I would not value education and have an appetite for knowledge as I do. I know wherever I go and whatever I do, your support will be there. I'd also like to thank my identical twin brother, Kevin, who recently graduated with a doctorate degree in BME. Thank you for providing someone to relate to as we both went through this process and although you beat me to graduation by 3 months, I had more papers than you, and as my mentor, Ariella, always said "papers are the currency of research", so who is the true winner? Better luck next time.

All of you had a piece in completing this work and I genuinely thank you for providing me with that support.

TABLE OF CONTENTS

List of Figures

FIGURE

LIST OF TABLES

TABLE

ABSTRACT

Cancer patient survivorship has increased substantially over the past few decades due to advances in anticancer treatments. However, a deleterious effect of these lifesaving treatments is premature ovarian insufficiency (POI), as they are gonadotoxic. POI leads to infertility and loss of ovarian endocrine function, which is particularly devastating for female cancer survivors who experience POI prior to puberty, because puberty is an important developmental in a female's life. Lack of ovarian endocrine function and absence of puberty leads to long-term co-morbidities such as poor bone health, diminished metabolic turnover, and high risk of cardiovascular events. Current treatment options such as hormone replacement therapy and ovarian auto-transplantation are associated with non-physiological delivery of hormones and risk of re-implanting cancerous cells. We hypothesized that allo-transplantation of encapsulated and immuno-isolated donor ovarian tissue restores ovarian endocrine function without evoking an immune response. This thesis describes how we tested the concept of immuno-isolation to protect encapsulated allogeneic ovarian tissue in murine and non-human primate models. First, we developed a dual capsule made with poly(ethylene glycol) (PEG) contained a proteolytically degradable core which was conducive for the dynamic growth of ovarian tissue and a non-degradable PEG shell that would serve as the immuno-protective barrier. We demonstrated in an ovariectomized syngeneic murine model that ovarian tissue encapsulated in Dual PEG survived

and functioned until it was removed 60 days post-implantation. The serum level of follicle-stimulating hormone significantly decreased from 64 ng/mL in ovariectomized mice to 34 ng/mL in mice that received implants. Multiple follicles with healthy morphology were present in the grafts retrieved after 60 days of implantation. Next, allogeneic ovarian tissue encapsulated in Dual PEG and implanted in recipient mice did not evoke detectable production of allo-specific antibodies, while non-encapsulated controls resulted in a 23-fold increase compared to pre-implantation levels; the capsule proved to be immuno-isolating and protected the encapsulated allograft from the outside immune environment and led to ovarian endocrine restoration. We demonstrated that the Dual PEG capsule prevented cellular infiltration and also retained cells encapsulated within. We then investigated the question whether the immuno-isolating capsule could be utilized towards auto-transplantation ovarian tissue from leukemia patients through retention of cancerous cells present in the graft and prevent cancer spreading and metastasis. Encapsulation of 1,000 4T1 cancer cells prevented proliferation, migration and metastasis to other organs through 28 days transplantation, while control mice had to be euthanized because of the spread disease. We then demonstrated encapsulation of ovarian allografts in Dual PEG precludes sensitization of the host immune system which confirms the capsule is immuno-isolating and the host immune system is not exposed to allo-antigens while the graft is encapsulated, possibly allowing multiple implantations of the capsule. Lastly, we demonstrated that non-human primate (NHP) ovarian tissue can develop in the Dual PEG capsule restoring estradiol and progesterone levels to 50 and 70 pg/mg creatine, respectively. Additionally, the encapsulated tissue was protected from an immune response as indicated by the lack of active, dividing T cells in a syngeneic and allogeneic NHP model. We show the capsule can withstand the

multi-fold volumetric expansion of NHP follicles, protecting the encapsulated allograft, which promotes graft survival and ovarian endocrine restoration. Taken together, this dissertation works towards allowing the implantation of allogeneic ovarian tissue to restore ovarian endocrine function in a physiological manner without the risk of immune rejection.

CHAPTER I

INTRODUCTION

Partially adapted from: Immuno-isolation to prevent tissue graft rejection: Current knowledge and future use

1.1 Authors: Anu David, James Day, Ariella Shikanov

1.2 Life-Saving Cancer Therapies Induce Premature Ovarian Insufficiency

The development of modern and much-improved anti-cancer treatments contributed to significantly increased rates of survival particularly in childhood cancer cases, reaching in most cases 85%. The severity and extent of complications has decreased with the introduction of newer treatments as well. However, premature ovarian insufficiency (POI) remains one of the most persistent and deleterious effects having an impact on survivors far past remission. POI results from ovarian susceptibility to gonadotoxic treatments such as pelvic or whole body radiotherapy and alkylating agents [1-7]. These treatments affect rapidly dividing cells and destroy the interactions between the oocyte and hormone-producing granulosa cells, affecting both fertility and ovarian endocrine function. Clinically POI is defined as persistent amenorrhea combined with elevated levels of follicle-stimulating hormone (FSH) before age 40 [8]. Cancer treatments can lead to POI during or immediately following the completion of cancer treatments [2] or years following the completion of treatments [3].

Adolescent patients treated for cancer before undergoing puberty experience delayed or absent puberty, which is particularly detrimental as puberty is an important physiological milestone in a female's life. Puberty initiates physical and psychological changes into adulthood that determine height, bone health, insulin responsiveness, lipid metabolism, cardiovascular health, and cognition [9-11]. This development process is initiated before puberty and orchestrated by a pulsatile secretion of gonadotropin releasing hormone (GnRH) and growth hormone (GH) from the hypothalamus, which in turn regulates the release of gonadotropins, luteinizing hormone (LH) and follicle-stimulating hormone (FSH) from the pituitary. Further, FSH and LH stimulate the ovaries to produce estradiol, androstenedione, progesterone, inhibins A and B, activin and follistatin which have systemic effects in many organs and tissues including endocrine glands and the regulation of reproductive functions (**Figure 1.1**).

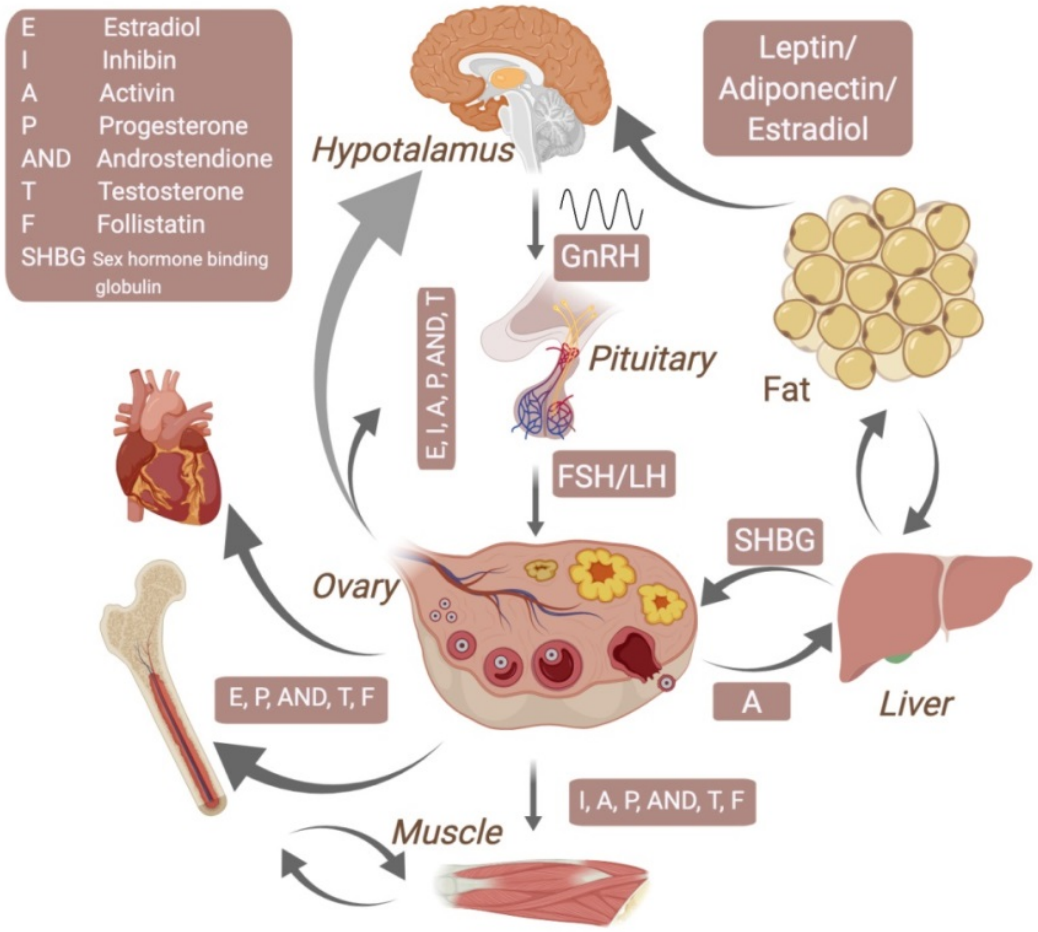

Figure 1.1: Schematic of hypothalamic-pituitary-gonadal axis and the integration into other systems of the body

The intricate and highly connected crosstalk between the ovary and the rest of the body is regulated with ovarian hormones that create a negative feedback loop by inhibiting the production of GnRH and FSH in the brain, resulting in dynamic pulsatile levels of circulating hormones and gonadotropins[12-14]. The pulsatility of the hypothalamic-pituitary-gonadal (HPG) axis is crucial to proper development and regulation of a plethora of systems including reproductive, fat, musculoskeletal, cardiovascular, and immune systems [15,16]. For female childhood cancer survivors who experience POI due to gonadotoxic treatments, the hormonal

balance is disrupted which inhibits the normal pubertal development, leading to irreversible co-morbidities such as unbalanced bone growth, poor bone health, abnormal fat distribution, high risk of cardiovascular disease, and metabolic changes [17-21].

1.3 Fertility Preservation Options for Cancer Survivors

To combat the ovarian damage caused by chemo and radio therapy, there have been efforts to use ferto-protective adjuvant therapies, such as sphingosine-1-phosphate, imatinib, and AS101; however, these treatments are still considered experimental and were not tested on adolescents [22-24] The only clinically approved ferto-protective intervention is gonadotropin-releasing hormone (GnRH) agonist, which shuts down the ovarian function and preserves the follicular pool to some extent [25,26]. For female patients, strategies to preserve fertility include embryo cryopreservation, oocyte cryopreservation, and ovarian tissue cryopreservation. For embryo cryopreservation, patients undergo in vitro fertilization (IVF), which has a relatively high success rate [27,28]; however, this option is limited by the fact that anti- cancer treatments must be delayed to complete the ovarian stimulation cycle, which excludes a significant percentage of patients [8]. For prepubescent cancer patients, embryo or oocyte cryopreservation are not an option, because ovaries are dormant and not responsive to gonadotropin stimulation. A relatively new, but still experimental option to preserve fertility and restore ovarian endocrine function is ovarian tissue cryopreservation and subsequent auto-transplantation after remission [29]. Tissue can be transplanted orthotopically in the pelvis or heterotopically outside the pelvis-abdominal wall. Spontaneous pregnancies have been reported after orthotopic ovarian tissue transplantation and have resulted in over 100 babies born, mostly in the cases of identical twins [30-36]. Stern et al [37] reported a pregnancy from a heterotopic implantation of ovarian tissue

into the abdominal wall. While cryopreservation and auto-transplantation of ovarian tissue is the only available option to preserve both fertility and endocrine function in prepubertal patients experiencing POI, it is associated with the risk of re-introducing cancerous cells harbored in the stroma of the ovarian tissue [38-41]. To date, there is no standard universal protocol to ensure the absence of malignant cells in ovarian autografts removed from the patient prior to anti-cancer treatments. Several studies have attempted to identify and quantify cancerous cells present in ovarian tissue using histological analysis or PCR [39,41.42]. In some cases histological analysis showed no evidence of malignant cells, but cancer-related biological markers were elevated in PCR analysis [39,41,42]. It is currently recommended to use of molecular markers for detection of malignant cells, but unfortunately not all cancers display specific genetic markers that can be detected via PCR complicating tissue characterization [43]. Additionally, there is no consensus as to which markers are most sufficient to detect malignant cells present in ovarian tissue, dependent on the strain of cancer [42], further complicating the classification of the ovarian tissue as safe. As the result, challenges in identifying cancer cells harbored in the tissue prevent clinical translation of this approach, especially in the case of hematologic malignancies, such as acute lymphoblastic leukemia, acute myeloid leukemia, and non-Hodgkin's lymphoma, where ovarian involvement can be high.

1.4 Restoration of Ovarian Endocrine Function with Hormone Replacement Therapy

Girls with POI who experience delayed onset of puberty require hormone replacement therapy (HRT) to initiate and sustain pubertal development and changes associated with sex development. HRT, originally designed to treat postmenopausal symptoms in women, lacks long-term safety data in children [44]. For puberty induction, the prescribed regimen starts with

increasing doses of estrogen, followed by a combination of estrogen and progesterone as a life-long treatment, until menopause. Unfortunately, HRT only delivers a fraction of ovarian hormones, e.g. estrogen and progesterone, at higher doses and at a constant and non-pulsatile rate, which does not mimic physiological puberty [45]. As a result, HRT-mediated puberty in girls with POI results in premature closure of the bone growth plate, cessation of bone growth and long-term metabolic imbalances [44,46-48]. Achieving an optimal pharmaceutical delivery of all the ovarian hormones is challenging due to the complexity of the regulation of the HPG axis.

1.5 Allo-transplantation of Ovarian Tissue to Restore Ovarian Endocrine Function

In the light of limitations of the current techniques to physiologically restore ovarian endocrine function in female cancer survivors with POI, in this thesis I propose a different strategy. I hypothesized that encapsulation of ovarian allograft in immuno-isolating hydrogel-based capsule will restore the physiological crosstalk of the HPG axis and the hormonal balance. The proposed design of the capsule with a biomimetic degradable core and inert non-degradable shell will promote survival and function of the encapsulated ovarian tissue and minimize the risk of an immune reaction, thus eliminating the need for immunosuppression.

1.6 Immuno-Isolation to Protect Allogeneic Tissue

Transplantation of a donor tissue requires systemic immunosuppression to prevent rejection; however, systemic immunosuppression in turn carries significant side effects, at times more debilitating than the disease treated by the transplant. Immuno-isolation of the graft can elegantly solve this problem by providing local protection and avoiding systemic immunosuppression.

An immuno-isolating construct or device creates a physical barrier around the implanted cells or tissues, and precludes contact with immune cells from the host. To ensure graft viability, such a device must allow bidirectional diffusion for nutrients and oxygen, as well as endocrine and paracrine factors to the implanted cells and exchange soluble factors for an extended period of time. To date, most studies have focused on immuno-isolation of allogeneic and xenogeneic pancreatic islets in mice and non-human primate (NHP) models for the treatment of diabetes [49-55].

One of the early attempts to implement immuno-isolation goes back to 1933, when an Italian scientist Bisceglie enclosed mice tumor cells in a polymer membrane and transplanted these cells into peritoneum in guinea pigs. He observed that the cells survived for 12 days and concluded that tumor cells were not attacked by the immune system of the host while receiving the nutrients through diffusion [56]. It was not until the 1960–1970s that the idea of using encapsulation of cells for immune protection gained traction again [57]. Chick et al. [58] and Lim and Sun [59] were the first to successfully use encapsulated pancreas islets in a hydrogel to develop a functional pancreatic transplant. Following these early experiments, substantial progress has been made in biological and polymer sciences leading to development of encapsulation devices for delivery of drugs and peptides for treatment of renal failure, hemophilia, and diabetes [60-64].

Immunoisolation can be achieved through either hydrogels or synthetic devices composed of membranes. The advantage of natural and synthetic hydrogels in biomedical applications comes from their excellent biocompatibility and high-equilibrium water content. The mechanical properties of hydrogels are similar to that of native extracellular matrix [65]. Importantly, these

properties can be tuned to mimic the environment that is most compatible with a specific tissue requirement in order to optimize graft viability and functionality. Examples of such tuning are modification of crosslinking density, molecular weight, and concentration of the polymeric material, which in turn defines the mechanical properties of the hydrogel, such as swelling ratio, mesh size, and diffusivity [66-69].

There are a few commercially available membrane-based immunoisolation devices. One of them is TheraCyte which is comprised of a 0.4 -µm pore cell-impermeable polytetrafluoroethylene (PTFE) membrane, laminated to a 5-mm pore membrane. The outer membranes support neovascularization, whereas the inner membrane prevents the encapsulated tissue within it to come in contact with the host immune cells [70]. Encaptra created by ViaCyte company is another example. This device was tested with pancreatic endoderm cells derived from human embryonic cells. After device implantation in mice, pancreatic cells matured and secreted insulin in response to rising blood glucose levels [71,72]. The design of both TheraCyte and Encaptra permits their retrieval once the implant is exhausted, with a potential follow-up implantation of a new device to sustain physiological function.

1.7 Hydrogels as Immuno-isolators

Hydrogels used for encapsulation and immune isolation include natural hydrogels, such as alginate, chitosan, agarose, fibrin, and synthetic hydrogels, such as poly (ethylene glycol) (PEG) [62, 73-76]. The versatility of hydrogels allows them to mimic the natural environment and extracellular matrix to provide cues for transplanted cells/tissue and support the desired cellular response. Specifically, ovarian follicles undergo significant expansion during active hormone-

secreting stage, after which they regress and die. For the purpose of this thesis I focused on two hydrogels, alginate and PEG that present with desirable physical, mechanical and chemical properties.

In general, factors that influence immunoprotective ability and capsule biocompatibility include the size of the capsule, wall thickness, mechanical strength, permeability, and surface characteristics [77-81]. Mechanical strength of the capsules is important to avoid physical breakage and infiltration of immune cells through the defects. Specifically for alginate, it was found that coating of the negatively charged alginate capsules with polycations, such as poly-L-lysine, poly-D-lysine, and poly-L-ornithine increases the mechanical stability and restricts permeability of immune cells [82]. However, coating with poly-L-ornithine and poly-D-lysine increased the inflammatory responses towards capsules [83], while coating with poly-L-lysine has been shown to improve the biocompatibility and inhibit adhesion of inflammatory cells [78-84]. Adherent inflammatory cells secrete cytokines that amplify the local inflammatory reaction and lead to formation of a fibrotic capsule around the device. As a result, cells inside the immuno-isolating alginate-based device cannot receive nutrients and oxygen, which leads to the failure of the graft.

Size and geometry of the capsule affect the function and survival of transplanted cells. Veiseh et al. [62] examined the effect of the size and geometry of alginate hydrogels on local immune response, resulting in fibrosis, as well as the functionality of the encapsulated cells. When comparing hydrogels with diameters ranging from 0.3 mm to 1.5 mm they showed improved survival and function in larger capsules. Islets encapsulated in 1.5 mm alginate spheres were able to restore blood glucose levels for a period of 180 days, while islets encapsulated in 0.5 mm

capsules lasted for only 25 days. The larger size of the hydrogel did not have a negative effect on graft functionality. In addition to maintenance of normoglycemia, they found that 1.5 mm alginate spheres were largely devoid of cellular deposition, whereas 0.3 mm spheres evoked significant deposition of fibrotic tissue. Other materials used in this study, such as stainless steel, glass, polycaprolactone and polystyrene, demonstrated a higher degree of fibrosis around the material compared to alginate [62].

PEG is a synthetic polymer also used in biomedical and immuno-isolating applications. Biological inertness and easy manipulation of mechanical properties provide a high degree of reproducibility [85]. By controlling the PEG concentration in the hydrogel, one can tune the mechanical properties (i.e. shear modulus) to elicit the desired cellular response [86,87]. This is essential because the stiffness of the hydrogel impacts the severity of the foreign body response (FBR). Softer gels cause a less extensive reaction compared to stiffer gels. Additionally, softer gels induce secretion of lower levels of inflammatory cytokines, such as TNF-α, IL-1β, and IL-6, compared to stiffer gels *in vitro* [88]. Through the process of mechanotransduction, macrophages behave differently based on F-actin localization. On softer gels, macrophages experience attenuated force compared to stiffer gels leading to a pronounced effect on macrophage spreading and attachment [89]. Furthermore, the crosslinking mechanism and density of PEG hydrogels can be manipulated. Although PEG's molecular structure is conserved – PEG diol with two hydroxyl end groups – the structure of the end-groups can be modified and functionalized allowing for a high degree of versatility and crosslinking chemistry, such as free radical polymerization [90-94] and Michael-type addition [95.96].

The molecular weight cut-off (MWCO) of the molecules that can diffuse through the PEG hydrogel is a tunable property as well. Tugba et al. [97] compared the diffusion of a physiologically active glucagon like peptide-1 (GLP-1) and a relatively inert bovine serum albumin (BSA) through PEG diacrylate (PEGDA) hydrogels. Given a PEG concentration of 5% w/v, 100% of encapsulated BSA was released from 20 kDa PEG hydrogels in the initial 30 h of the release experiment, while only 84% BSA was released over the same period from 10 kDa PEG. Whereas, in 10% w/v PEG, BSA release decreased to 73% and 67% for 20 kDa and 10 kDa PEGDA hydrogels, respectively. They determined that diffusivity was dependent on PEG concentration and molecular weight of the PEG macromer enabling only molecules of a specific size and below to diffuse through the PEG hydrogels. When tuning the size exclusion of a polymeric membrane, one must be vigilant, as a MWCO of approximately 20 kDa would be needed to exclude secreted cytokines, but this may also affect cell viability due to restricted diffusion of large proteins [98]. A balance needs to be reached to prevent infiltration of host immune cells while not inhibiting the exchange of nutrients and oxygen.

Several studies proved that encapsulation of pancreatic islets in PEG hydrogels can restore glucose to physiological levels *in vitro* and *in vivo* [49-52]. Cruise et al [49] showed that PEGDA acted as a passive membrane barrier around the encapsulated islets. Additionally, PEGDA did not affect islet cell functionality as streptozotocin-induced mice maintained normoglycemia up to four months [50]. Although PEGDA has been shown to support islet survival and act as a passive barrier to host immune cells, its immunoprotective qualities are limited in time due to its hydrolytically degradable structure. To further promote the functionality of the encapsulated cells, Weber et al. [51] created a dual PEG hydrogel system. This multilayered hydrogel consists

of a PEG-laminin core and an exterior inert PEG layer. The core provides a biologically active environment for the islets allowing the islets to survive 28 days in culture, while the outer shell provides a protective barrier against a host immune response [51] Headen et al. [52] showed that encapsulation of islets in PEG-maleimide did not affect cell viability and provided a tunable hydrogel network that supported insulin production in encapsulated human islets similar to the non-encapsulated islets in culture.

Due to PEG's non-fouling properties, PEGylation of other materials has been investigated as a method for immunoprotecting islet cells, and it has been shown that the PEGylated capsules reduced IL-2 secretion compared to alginate-poly-L-ornithine capsules [64]. Although PEG protects from infiltration of cytotoxic T-cells and reduces host-cell interactions, smaller components of the immune system, such as cytokines and antibodies produced by immune cells can still potentially diffuse through the passive barrier. This may lead to islet destruction, and shorten graft longevity [53]. To address this deficiency, Cheung and Anseth [99] demonstrated that conjugating apoptosis-inducing anti-Fas monoclonal antibodies to the surface of PEG hydrogels attenuates the immune response to the pancreatic islet cells further by destroying auto-reactive T-cells. The inclusion of anti-Fas monoclonal antibodies on the surface of the hydrogels induced apoptosis of Fas-sensitive Jurkat T cells.

TheraCyte, which is a membrane immunoisolator [70], has been used for encapsulation of pancreatic tissue to restore glucose levels in different animal models. Itkin-Ansari's group showed that TheraCyte protected pancreatic allograft from immune rejection in Rhesus monkeys for 1 year compared to a non-encapsulated allo-graft, which lasted only 14 days [100]. A study by Kumagai-Braesch et al. [101] showed that TheraCyte supports islet allografts for six months in

rats with normal and sensitized immune system. Bruin et al. [102] showed that human embryonic stem cells can differentiate into pancreatic progenitors in TheraCyte and were able to restore glucose levels in diabetic mice. Recently, Boettler et al. [63] encapsulated pancreatic tissue in TheraCyte and observed that the diabetic mice were able to maintain normoglycemia following implantation of TheraCyte. **Table 1** illustrates the advantages and limitations of natural and synthetic materials as immuno-isolating devices.

Table 1: Advantages and disadvantages of alginate, PEG, and TheraCyte as encapsulating materials for allogeneic cells

Gel/device	Advantages	Disadvantages
Alginate	(a) Low toxicity towards encapsulated cells (b) Bio inert (c) Minimal FBR (d) Low cost	(a) Limited control of mechanical properties (b) Ion-leaching leading to instability
PEG	(a) Easily tunable mechanical properties (b) Low toxicity (c) Synthesis reproducible (GMP grade) (d) Robust chemical modification with bioactive agents (RGD, FASL)	(a) Certain formulations can cause a more severe FBR (b) Pore size and stiffness must be adjusted for each application separately
TheraCyte	(a) A proven immunoisolator (b) Induces neovascularization (c) Commercially available (d) Easy retrieval and shape maintenance	(a) Limited variability in terms of geometry, stiffness, size and volume (b) Prone to physical damage (c) Limited space for loading of cells (d) Expensive

1.8 Use of Immuno-isolation to Support Ovarian Tissue Allo-Transplantation and Restore Ovarian Endocrine Function

The experimental success with allogeneic implantations of pancreatic islets and parathyroid cells led to the investigation of the feasibility of treatment of additional endocrine disorders, such as ovarian insufficiency in young female patients. Premature ovarian failure is a common side effect of anticancer treatments in girls and young women. Allogeneic ovarian tissue implantation has a promising potential as a means to restore ovarian endocrine function physiologically and avoid the side effects associated with delayed puberty and ovarian insufficiency.

The application of biomaterials for immuno-isolation of a gonadal tissue has promising potential for restoring endocrine function in males and females who suffer from premature gonadal insufficiency caused by cytotoxic therapy or autoimmune diseases. Just as islet transplantation is used to treat endocrine disruption in Type 1 Diabetes [49-52,62-64] as depicted in **Figure 1.2**.

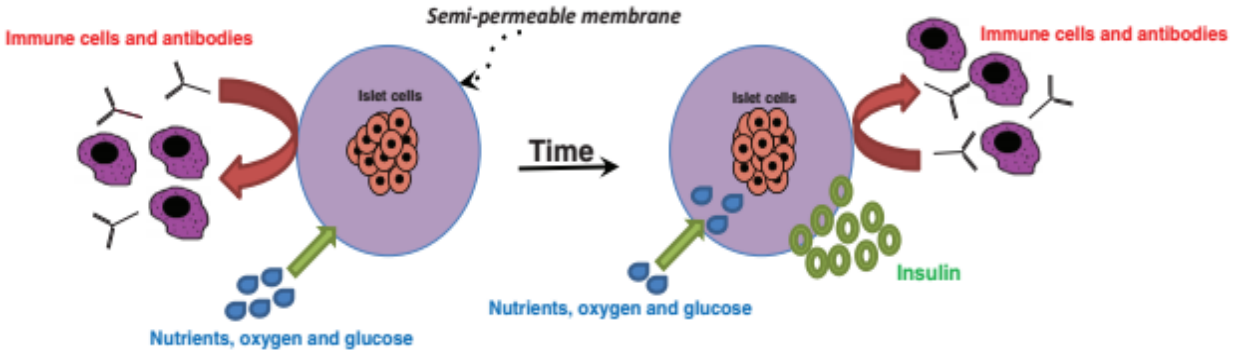

Figure 1.2: Immunoisolation of islet cells in a hydrogel. The basic principle is encapsulating islets in a semipermeable membrane which after a period of implantation results in the release of insulin. These hydrogels ideally allow the inflow of nutrients and exchange of hormones while minimizing immune cell infiltration.

Transplantation of ovarian follicles secreting sex hormones in response to endogenous circulating gonadotropins, could establish normal physiological endocrine ovarian function. The transplantation of ovarian follicles has similarities to islets, yet also presents unique challenges as well as opportunities. Follicles have a similar initial size to islets and secrete sex hormones (estradiol and progesterone) in response to circulating stimuli. Unlike islets, however, follicles expand and contract as they undergo structural and functional changes during the menstrual cycle. Furthermore, follicles are avascular and relatively resistant to hypoxia, allowing them to survive when implanted as larger structures. Due to these similarities and advantages compared to islets, immuno-isolation methods can be utilized towards follicles or ovarian tissue (**Figure 1.3**).

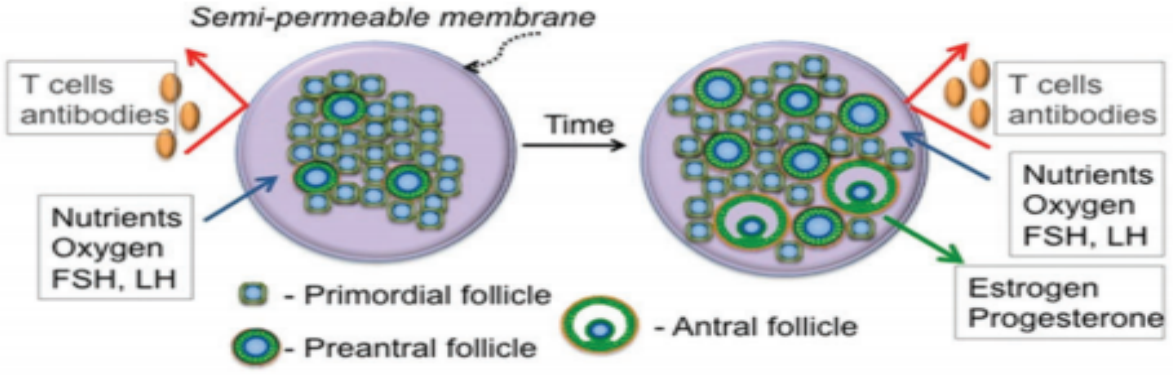

Figure 1.3: Immunoisolation of multiple follicles in a hydrogel. The basic principle is encapsulating follicles in a semipermeable membrane which after a period of implantation results in follicular development. These hydrogels ideally allow the inflow of nutrients and exchange of hormones while minimizing immune cell infiltration.

By protecting ovarian follicles or tissue from the host using PEG, alginate, and TheraCyte, successful restoration of ovarian endocrine function can be potentially achieved. This is possible

by maintaining the viability and functionality of a sufficient number of follicles secreting gonadal hormones in response to the circulating gonadotropic factors. It has been shown that proteolytically degradable synthetic PEG-based hydrogels support mice follicle growth and maturation [103]. Sittadjody et al. [104] encapsulated rat granulosa and theca cells in multilayered alginate to engineer an artificial ovarian tissue *in vitro*. They observed that sex steroids and peptide hormones were released in response to added gonadotropins.

1.9 Conclusion

The life-saving chemo and radiotherapies may cause premature ovarian insufficiency (POI), which is associated with ovarian damage, loss of fertility and endocrine function. For childhood cancer survivors who experience POI prior to puberty, the impact is particularly detrimental as the absence of puberty leads to co-morbidities such as poor bone health, altered metabolism, and poor cardiovascular health. Current options to restore endocrine function are HRT and ovarian tissue cryopreservation and auto-transplantation but are associated with limitations such as non-physiological delivery of hormones and risk of re-introduction of cancerous cells. This thesis details the work to study the hypothesis that allo-transplantation of ovarian tissue can restore ovarian endocrine function utilizing the concept of immune-isolation to protect ovarian allografts from an immune response. In **Chapter 2**, we describe the design and development of different formulations of PEG-based hydrogel for encapsulation of ovarian tissue. Here we further investigated the inflammatory reaction with the PEG-based capsules in the host surrounding tissues to determine which formulation attenuates the inflammation and fibrotic capsule formation around the implanted graft. **In Chapter 3**, we describe the development of a Dual PEG capsule with a degradable core and non-degradable shell that is conducive for ovarian tissue

development and is immuno-isolating. Multiple formulations of PEG-based capsules were tested in a syngeneic mouse model of POI to assess ovarian endocrine restoration and graft function. In **Chapter 4**, we tested the ability of the Dual PEG capsule to immuno-isolate the encapsulated allogeneic mouse ovarian tissue and assessed restoration of ovarian endocrine function and immune response in an allogeneic mouse model. In **Chapter 5**, we describe the ability for the Dual PEG capsule to retain cancer cells when co-encapsulated with syngeneic mouse ovarian tissue in application towards ovarian tissue auto-transplantation. In **Chapter 6,** we tested whether allogeneic ovarian tissue sensitizes the immune system when encapsulated in Dual PEG using an allogeneic mouse model and subsequent implantations of either encapsulated or non-encapsulated ovarian allografts. **In Chapter 7**, we tested whether non-human primate (NHP) ovarian tissue encapsulated in Dual PEG survives and develops in a syngeneic and allogeneic NHP model of POI. Additionally, we studied whether the encapsulated allografts provoked an immune response, testing the immuno-isolating capability of Dual PEG when encapsulating NHP ovarian tissue. In **Chapter 8**, the overarching conclusions of this thesis are made and possible future directions of this work are detailed.

CHAPTER II

Developing a synthetic hydrogel system appropriate for immuno-isolation of ovarian tissue

2.1 Authors:

James R. Day*, Anu David*, Jiwon Kim, Evan A. Farkash, Marilia Cascalho, Nikola Milašinović, Ariella Shikanov

2.2 Abstract

Poly(ethylene glycol) (PEG) can be functionalized and modified with various moieties allowing for a multitude of cross-linking chemistries. Here, we investigate how vinyl sulfone, acrylate, and maleimide functional end groups affect hydrogel formation, physical properties, viability of encapsulated cells, post-polymerization modification, and inflammatory response of the host. We have shown that PEG-VS hydrogels, in the presence of a co-monomer, N-vinyl-2-pyrrolidone (NVP), form more efficiently than PEG-Ac and PEG-Mal hydrogels, resulting in superior physical properties after 6 minutes of ultraviolet light exposure. PEG-VS hydrogels exhibited hydrolytic stability and non-fouling characteristics, as well as the ability to be modified with biological motifs, such as RGD, after polymerization. Additionally, unmodified PEG-VS hydrogels resulted in lesser inflammatory response, cellular infiltration, and macrophage recruitment after implantation for 28 days in mice. These findings show that altering the end group chemistry of

PEG macromer impacts characteristics of the photo-polymerized network. We have developed a tunable non-degradable PEG system that is conducive for cell or tissue encapsulation and evokes a minimal inflammatory response, which could be utilized for future immuno-isolation applications.

2.3 Introduction

The use of synthetic hydrogels presents a unique opportunity for tissue engineering applications, because the polymer network can be tuned to mimic the microenvironment of the native tissue to achieve desired function [85,87, 105]. Poly(ethylene glycol) (PEG) is one of the most studied and widely utilized biomaterial for synthetic hydrogels. Due to its high-water content and non-fouling properties, PEG based hydrogels are highly biocompatible and tunable [85, 106]. Additionally, the viscoelastic properties of PEG hydrogels allow for expansion and growth of encapsulated tissue, which is vital for engineering a hydrogel based immuno-oisolating construct [107, 108].

An immuno-isolating construct or device creates a physical barrier around the implanted cells or tissues, precludes contact with immune cells from the host and prevents sensitization. For the immuno-isolation of implanted allogeneic tissue, it is important for the network to be non-degradable yet porous enough to allow effective diffusion of nutrients and metabolites and, on the other hand, block transport of allo-antigens and cells out of the device and into the surrounding tissues of the recipient. An important design criteria when engineering an immuno-isolating construct is to create an interface with the host tissues that elicits a minimal inflammatory response. Evoking a strong inflammatory response would result in a thick fibrotic capsule in addition to immune cell recruitment around the construct, thereby hindering function

[109]. Due to its non-fouling properties, PEG coating and encapsulation has been shown to be a successful strategy to reduce acute inflammatory responses [110,111]. Additionally, PEG chain density, length, and conformation contribute to the ability to resist protein absorption [112-114].

Functionalization of the end hydroxyl groups of the otherwise inert PEG macromer with reactive end groups allows for a variety of crosslinking chemistries [90, 91, 94-96]. Multiple chemistries have been developed to functionalize PEG, such as vinyl sulfone, acrylate, amine, or maleimide end groups [115-119]. Presence of acrylate groups promotes the formation of a crosslinked network via photo-polymerization in the presence of a photo-initiator [90, 120,121], while vinyl sulfone and maleimide end groups are used for Michael-type addition chemistry with cysteine containing enzyme sensitive peptides to create a proteolytically degradable network [95,96,115]. Additionally, PEG macromers can be modified with biological motifs such as integrin binding peptides to create a microenvironment conducive for cell attachment [122].

Crosslinking of hydrogels using photo-polymerization is expedient, results in hydrogels with superior physical properties for *in situ* encapsulation, and creates networks that are resistant to proteolytic degradation [120]. Furthermore, several groups have shown photo-polymerized systems are cytocompatible and useful for a multitude of engineering applications [90, 123-130]. During the photo-polymerization process, light exposure creates free radicals in the presence of photo-initiators, which react as electron donors with the terminal double bonds and form crosslinked networks. Free radical mediated crosslinking is dependent on the reactivity of the free radical and the electrophilic nature of the available double bonds. Since this reaction is dependent on the presence of double bonds, we hypothesize that the chemistry of the functional end groups of a multi-arm PEG macromolecule will alter the susceptibility of double

bonds to react with free radicals, therefore, affecting the integrity of the crosslinking network and physical properties of the hydrogel. To test this hypothesis, we prepared photo-polymerized vinyl sulfone (PEG-VS), acrylate (PEG-Ac), and maleimide (PEG-Mal) hydrogels (**Figure 2.1**) and assessed how changing chemistry of the functional end group of the multi-arm PEG backbone impacted the crosslinking efficiency, bulk properties, stability, cell compatibility, modification efficiency, and the degree of inflammatory response. Our end objective was to develop a tunable non-degradable PEG system that is conducive for cell or tissue encapsulation and evokes a minimal inflammatory response, which could be utilized for immuno-isolation applications.

Figure 2.1: Chemical schematic of photo-polymerization of PEG-VS, PEG-Ac, and PEG-Mal in the presence of a photoinitiator.

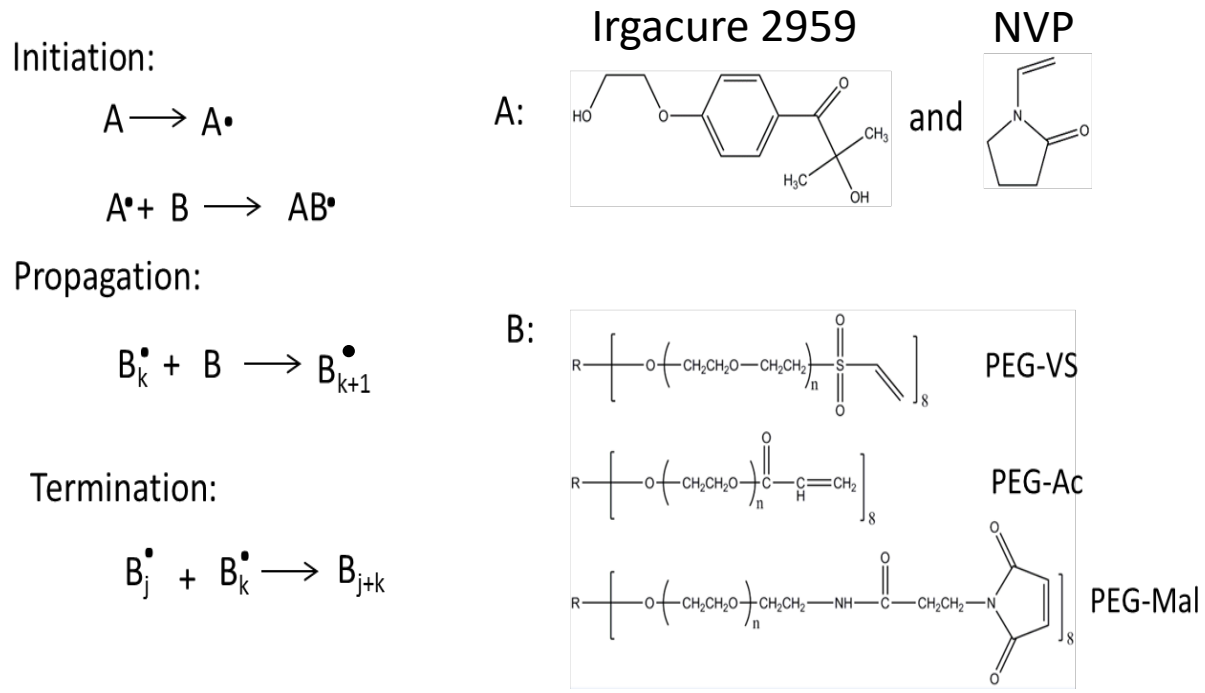

2.4 Results

2.4.1 The end group chemistry in PEG hydrogels impacts gelation efficiency and physical properties

We hypothesized that altering the functional end group attached to a multi-arm PEG backbone would alter the gelation efficiency and physical properties of the resultant photo-polymerized hydrogel due to a change in the reaction environment and reactivity of the respective group. To determine the effect of functional end groups on efficiency of gelation, we exposed the respective precursor solutions to 6, 15, and 30 minutes of UV light and measured gel fraction. When comparing across the three functional groups, PEG-VS hydrogels formed most efficiently, as demonstrated by the largest gel fraction at all exposure times and compositions (**Figure 2.2A**, **Table 2**).

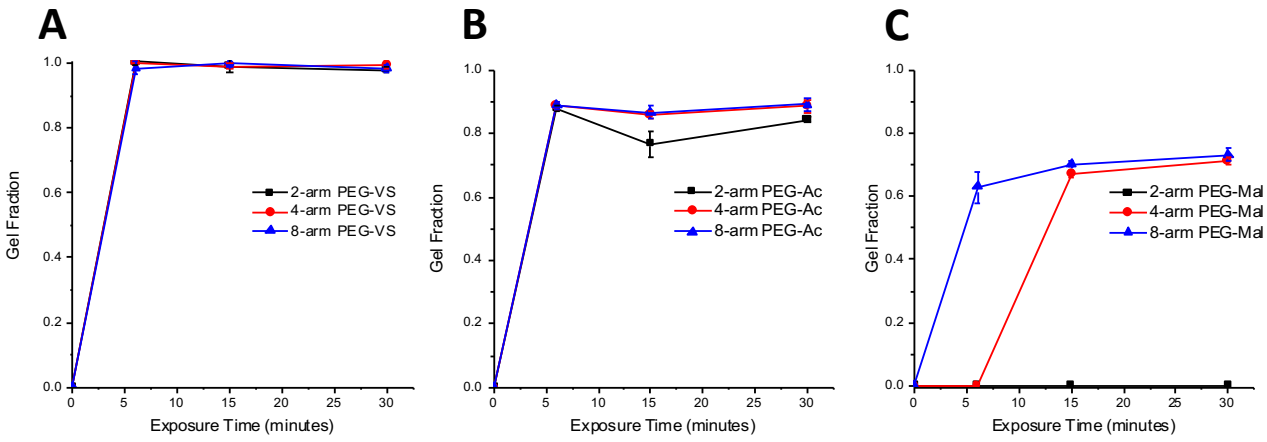

Figure 2.2: Gel fraction of 2-, 4-, and -8-arm 5% w/v **(A)** PEG-VS, **(B)** PEG-Ac, and **(C)** PEG-Mal hydrogels with 0.1% v/v NVP exposed to UV light (1090 µW/cm^2) for 6, 15, and 30 minutes (n=5 for all compositions).

Table 2: Gel fraction of -2, -4, and -8-arm 5% w/v PEG-VS, PEG-Ac, and PEG-Mal hydrogels with .1% v/v NVP and without RGD modification (n=15 for 8-arm, n=5 for 2- and 4-arm compositions), without NVP and without RGD modification (n=5 for all compositions), and with .1% v/v NVP and with .5mM RGD (n=5 for all compositions). All gels were exposed to UV light for 6 minutes. "–" indicates the hydrogels did not form.

Gel Composition	Gel Fraction		
	NVP(-), RGD(-)	NVP(+), RGD(-)	NVP(+), RGD(+)
8-arm PEG-VS	0.99±0.02	0.99±0.02	0.73±0.05
8-arm PEG-Ac	0.88±0.01	0.89±0.02	0.71±0.01
8-arm PEG-Mal	-	0.63±0.05	0.52±0.02
4-arm PEG-VS	1.0±0.01	1.0±0.0	-
4-arm PEG-Ac	0.88±0.01	0.89±0.01	0.64±0.02
4-arm PEG-Mal	-	-	-
2-arm PEG-VS	-	1.0±0.01	-
2-arm PEG-Ac	0.81±0.01	0.88±0.01	0.64±0.01
2-arm PEG-Mal	-	-	-

After 6 minutes exposure to UV light (1090 μW/cm^2), 8-arm PEG-VS, PEG-Ac, and PEG-Mal (NVP(+), RGD(-)) hydrogels formed with 99%, 89%, and 63% efficiency, respectively. All tested multi-arm PEG-VS hydrogels that included NVP formed completely by 6 minutes of exposure, while PEG-Ac and PEG-Mal hydrogels did not form completely up to 30 minutes of UV light exposure (**Figure 2.2**). All multi-armed PEG-VS hydrogels incorporated 99% of solid content by 6 minutes, while PEG-Ac and PEG-Mal hydrogels incorporated up to 89% and 70% solid content by 30 minutes, respectively (**Figure 2.2**).

Formation of PEG-VS photo-crosslinked hydrogels is the result of the reaction between the electron deficient activated vinyl group and free radicals, similar to the nucleophile-catalyzed thiol Michael-type addition reaction of PEG hydrogels. The stronger reactivity of the vinyl sulfone group is due to the vinyl moiety being more electron deficient than that of the acrylate or maleimide[24], which was confirmed by the downfield shifting of the VS protons in the PEG-VS ^{1}H NMR spectrum (**Supplemental Figure 2.1A**). The sulfone group of the PEG-VS is a stronger electron withdrawing group compared to the neighboring carbonyl group of acrylate and amide, attracting more electrons away from the neighboring double bond, causing electron deficiency. Thus, the double bond in vinyl sulfone is more susceptible to reacting with free radicals and the rate of propagation is increased. During propagation, the electron withdrawing force of the sulfone moiety further destabilizes the secondary free radical resulting in an increase in reactivity [131]. Interestingly, PEG-Mal did not crosslink as quickly or efficiently as PEG-VS or PEG-Ac, across all compositions. One of the proposed explanations could be that the reaction of free radicals with the double bond resulted in bond dimerization, thereby, stabilizing the resultant free radical via resonance [132]. To further investigate the impact the functional end groups had on the network, swelling ratio (**Figure 2.3**) and storage modulus (**Figure 2.4A**) of PEG-VS, PEG-Ac, and PEG-Mal hydrogels were investigated.

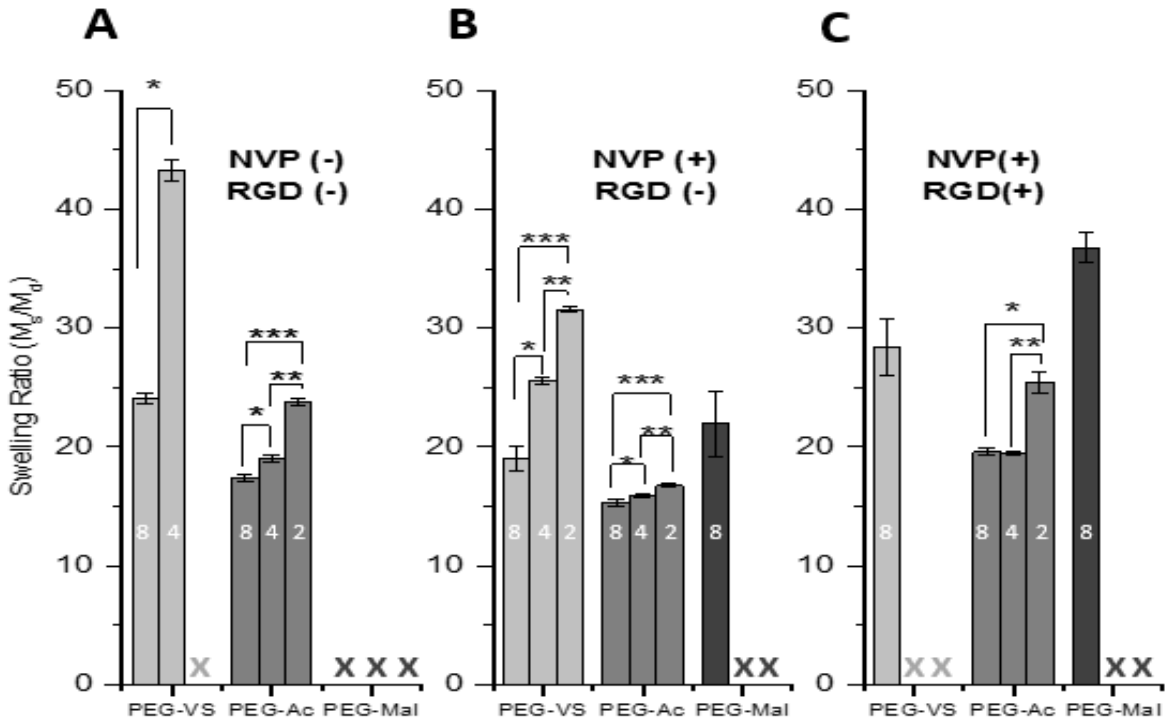

Figure 2.3: Swelling ratio of **(A)** 5% w/v 2-, 4-, and -8-arm 5% w/v PEG-VS, PEG-Ac, and PEG-Mal hydrogels without NVP and without RGD modification (n=5 for all compositions), **(B)** with NVP and without RGD modification (n=15 for 8-arm, n=5 for 2- and 4-arm), and **(C)** with NVP and with .5mM RGD (n=5 for all compositions) after 6 minutes exposure to UV light (1090 µW/cm2). Numbers (2,4, or 8) within columns indicate arms around PEG macromer. "X" indicates the hydrogel composition did not form. Differing letters (a, b, c) and indicate statistical significance ($p<0.05$). Significance was determined by a Welch two-sample t-test.

Altering the functional end group in a multi-arm PEG macromer impacted the crosslinking network as shown by the significant difference between swelling ratio (**Figure 2.3B**) and storage moduli (**Figure 2.4A**) of 5% w/v 8-arm PEG-VS, PEG-Ac, and PEG-Mal (NVP(+), RGD(-)) hydrogels. Photo-crosslinked PEG-Mal exhibited the highest swelling ratio (Q_m=22) which corroborated that the PEG-Mal network was less dense compared to that of PEG-VS (Q_m=19) and PEG-Ac (Q_m=15) (**Figure 2.3B**). PEG-VS and PEG-Ac hydrogels exhibited a storage modulus of 4500-5000 Pa, while

PEG-Mal hydrogels had a storage modulus of 2400 Pa, indicating a less mechanically strong network (**Figure 2.4A**).

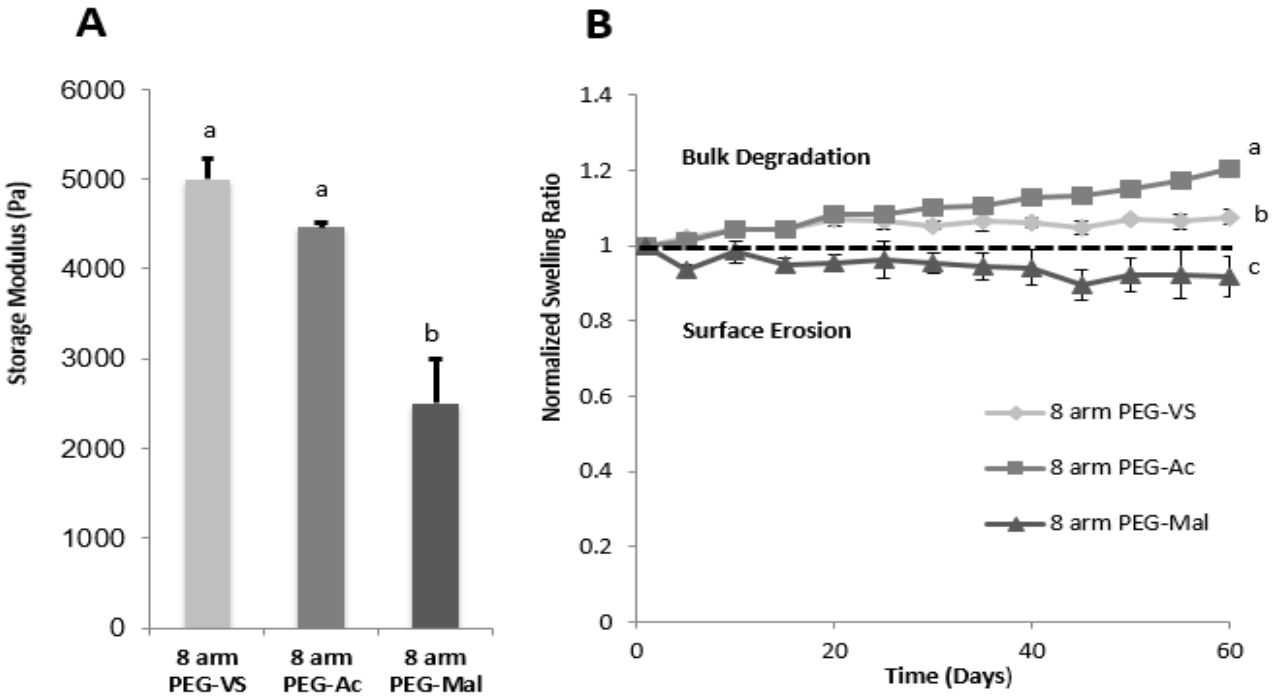

Figure 2.4: A) Storage modulus of 5% 8-arm w/v PEG-VS (n=3), PEG-Ac (n=3), and PEG-Mal (n=3) with NVP and without RGD modification after 6 minutes exposure to UV light and **(B)** Degradation over 60 days in PBS of 8-arm 5% w/v PEG-VS (n=5), PEG-Ac (n=5), and PEG-Mal (n=4) hydrogels with NVP and without RGD modification after 6 minutes exposure to UV light. "*" indicate statistical significance ($p<0.05$). Significance was determined by a Welch two-sample t-test.

In addition to the functional end group, the number of reactive ends in the multi-arm PEG macromer affected the properties of the photo-crosslinked hydrogels. Decreasing the number of arms around a PEG macromer from 8 to 4 to 2 arms decreased the efficiency of the photo-initiated reaction, similar to what we observed when the hydrogels were formed using Michael-type crosslinking chemistry [133]. The most dramatic effect of decreasing number of arms was

observed in PEG-Mal hydrogels with NVP, because 2 and 4-arm PEG-Mal did not form after 6 minutes of UV light exposure (**Figure 2.2C**, **Table 2, Figure 2.3B**); this finding further confirmed that maleimide end functional group does in fact stabilize the double bond and sterically hinder free radical attack more than vinyl sulfone or acrylate groups. To further investigate why the 8-arm PEG-Mal network was not fully formed after 6 minutes of exposure and whether the irradiation time was the limiting factor, we increased the UV exposure time to 30 minutes. The storage moduli of 8-arm PEG-Mal hydrogel after 30 minutes of exposure reached on average 9470 Pa (n=3). The volume of the crosslinked hydrogel remained unchanged and we concluded that the 3.5-fold increase in the storage modulus compared to shorter irradiation times was due to improved network formation and not due to the evaporation of solvent. These results indicated incomplete network formation after 6 minutes of UV exposure, as corroborated by the gel fraction (**Figure 2.2C**). When considering 8-arm and 4-arm PEG-VS and acrylate gels, with the increase in functionality (number of arms) of the macromer, the fraction of arms that must become crosslinked in order to produce a gel decreases, allowing macromer structure to set the fractional conversion of end groups that must be achieved to reach the gel point [134].

To validate network formation, FTIR analysis was performed (**Supplemental Figure 2.2**). The observed peak at 1420 cm^{-1} represents C–H of C=C, which is related to formation of free radicals after decomposition of the photo-initiator (**Supplemental Figure 2.2A-C**) [135,136]. All FTIR spectra showed a broad absorption band around 3430 cm^{-1} due to the –OH stretching frequencies [136]. Peaks around 2920 and 2864 cm^{-1} are related to asymmetric and symmetric behavior (stretching) of methyl group (namely =C–H vibrations) (**Supplemental Figure 2.2A-C**) [137], as complemented by the NMR spectra (**Supplemental Figure 2.1**). The spectrum of 8-arm

PEG-Ac (NVP(+)) gels suggests network formation due to the formation of C–C bonds between PEG polymer backbone chains in the hydrogel (**Supplemental Figure 2.2B**) that affects the mobility of the PEG backbone [138], as observed by the spectrum peak broadening. This observation was supported by the finding that PEG-Ac hydrogels have a swelling ratio of approximately 15 independent of the number of arms around the macromer (**Figure 2.3B**). A peak around 1720 cm^{-1} in the spectra of hydrogels indicates double bond conversion (**Supplemental Figure 2.2B, C**) [139]. The FTIR spectra of 8-arm PEG-Ac and 8-arm PEG-Mal hydrogel had a stronger peak compared to the spectrum of 8-arm PEG-VS gel (**Supplemental Figure 2.2A**), suggesting that a greater portion of double bonds stay intact, which presents an option of post crosslinking modification of the unreacted double bonds.

2.4.2 Inclusion of NVP alters hydrogel physical properties and has a protective effect on cell viability during encapsulation

It has been demonstrated NVP accelerates gelation due to the increase in vinyl group concentration and diffusion of free radicals [140]. To investigate this effect on gelation and network formation after 6 minutes of UV light exposure, gel fraction and swelling ratio with and without NVP was acquired (**Table 2, Figure 2.3A,B**). The presence of NVP in the precursor solution is essential for formation of 2-arm PEG-VS gels in 6 minutes, but had a less pronounced effect on gelation of 4- and 8-arm PEG-VS networks (**Table 2**). Inclusion of NVP impacted the physical properties of the network as indicated by the significant decrease in swelling ratio (**Figure 2.3A, B**). NVP demonstrated no impact on PEG-Ac network formation and a minimal impact on the physical properties. For all PEG-Mal networks, the inclusion of NVP is essential for gelation (**Table**

2, Figure 2.3A). Furthermore, steric hindrance of the free radicals on the macromer ends would explain the improved gelation in the presence of NVP [141]. In radical polymerization, the reactivity of a free radical depends upon the electrons' delocalization, polarity and volume nature of the side groups linked to the radical carbon [142]. The effect was more pronounced for vinyl sulfone, meaning that the radicals at the end of the chain in PEG-VS are more sterically hindered than those of acrylates. We hypothesize the electron deficiency of the vinyl moiety and destabilization of the radical in PEG-VS is able to overcome steric hindrance to efficiently form hydrogels via free radical reaction (**Figure 2.3A, Table 2**). In this reaction, NVP acts as a facilitator and creates more free radicals that are accessible by larger sterically hindered VS and Mal groups. We demonstrated that the degree to which NVP facilitates the reaction was dependent on the chemistry and structure around the vinyl groups in a multi-arm PEG macromer.

Additionally, for any cell/tissue encapsulation, the ability for the cells to survive the encapsulation process is vital. To investigate whether cells or tissue can survive the encapsulation process, we encapsulated mouse embryonic fibroblasts (MEFs) in PEG-VS, PEG-Ac, and PEG-Mal hydrogels with and without NVP and assessed survival after one day in culture. Similar to Hao et al. [140], we observed that after the addition of NVP to the precursor solution the encapsulated cells exhibited greater viability (**Figure 2.5A**). Cells encapsulated in PEG-VS, PEG-Ac, and PEG-Mal hydrogels with NVP exhibited a viability of 87%, 89%, and 68%,respectively, which decreased significantly to 60% and 40%, when NVP was not included in PEG-VS and PEG-Ac hydrogels(**Figure 2.5A(F)**). PEG-Mal hydrogels did not form when NVP was not included. It was hypothesized that the protective effect of NVP was due to improved formation kinetics of the network, decreasing the time and absolute exposure of the cells to free radicals. Overall, we showed that NVP can be

added in the precursor solution to increase the kinetics of the reaction, the physical properties of the network, and does not negatively impact cell viability upon encapsulation. When comparing cellular response to encapsulation between the end functional groups of PEG macromers, cells encapsulated in PEG-VS and PEG-Ac exhibited a significantly higher viability (87% and 89%, respectively) than cells encapsulated in PEG-Mal hydrogels (68% viability) (**Figure 2.5A(F)**). We hypothesize that this is due to the kinetics of the reaction and cells being exposed to more absolute free radicals during the PEG-Mal encapsulation, as well as toxicity from residual maleimide groups.

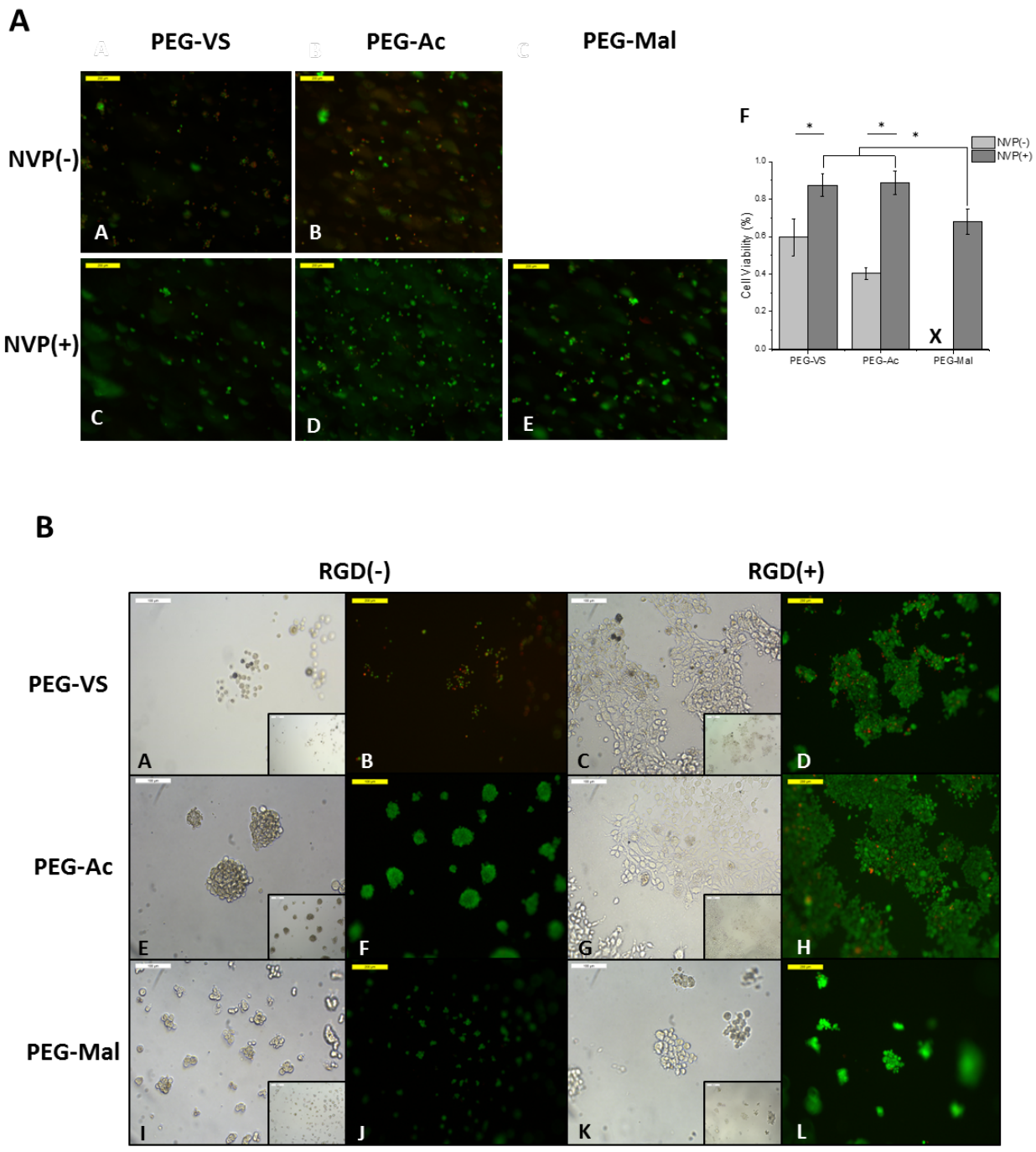

Figure 2.5: A) Fluorescent images of MEFs encapsulated in 5% 8-arm PEG-VS and PEG-Ac without NVP **(A,B)**, respectively and 5% 8-arm PEG-VS, PEG-Ac, and PEG-Mal with .1% v/v NVP **(C,D,E)**, respectively. Cells were stained with calcein AM and ethidium homodimer-1 for 30 minutes. Magnification 10×. **(F)**Quantification of cell viability in PEG-VS, PEG-Ac, and PEG-Mal hydrogels (n=3). "*" indicates statistical significance ($p<0.05$). "X" indicates the hydrogel did not form. **(B)** Brightfield and fluorescent images of MEFS seeded on 5% 8-arm PEG-VS, PEG-Ac, and PEG-Mal hydrogels without RGD modification **(A,B,E,F,I,J)** and 5% 8-arm PEG-VS, PEG-Ac, and

PEG-Mal hydrogels incubated in a 5mM RGD solution after polymerization **(C,D,G,H,K,L)**. Magnification 20×, inset magnification 10×.

2.4.3 The functional end group of a PEG macromer impacts the efficiency of RGD modification

We determined the efficiency of RGD conjugation to PEG-VS and PEG-Ac by analyzing NMR spectra of the macromers before and after the conjugation reaction. By reacting 5% 8-arm PEG monomers, which have 10 mM reaction arms with 5 mM RGD we expected to see a 50% depletion of vinyls. Using NMR and assigning a vinyl peak an integration value of 1.0, the ratio between the protons in the double bond and in the PEG backbone can be calculated and compared between unmodified and RGD modified PEG macromers (**Supplemental Figure 2.1**). For PEG-VS, there was a 53.5% reduction in vinyl protons when comparing modified to unmodified, indicating 100% binding efficiency. For 8-arm PEG-Ac, there was a 24.5% reduction of vinyls from unmodified to modified. The double bonds in PEG-Mal undergone hydrolysis during dialysis and the ratio between the modified and unmodified macromers could not be determined (**Supplemental Figure 2.1**). Based on these results, we concluded that RGD binds with 100% efficiency to vinyl sulfone moieties because of the vinyls' electron deficiency and susceptibility to thiol-mediated reactions.

RGD modification of multi-armed PEG impacted gelation and the physical properties of the resultant hydrogel. When 0.5mM RGD was added to PEG-VS, PEG-Ac, and PEG-Mal hydrogels, solid content incorporation decreased after 6 minutes of gelation (**Table 2**) and swelling ratio increased compared to unmodified hydrogels (**Figure 2.3B,C**), indicating a less dense network. The most drastic impact was seen in PEG-VS hydrogels as 2- and 4-arm PEG-VS hydrogels modified with .5mM RGD did not form after 6 minutes of gelation (**Table 2**).

2.4.4 Available double bonds allow for post-polymerization RGD modification of PEG hydrogel networks

To investigate whether post-polymerization modification of the crosslinked hydrogels with RGD was possible we incubated the gels with 5mM RGD solution for 15 min. After a thorough washing step, we seeded mouse embryonic fibroblasts (MEFs) on top of the gels. We compared cell adhesion to 5% w/v 8-arm PEG-VS, PEG-Ac, and PEG-Mal hydrogels with RGD modification (RGD(+)) and without RGD (RGD(-)) added after polymerization (**Figure 2.5B**). Cells seeded on the hydrogels treated with RGD post-polymerization attached to the gel surface and demonstrated a spindle-shaped morphology. Without the RGD modification, cells seeded on the gels formed clusters and did not spread. Post-polymerization modification with RGD also improved the viability of the seeded cells for PEG-VS hydrogels, which was 49% without and 95% with RGD modification. Larger clusters and 100% viability was observed when cells were seeded on unmodified PEG-Ac and PEG-Mal hydrogels (**Figure 2.5B**). This can be explained by the fact that vinyl sulfone groups are more hydrophilic than acrylate and maleimide groups and hardly promote any protein absorption, increasing the non-fouling properties [110]. The possibility of modifying a hydrogel with bioactive peptides after polymerization enables the creation of a bio-responsive surface without drastically impacting the physical properties of the network.

2.4.5 Hydrolytic stability of photo-crosslinked PEG hydrogels for immuno-isolation application

In immuno-isolation applications, proteolytic or hydrolytic degradation of the hydrogel leads to exposure of the recipient immune system to the donor tissue and may result in

sensitization of the host and rejection of the implanted tissue causing premature graft failure. For this reason, an immuno-isolating hydrogel system must be designed to be non-degradable and stable *in vivo*. Photo-polymerization of functionalized PEG forms crosslinks between the carbon atoms, through the double bonds at the end-groups of the otherwise biologically inert macromer. Similar to previous findings demonstrating significant hydrolytic degradation of PEG-Ac hydrogel [143], we found that in physiological conditions, PEG-VS hydrogels were more stable than PEG-Ac hydrogels (**Figure 2.4B**). PEG-VS hydrogel swelling ratio changed the smallest percentage over a span of 60 days in DPBS. The presence of carbonyls in PEG-Ac and PEG-Mal hydrogels make them more susceptible to hydrolytic attack of hydroxyl groups. In addition to being hydrolytically stable, differential scanning calorimetry (DSC) demonstrated PEG-VS samples show good thermal behavior within the application temperature (**Supplemental Figure 2.3)**. Within the application temperature, no significant changes are seen, since the two curves, before and after gelation, are similar. The T_m of the polymer has been shifted from 51.3 °C to 54.6 °C, as a result of UV polymerization. As a consequence of network formation, and hence more complex, less flexible structure, the decrease in endothermic peak is evident (**Supplemental Figure 2.3**).

2.4.6 Inflammatory response of the surrounding host tissues to the implanted PEG hydrogels

Attenuated inflammatory response at the interface between the immuno-isolating device and the host tissues contributes to extended immuno-isolation and survival of the graft. We investigated the local interactions at the interface between the hydrogel implant and host tissues. We implanted subcutaneously for 28 days PEG-VS, PEG-Ac, and PEG-Mal hydrogels, and performed macro- and microscopic characterization. Interestingly, hydrogels at the retrieval

showed blood vessel development around the hydrogels, yet the hydrogels were intact and were easily removable. PEG-Mal hydrogels with and without RGD induced a strong response from the host, compared to other groups showing dense collagen deposition with stratified cells. In addition to the presence of multinucleated giant cells, PEG-Mal based hydrogels with and without RGD showed clear infiltration of cells into the hydrogel (**Figure 2.6Q, R, U and V**) with presence of macrophages M1 and M2, as was confirmed with CD-68 and CD-163 antibody staining (**Figure 2.6S, T, W and X**), which will hinder the immuno-isolating properties of the hydrogel (**Figure 2.6Q, R, U and V**). Similarly, PEG-Ac hydrogels became encapsulated in a pseudostratified cell lining with giant cells, with some infiltration into the hydrogel (**Figure 2.6I, J, M and N**). Neovascularization was observed in the surrounding dense collagen with increased macrophage infiltration in PEG-Ac gels without RGD compared to those with RGD (**Figure 2.6I, J, K, L, M, N, O, P**). PEG-VS hydrogels showed the least inflammatory response with an attenuated cell lining and a thinner but dense collagen deposition with only occasional giant cells. No cellular infiltration in PEG-VS hydrogels occurred after 28 days (**Figure 2.6A, B**) compared to PEG-VS-RGD hydrogels (**Figure 2.6E, F**). This observation corroborated with what was seen in **Figure 2.5B**, as unmodified PEG-VS hydrogels elicited minimal cellular attachment and spreading compared to PEG-Ac and PEG-Mal hydrogels (**Figure 2.5B**), indicating less protein absorption. Interestingly, PEG-VS hydrogels with and without RGD showed stronger presence of macrophage M2 (**Figure 2.6D, H**) and lesser presence of M1 (**Figure 2.6C, G**) compared to PEG-Ac and PEG-Mal hydrogels, possibly indicating a healing response.

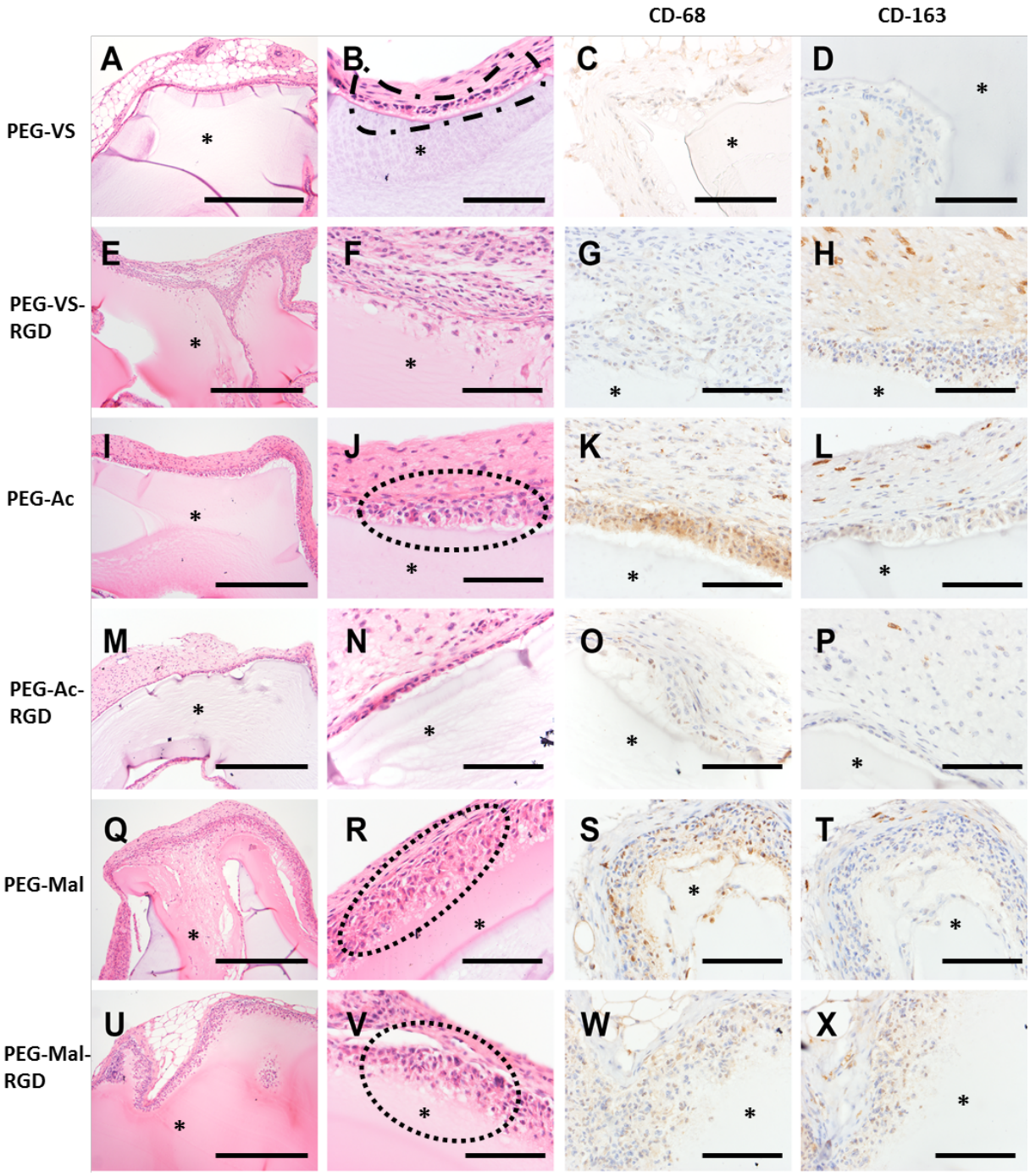

Figure 2.6: Histological images of 8-arm PEG types after implantation for 28 days. **(A, B)** PEG-VS, **(E, F)** PEG-VS-RGD, **(I, J)** PEG-Ac, **(M, N)** PEG-Ac-RGD, **(Q, R)** PEG-Mal and **(U, V)** PEG-Mal-RGD. Host response to implanted PEG types as observed: **(B)** PEG-VS implant with retraction artifact and loosely adherent capsule composed of attenuated epithelioid cells (dashed outline). **(J)** PEG-Ac implant with multilayered cellular capsule overlying granulation tissue with prominent angiogenesis and frequent multinucleate giant cells (dashed outline). **(R, V)** PEG-Mal

implant with infiltration into and partial resorption of the hydrogel matrix (dotted outline). **(C, G)** Presence of macrophage M1 (CD-68 staining) were observed in **(G, K)** PEG-Ac and **(S, W)** PEG-Mal hydrogels. Whereas macrophage M2 (CD-163 staining) observed in weak to strong presence between PEG hydrogel types **(P, T, X, D, H and L)**. **(*)** PEG hydrogel. Magnification 10× **(A, E, I, M, Q, U**) **scale bar, 500 µm**. Magnification 40× **(B, C, D, F, G, H, J, K, L, N, O, P, R, S, T, V, W, X), scale bar, 50 µm**.

2.5 Discussion

The design of an immuno-isolating hydrogel system has to address cytocompatibility upon encapsulation, the physical properties of the network that match the physiological host environment, resistance to proteolytic and hydrolytic degradation, and minimal inflammatory response. In a previous study, we investigated the ability of TheraCyte and alginate to support and protect ovarian tissue in a syngeneic and allogeneic model [144]. We found that alginate was not able to withstand the volumetric expansion of ovarian tissue, compromising its immuno-isolating capability. Immuno-isolating non-degradable PEG hydrogels have been used for encapsulating pancreatic cells [49-52] using crosslinking chemistries with non-degradable peptides[52, 136, 145], scramble peptides [146-148], and photo-polymerization [120, 140, 149]. However, non-degradable and scramble peptides can require longer gelation times compared to photo-polymerization[136], and gelation upon monomer-peptide introduction may limit advanced patterning opportunities. During photo-crosslinking, expedient polymerization only upon light exposure presents the opportunity for advanced patterning and spatiotemporal control. To our knowledge, non-degradable PEG-VS hydrogels have not been developed using solely photo-polymerization. Photo-polymerized PEG-VS based hydrogels, described here, meet the design criteria for an immuno-isolating device and are advantageous towards microencapsulation due to the high degree of tunability, biocompatibility, and non-fouling

surface [85,106]. We hypothesized that utilizing PEG-VS as the backbone polymer would create a hydrolytically stable hydrogel system in a physiological environment without impacting tissue viability upon encapsulation. In this study, we investigated how changing the end functional group around a PEG macromer impacts gelation, physical properties, and compatibility, with the objective of designing a hydrogel system that could be used towards immuno-isolating applications.

We first compared how vinyl sulfone, acrylate, and maleimide impacted gelation efficiency and physical properties of the resultant PEG hydrogels. PEG-VS hydrogels form most efficiently across the functional groups given the same exposure time, because double bonds in the vinyl sulfone moiety are more electron deficient [121], leading to faster free radical reaction and propagation. The physical properties of PEG-VS hydrogels were also superior to that of PEG-Ac and PEG-Mal given the same crosslinking time, which would be vital for tissue encapsulation and tuning the mesh size for immuno-isolation applications. A shorter crosslinking time to complete the encapsulation minimizes the impact on cell viability. Additionally, including NVP, a co-monomer, at a low concentration demonstrated a protective effect on cell viability upon encapsulation. We hypothesized that in the presence of NVP the cells were exposed to a decreased absolute number of free radicals for a shorter time due to the improved gelation kinetics. Overall, we have demonstrated that addition of NVP improves gelation, physical properties, and cell cytocompatibility.

Unmodified PEG hydrogels are inert to protein absorption and cell interactions. We showed the efficiency of RGD binding was impacted by the functional end group that was present during the thiol-mediated reaction. In this reaction the thiol present in the side chains of RGD

reacts with vinyl groups present in the functional group on the PEG arms. PEG-VS incorporated RGD most efficiently due to the electron deficiency of the double bond and availability to react with thiol groups. We have been able to demonstrate that RGD can be incorporated into PEG-VS and PEG-Ac hydrogel networks after photo-polymerization due to the presence of unreacted double bonds. Post-crosslinking modification could be important for tissue engineering applications as one can create a hydrogel system with the desired physical properties and then modify the network with bioactive motifs post-polymerization.

Resistance to hydrolytic degradation is an important design criterion for an immuno-isolating device. Photo-polymerization was used as the crosslinking chemistry to minimize the extent of proteolytic degradation. However, hydrolytic degradation of ester and maleimide bonds may lead to premature graft rejection. PEG-Ac and PEG-Mal hydrogels are susceptible to hydrolytic degradation due to the presence of carbonyls and/or ring opening, while PEG-VS hydrogels are more stable in physiological conditions. We confirmed that PEG-VS was the most hydrolytically stable over a span of 60 days. Additionally, biocompatibility of an implanted device with the surrounding tissues of the host and a minimal inflammatory response contribute to the graft longevity. Macrophages play a key role in inflammatory response after implantation of biomaterials [150]. Upon implantation, PEG-VS hydrogels had the least amount of cellular infiltration compared to PEG-Ac and PEG-Mal hydrogels. RGD incorporation in all PEG hydrogel types further facilitated cell infiltration. Interestingly, PEG-Ac-RGD hydrogels attracted less macrophage reaction when compared to the non-modified PEG-Ac, which corroborates with Blakney et al. who used PEG-DA hydrogels [151]. Overall, we demonstrated that PEG-VS hydrogels can form efficiently via photo-polymerization, are hydrolytically stable, maintain cell

viability upon encapsulation, and elicit a lesser inflammatory response compared to PEG-Ac and PEG-Mal hydrogels.

This study has demonstrated that reactive functional end groups of the multi-arm PEG macromers impact free radical mediated network formation. The PEG-VS network formed more efficiently via photo-polymerization, impacting bulk properties, was most stable in physiological conditions, and elicited an attenuated inflammatory response compared to PEG-Ac and PEG-Mal hydrogels. Further, NVP can be added to the precursor solution to expedite the cross-linking process without impacting cellular response upon encapsulation. One of the potential applications of these hydrogels would be their use for immuno-isolation methods. A shorter crosslinking time would improve the biocompatibility of a hydrogel when used with live cells or in proximity to live tissues and should have the least effect on the viability of cell or tissue encapsulated within the photo-polymerized hydrogel. These attributes are crucial for efficient encapsulation of tissue or cells, including those of allogeneic origin, for long-term immuno-isolating applications.

2.6 Materials and Methods

2.6.1 Hydrogel Preparation

To form the hydrogel network, 2, 4, or 8-arm PEG-VS, PEG-Ac and PEG-Mal (JenKem Technology, Beijing, China) macromer powder was dissolved in sterile Dulbecco's Phosphate Buffered Saline(DPBS) (pH 7.4, Gibco, USA) solution and 0.4 mg/100µL of photo-initiator Irgacure 2959 (Ciba, Basel, Switzerland, MW=224.3) to create a solid concentration of 5% w/v.

Furthermore, a co-monomer, N-vinyl-2-pyrrolidone (NVP) (Sigma-Aldrich, USA), was added in some compositions at a final concentration of 0.1%, as NVP has been shown to enhance the gelation mechanism without impacting the cell compatibility [140]. To form the gels, the precursor solution (PEG, Irgacure 2959 and NVP (in some compositions)) was exposed to UV light at a constant intensity (1090 μW/cm^2 at a distance of 4 cm) for a designated duration.

2.6.2 Gel Fractions of PEG- Hydrogels

5% w/v 2, 4, and 8-arm PEG-VS, PEG-Ac, and PEG-Mal hydrogels were tested with no NVP and no RGD (NVP(-), RGD(-)), with 0.1% v/v NVP and no RGD (NVP(+), RGD(-)), and with 0.1% v/v NVP and modified with 0.5 mM RGD (NVP(+), RGD(+)). PEG precursor solution of constructs containing 0.5 mM RGD was incubated with 0.5 mM RGD for 15 minutes in isotonic HEPES buffer prior to UV exposure. All precursor solutions were exposed to UV light (365 nm, 1090 μW/cm^2 at a constant height of 4 cm) for 6 minutes and precursor solution containing NVP and no RGD were exposed for 6, 15, and 30 minutes. Gels were swelled overnight at room temperature to remove soluble monomers and lyophilized to remove water content. Dry mass was obtained and divided by theoretical solid content to quantify gel fraction (n=5 for all compositions).

2.6.3 NMR Analysis to Characterize RGD Conjugation

We evaluated the effect of the end-group chemistries on the efficiency of Michael-type addition of RGD to 8-arm 5% PEG-VS, PEG-Ac, and PEG-Mal. 5% w/v PEG precursor solution was incubated with 5 mM RGD for 15 minutes in HEPES buffer. A 5% w/v 8-arm PEG solution contains 10 mM reactive arms; so theoretically, half of the arms should be reacted when 5 mM RGD is

added. After incubation, 1 mL of the respective precursor solutions were transferred to a dialysis tubing (3.5-5 kDa MWCO, Spectrum Laboratories, California, USA). Dialysis against Milli-Q water was performed overnight to remove unreacted RGD molecules. The solutions were then lyophilized and the solid content was dissolved in 600 μL of deuterium oxide and transferred to a respective NMR tube. The NMR data was acquired on a 500 MHz Varian VNMR spectrometer equipped with two high band and one low band radio frequency channels. All spectra were acquired at 25 °C.

2.6.4 Fourier Transform Infrared Spectroscopy (FTIR) Analysis

Samples of pure chemicals and powdered dry hydrogels (xerogels) were submitted to FTIR analysis and the spectra were obtained using a Bomem MB 100 FTIR Spectrophotometer applying the Potassium Bromide (KBr) disc method. 1.5 mg of the powdered dry hydrogels were mixed and grinded (sample/KBr ratio was kept at 1/50 constant) and then compressed into a pellet at a pressure of 11 t for about a minute, using the Graseby Specac Model: 15.011. Spectra were obtained in the 4000–400 cm^{-1} wave number range at 25 °C and at 4 cm^{-1} spectral resolution.

2.6.5 Swelling Ratio

The swelling ratios of PEG hydrogels with varying compositions were determined. The hydrogels were formed as described above and submerged in DPBS for 24 hours. After 24 hours, excess DPBS was removed and the swollen mass of the hydrogels was obtained. These hydrogels were then air dried at room temperature and lyophilized to remove any moisture. Larger volumes (100 μL) of hydrogels were used to minimize error from weighing. The mass swelling ratio (Q_m)

was determined by dividing the mass of the swollen gels (M_s) by the mass of the dry gels (M_d). Results shown are mean ± SD.

2.6.6 Rheology

The storage moduli of PEG hydrogels with varying compositions were investigated. After formation, the hydrogels were swollen in DPBS overnight. A TA HR-2 rheometer (TA Instruments) equipped with a 20 mm parallel plates and a Peltier stage was used for this study. To ensure the hydrogel was the same size as the geometry, 1 mm thick hydrogel slabs were made and a 20 mm diameter disc was punched out (n=3). A constant strain rate of 5% was maintained for all tested hydrogels and the storage modulus was obtained by performing an angular frequency sweep from 0.1 to 10 rad/s. Results shown are mean ± SD.

2.6.7 In Vitro Hydrolytic Degradation of PEG-VS, PEG-Ac and PEG-Mal Hydrogels

The sensitivity of PEG hydrogels with varying end groups to hydrolytic degradation was investigated by incubating the gels in DPBS (pH: 7.4) at 37 °C for a period of 60 days (n=5 for PEG-VS and PEG-Ac, n=4 for PEG-Mal). Fresh DPBS was added every other day. Degradation was measured by determining the swelling ratio which was calculated every fifth day relative to the average initial dry (polymer) mass. All swelling ratio measurements were normalized to the initial swelling ratio (Day 1) [143]. Results shown are mean ± SD.

2.6.8 Differential Scanning Calorimetry (DSC) Analysis

The DSC experiments were performed using a DSC 1 instrument (Mettler–Toledo, Switzerland). Dried hydrogel samples were crimped in standard 40 µl aluminum pans and tracings were performed between 0.0 and 350.0 °C, at a heating rate of 10 °C/min under constant nitrogen purge of 50 cm^3/min.

2.6.9 Assessment of the Protective Effect of NVP during Photo-polymerization on Cell Viability

Mouse embryonic fibroblasts (MEFs) were encapsulated in 5% w/v 8-arm PEG-VS, PEG-Ac and PEG-Mal with, NVP(+), and without, NVP(-), 0.1% v/v NVP. Cells were encapsulated at a density of 250,000 cells/mL in a 10 µl gel. All cell containing precursor solutions were exposed to UV light for 6 minutes (n=3 for each condition). To assess cell viability, a Live/Dead assay (Thermofischer Scientific, Waltham, MA), based on membrane integrity was utilized. Briefly, 20 µl of 2 mM ethidium homodimer-1 and 5 µl of 4 mM calcein-AM were added to 10 mL of sterile PBS to make the stock solution. After 24 hours of culture, media was removed and 500 µl of Live/Dead stock solution was added to each sample and allowed to incubate for 30 minutes at 37 °C before imaging. Cell viability was quantified via Image J software.

2.6.10 Post-polymerization RGD Modification

We investigated whether photo-polymerized PEG hydrogels contained unreacted end group that allow post-polymerization modification with the RGD peptide. 100 µL precursor solution of 5% w/v 8-arm PEG-VS, PEG-Ac, and PEG-Mal with 0.1% v/v NVP was laid on the bottom of a 96 well plate and exposed to UV light for 6 minutes. Gels receiving post-polymerization RGD modification (RGD(+)) were incubated in a 5 mM RGD solution for 15 minutes. All gels were

washed with sterile PBS and allowed to swell overnight. Mouse embryonic fibroblasts were then seeded onto the PEG layers at a density of 25,000 cells/mL and cultured for a period of 6 days to evaluate cell spreading. As previously described, cells were stained with a Live/Dead cytocompatibility kit to assess viability at day 6 of culture. Viability was quantified via Image J software.

2.6.11 Inflammatory Response to Implanted PEG- Hydrogels

To investigate the inflammatory response, we subcutaneously implanted PEG hydrogels with varying end-group chemistries with and without RGD modification. The Institutional Animal Care and Use Committee (IACUC) guidelines for survival surgery in rodents and Policy on Analgesic Use in Animals Undergoing Surgery were followed for all the procedures. Animal experiments for this work were performed in accordance with the protocol approved by the IACUC at the University of Michigan (PRO00005750). A small incision was made on the dorsal side of the anesthetized adult female B6CBAF1 mice and the PEG (-VS, -Ac and -Mal) hydrogels were implanted subcutaneously in the first group (n=3 mice/group). The second group of mice were implanted with PEG hydrogels modified with 0.5 mM RGD (n=3 mice/group). The skin was then closed using 5/0 absorbable sutures. The mice were placed in a clean warmed cage for recovery and monitored post-operatively for 10 days. The mice received Carprofen (RIMADYL, Zoetis, USA) (5 mg/kg body weight) for analgesia before the incision was made. The mice were euthanized after a period of 28 days following implantation and the PEG hydrogels were retrieved.

2.6.12 Histological Analysis

Retrieved PEG-VS, PEG-Ac and PEG-Mal hydrogels were fixed in Bouin's fixative solution (Sigma-Aldrich) at 4 °C overnight and then transferred to 70% ethanol at 4°C until processing. After fixation, the samples were processed at the Histology Core in Microscopy & Image Analysis Laboratory at the University of Michigan. Samples were embedded in paraffin and serially sectioned at 5 μm thickness and were stained with hematoxylin and eosin. Stained sections were then examined for the presence of cells and host immune response under the light microscope.

2.6.13 Immunohistochemistry for Macrophages

To analyze the macrophage infiltration following implantation with PEG hydrogels, paraffin-sectioned slides were stained for mouse CD-68 and CD-163. First, sections were deparaffinized with Xylene and rehydrated. Slides were incubated in peroxide blocking reagent (BUF017B, BioRad, USA) for 30 min at room temperature to block any endogenous peroxidase activity. The slides were then incubated in antigen retrieval buffer, pH8.0 (BUF025A, BioRad) for 20 min at 96 °C and additional 20 min at room temperature for antigen retrieval. Following which the slides were incubated with normal goat serum (ab156046, abcam, USA) to block non-specific binding sites for 30 minutes at room temperature. The sections were incubated overnight at 4 °C with primary antibodies: rat anti-mouse CD-68 antibody (1:100 dilution, MCA1957; BioRad), rabbit anti-mouse CD-163 antibody (1:100 dilution, ab182422, abcam). The slides were subsequently incubated for 60 minutes at room temperature with secondary antibodies: goat anti-rat (1:100 dilution, STAR72, BioRad) for CD-

68 and goat anti-rabbit (1:500 dilution, ab97051, abcam) for CD-163. Diaminobenzidine (ab94665, abcam) was used as a chromogen and hematoxylin as a counterstain. For negative-controls, paraffin sections were incubated without the primary antibody.

2.6.14 Statistical Methods

Statistical analysis was performed using R software. A Welch two-sample T-test was used to evaluate differences in swelling ratio, storage modulus, and cell viability. The results were considered statistically significant when $p<0.05$.

2.7 Supplemental Figures

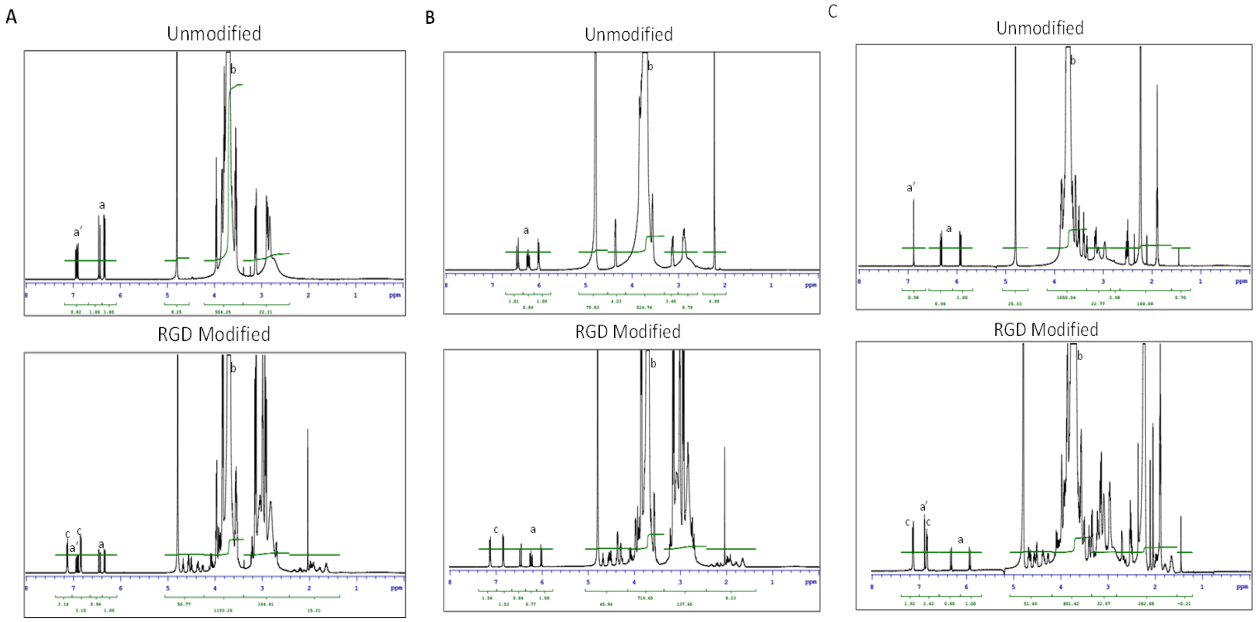

Supplemental Figure 2.1: NMR spectra of (A)unmodified and modified PEG-VS, (B) unmodified and modified PEG-Ac, (C) unmodified and modified PEG-Mal. a and a' indicate vinyl protons, b indicates methylene protons in the PEG backbone, and c indicates aromatic proteins from RGD.

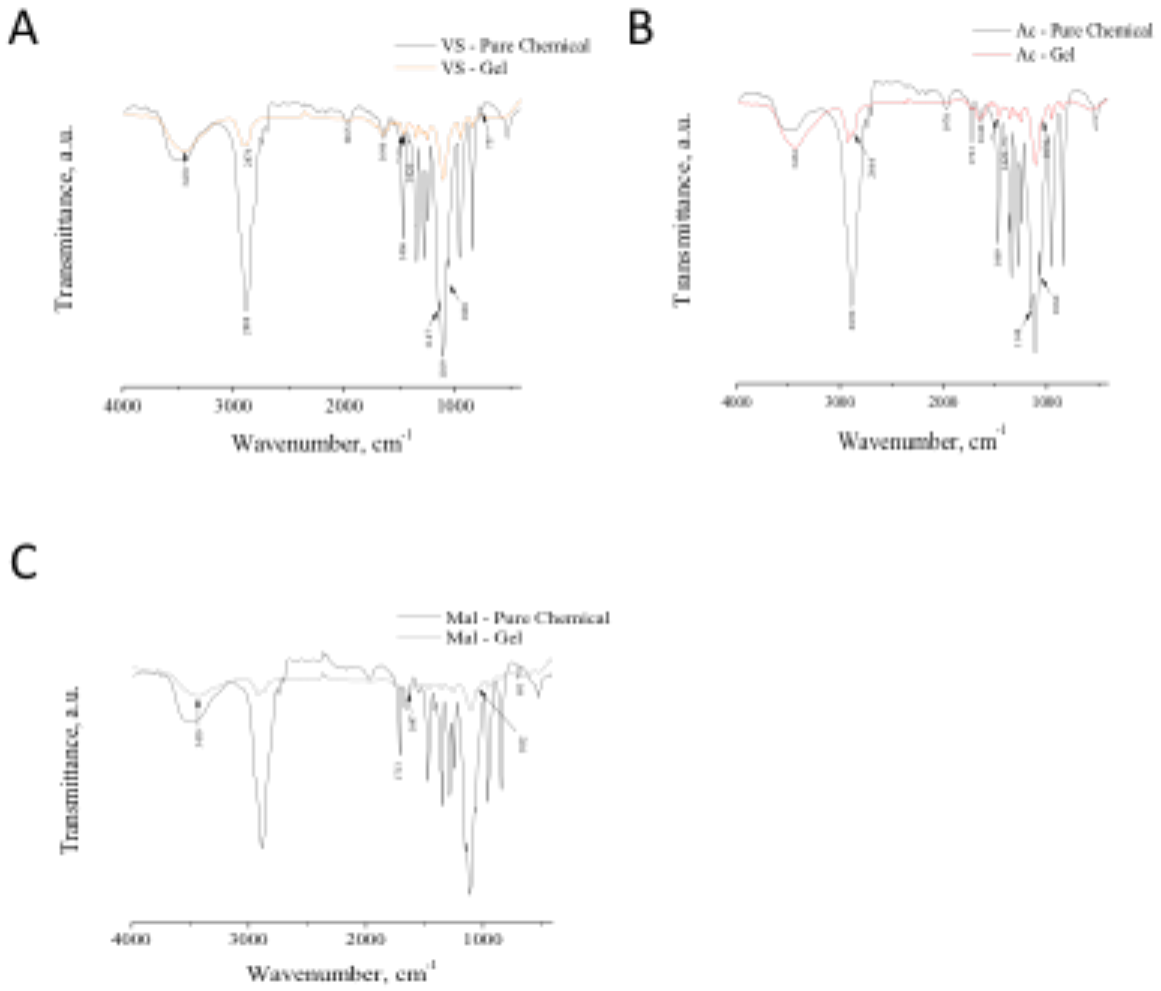

Supplemental Figure 2.2: FT-IR spectra of 8-arm (A) PEG-VS, (B) PEG-Ac, and (C) PEG-Mal before and after polymerization to assess network formation.

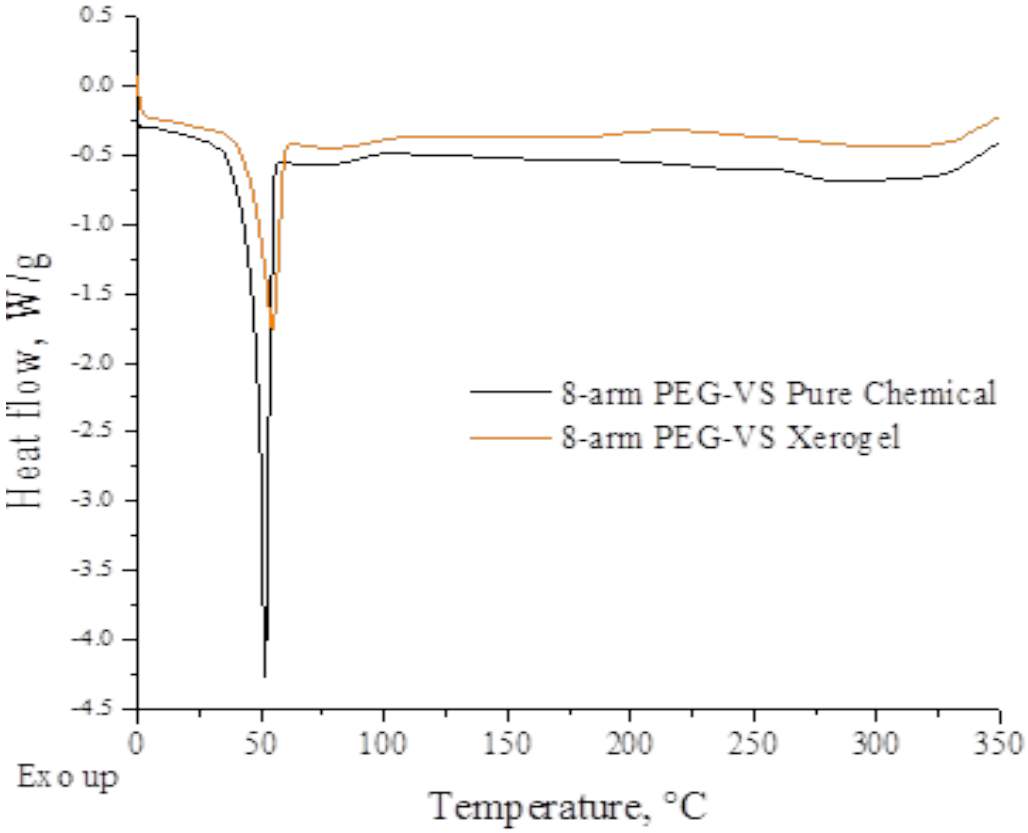

Supplemental Figure 2.3: DSC spectra of 8-arm PEG-VS powder and xerogel.

CHAPTER III

Immuno-isolating poly(ethylene glycol) based capsules support ovarian tissue survival to restore endocrine function

3.1 Authors

James R. Day, Anu David, Alexa L. Cichon, Tanay Kulkarni, Marilia Cascalho, Ariella Shikanov

3.2 Abstract

A common irreversible adverse effect of life-saving anticancer treatments is loss of gonadal endocrine function and fertility, calling for a need to focus on post-treatment quality of life. Here, we investigated the use of poly(ethylene glycol)-vinyl sulfone based capsules to support syngeneic donor ovarian tissue for restoration of endocrine function in mice. We designed a dual immuno-isolating capsule (PEG-Dual) by tuning the physical properties of the PEG hydrogels and combining proteolytically degradable (PEG-PD) and non-degradable (PEG-NPD) layers to meet the numerous requirements for encapsulation and immuno-isolation of ovarian tissue, such as nutrient diffusion and tissue expansion. Tuning the components of the PEG-Dual capsule to have similar physical properties allowed for concentric encapsulation. Upon implantation, the PEG-based capsules supported ovarian tissue survival and led to a significant decrease in FSH levels 60 days post-implantation. Mice that received the implants resumed regular estrous cycle activity and follicle development in the implanted grafts. The PEG-Dual capsule provided an environment conducive for tissue survival, while providing a barrier to the host environment. This study

demonstrated for the first time that immuno-isolating PEG-VS capsules can support ovarian follicular development resulting in the restoration of ovarian endocrine function and can be applied to future allogeneic studies.

3.3 Introduction

Loss of gonadal endocrine function and fertility in cancer patients undergoing chemo- and radiotherapy is a common irreversible consequence of these lifesaving therapies [46,152-156]. With improved survival rates of up to 80%, survivors of childhood cancer are a rapidly growing population, necessitating a shift in focus from simply survival to quality of life post-treatment. Abnormal puberty, osteopenia, muscle wasting, cardiovascular disease, frailty, sterility and risk of premature death all stem from impaired gonadal function[157-160. The restoration of reproductive and endocrine function is uniquely challenging due to the limited and non-renewable ovarian reserve. Cryopreservation of ovarian or testicular tissue obtained prior to exposure to gonadotoxic treatments, with subsequent implantation in survivors can restore both fertility and endocrine function, but the risk of re-introducing malignant cells present in the ovarian tissue limits its translation to the clinic[39,40, 161. To avoid this risk, implantation of the donor ovarian tissue encapsulated in an immuno-isolating capsule has the potential to restore ovarian endocrine function by secreting the gonadal hormones, while eliminating the risk of reseeding cancer cells and the need for immunosuppressant therapy.

Implantation of hormone secreting cells, such as pancreatic islets, in immuno-isolating capsules has been investigated for treating Type I diabetes[50,51,63,64]. For this purpose, hormone secreting cells are encapsulated in a semi-permeable membrane that prevents or attenuates the interaction between the encapsulated allogeneic cells or tissue and the host immune system, while allowing diffusion of nutrients and waste[162]. Ovarian follicles, which are the functional hormone secreting units of the ovary, are similar to islets in that they synthesize and secrete hormones in response to circulating stimuli, in this case follicle stimulating hormone (FSH); however, unlike islets, ovarian follicles are dynamic in growth. At the beginning of each cycle only a small portion of follicles activates and enters the growing pool. The growing follicles

undergo a multiple fold volumetric expansion, which when encapsulated in an immuno-isolating capsule must be accommodated by a degradable matrix that mirrors and allows the follicle expansion. Furthermore, follicles are avascular and relatively resistant to hypoxia, allowing them to survive and function with diffusion through the encapsulating matrix being the only mechanism to supply oxygen and nutrients.

We have reported earlier that hydrogels prepared with poly(ethylene glycol) vinyl sulfone (PEG-VS) and crosslinked with proteolytically sensitive peptides supported follicle development in vitro and in vivo[133,146]. For the purposes of immuno-isolation, we investigated whether the tunable properties of PEG hydrogels and inert non-immunogenic interface with the host[85,106] can match the requirements to allow follicle expansion while preventing infiltration of the cells from the host and immune reaction. We encapsulated syngeneic ovarian tissue in three different PEG-VS constructs: a non-degradable photo-polymerized PEG-VS hydrogel (PEG-NPD), a proteolytically degradable PEG-VS hydrogel (PEG-PD), and a dual PEG-VS hydrogel (PEG-Dual) construct containing a proteolytically degradable PEG-VS core with a non-degradable PEG-VS shell (**Figure 3.1**).

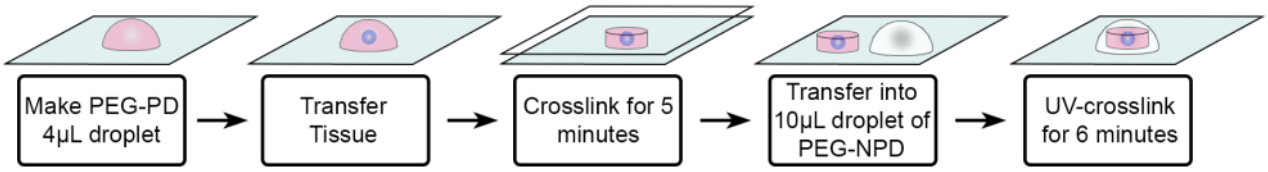

Figure 3.1: Schematic of encapsulating ovarian tissue in Dual PEG.

The objectives of this study were to: 1) answer the question whether the viscoelastic properties of a non-degradable PEG-VS hydrogel are sufficient to allow follicle expansion; 2) create a dual construct with a degradable core and non-degradable shell with controlled physical properties to match follicle expansion; and 3) to identify the PEG-VS-based hydrogel construct that supports ovarian tissue survival and function, leading to ovarian endocrine function restoration.

3.4 Results

3.4.1 Visco-elastic properties of PEG-VS hydrogels

To determine the physical properties of the PEG hydrogels encapsulating the ovarian tissue, we measured the equilibrium mass swelling ratio and storage modulus of 5% PEG-NPD and PEG-PD. We found that PEG-NPD, prepared via free radical photo-polymerization chemistry, and PEG-PD, prepared with thiol-ene Michael type addition chemistry, had comparable swelling ratios (**Figure 3.2A**). The Q_m of PEG-PD hydrogels was 32.2, and the Q_m of PEG-NPD hydrogels was 30.2. Similarly to the swelling ratio, the storage modulus for PEG-PD hydrogels was 2403 Pa and 2876 Pa for PEG-NPD (**Figure 3.2B,C**). Specifically important for the PEG-Dual capsule, similar swelling ratios and visco-elastic properties of the two types of the hydrogels allow concentric encapsulation of the PEG-PD as a core inside a PEG-NPD shell without further modification.

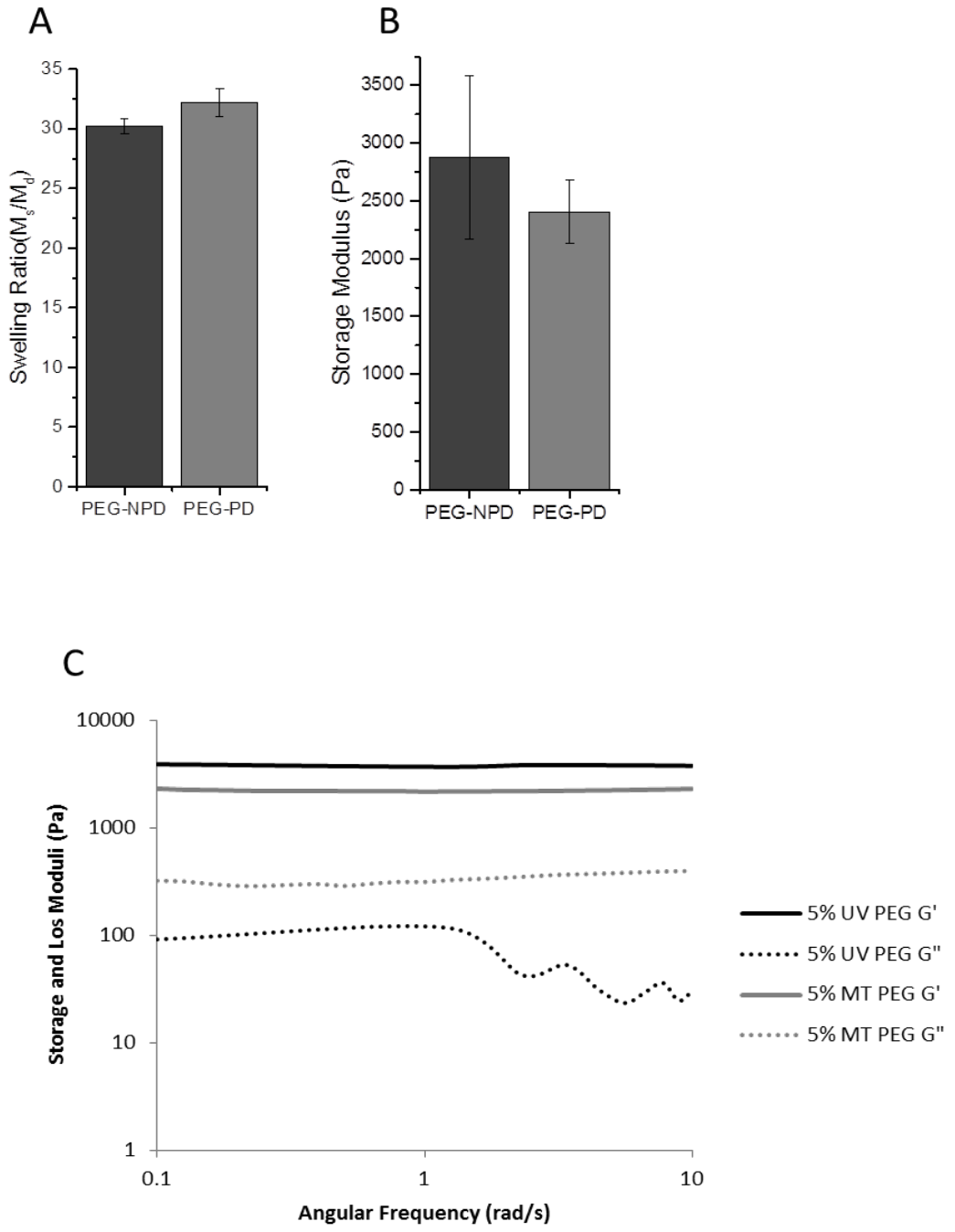

Figure 3.2: Swelling ratio (n=5 for all compositions) and **(B)** storage modulus of 5% PEG-PD (n=3) and PEG-NPD (n=4). **(C)** Illustration of storage modulus and loss modulus of 5% PEG-PD and 5% PEG-NPD. All data reported **A,B** is mean ±SD.

3.4.2 Encapsulation and subcutaneous implantation of ovarian tissue

The ovarian tissue encapsulated in PEG-NPD, PEG-PD, or PEG-Dual hydrogel was completely surrounded in the respective hydrogel network (**Figure 3.3A,D,G**). For the PEG-Dual hydrogel, the ovarian tissue was encapsulated in PEG-PD core, which was surrounded by a PEG-NPD shell (**Figure 3.3G**). At the time of sacrifice, the hydrogels were easily identified and retrieved from the subcutaneous space. No difference in the appearance of the different capsules was noted. Because of the inert and non-fouling properties of PEG hydrogels, we observed minimal interaction with the host tissue at the area around the implanted capsules (**Fig 3.3B,E,H**). At the macroscopic evaluation of the capsules, which were easily removed from the host, the ovarian tissue was visible and fully encapsulated in the center of the capsules. No signs of revascularization or cell infiltration were observed, which was the anticipated result to ensure efficient immuno-isolation (**Figure 3.3C,F,I**).

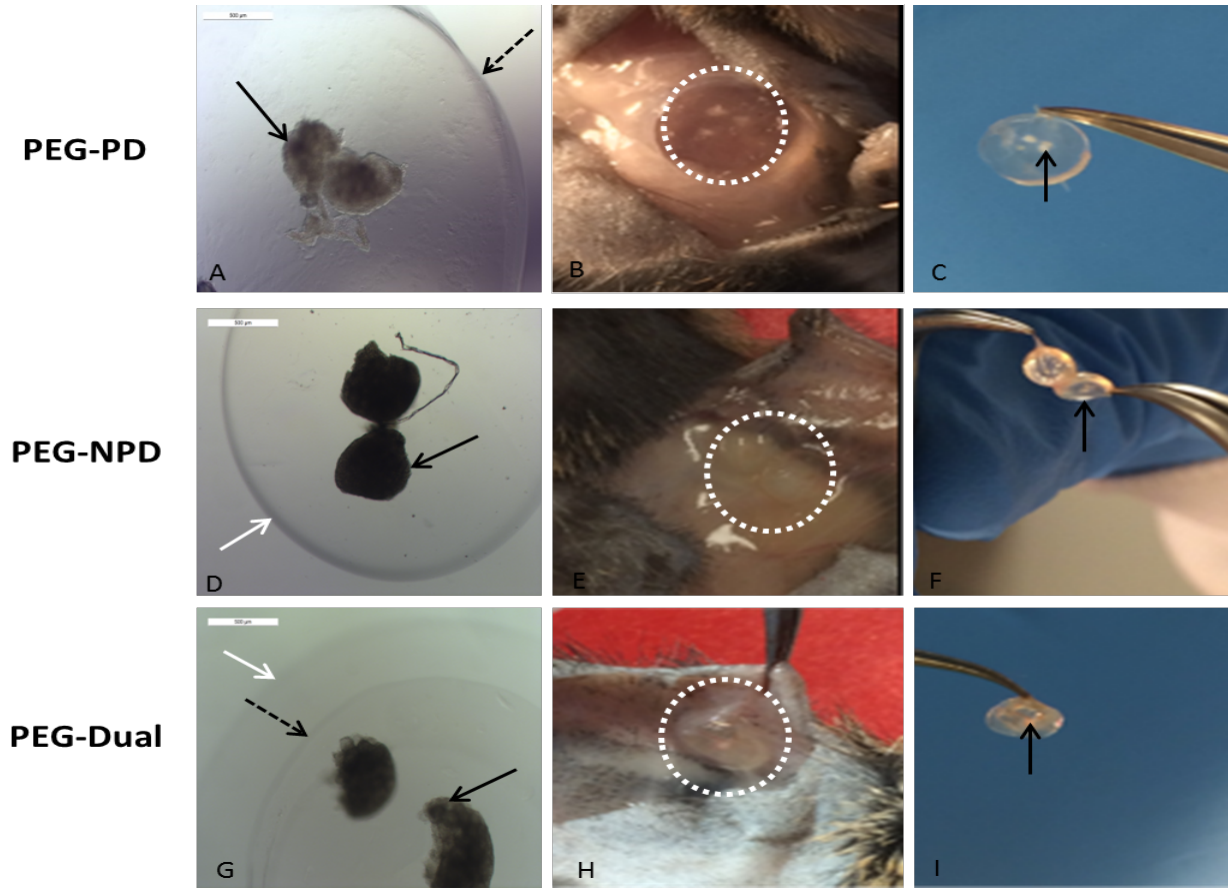

Figure 3.3: Macroscopic images of PEG-VS hydrogels before and after implantation. **(A)** Ovarian tissue encapsulated in PEG-PD, **(B)** PEG-PD at the time of sacrifice, **(C)** PEG-PD after removal, **(D)** Ovarian tissue encapsulated in PEG-NPD, **(E)** PEG-NPD at the time of sacrifice, **(F)** PEG-NPD after removal, **(G)** Ovarian tissue encapsulated in PEG-Dual, **(H)** PEG-Dual at the time of sacrifice, **(I)** PEG-Dual after removal. White dotted circle indicates the localization of the hydrogel on the mice. Solid black arrows indicate encapsulated ovarian tissue. Dashed black arrows indicate the border of PEG-PD and solid white arrows indicate the border of PEG-NPD. Magnification 5X **(A, D, G)**

3.4.3 Follicle development and growth in the immuno-isolation capsules

We performed histological analysis of the retrieved ovarian tissue in immuno-isolating capsules to investigate the growth and development of the follicles, up to 60 days post implantation. After 7 days of implantation in the immuno-isolating capsule small primordial and primary follicles were found in all the capsules (**Figure 3.4A,D,G**). After 30 days of implantation multiple large antral follicles developed in the ovarian tissue implanted in PEG-PD and PEG-Dual, supporting our initial hypothesis that proteolytic degradation was essential to promote follicular growth (**Figure 3.4B,H**). We identified multiple follicles in the PEG-NPD capsule after 30 and 60 days, yet the antral follicles failed to develop an antral cavity, as demonstrated in Figure 3F. Similar to the findings at 30 days post implantation, multiple growing and fully developed antral follicles were observed in the ovarian tissue implanted in PEG-PD and PEG-Dual, but not in PEG-NPD. In agreement with our macroscopic findings, we did not find evidence of blood vessel infiltrating the implanted tissue, which further confirmed the barrier to the host by the gels.

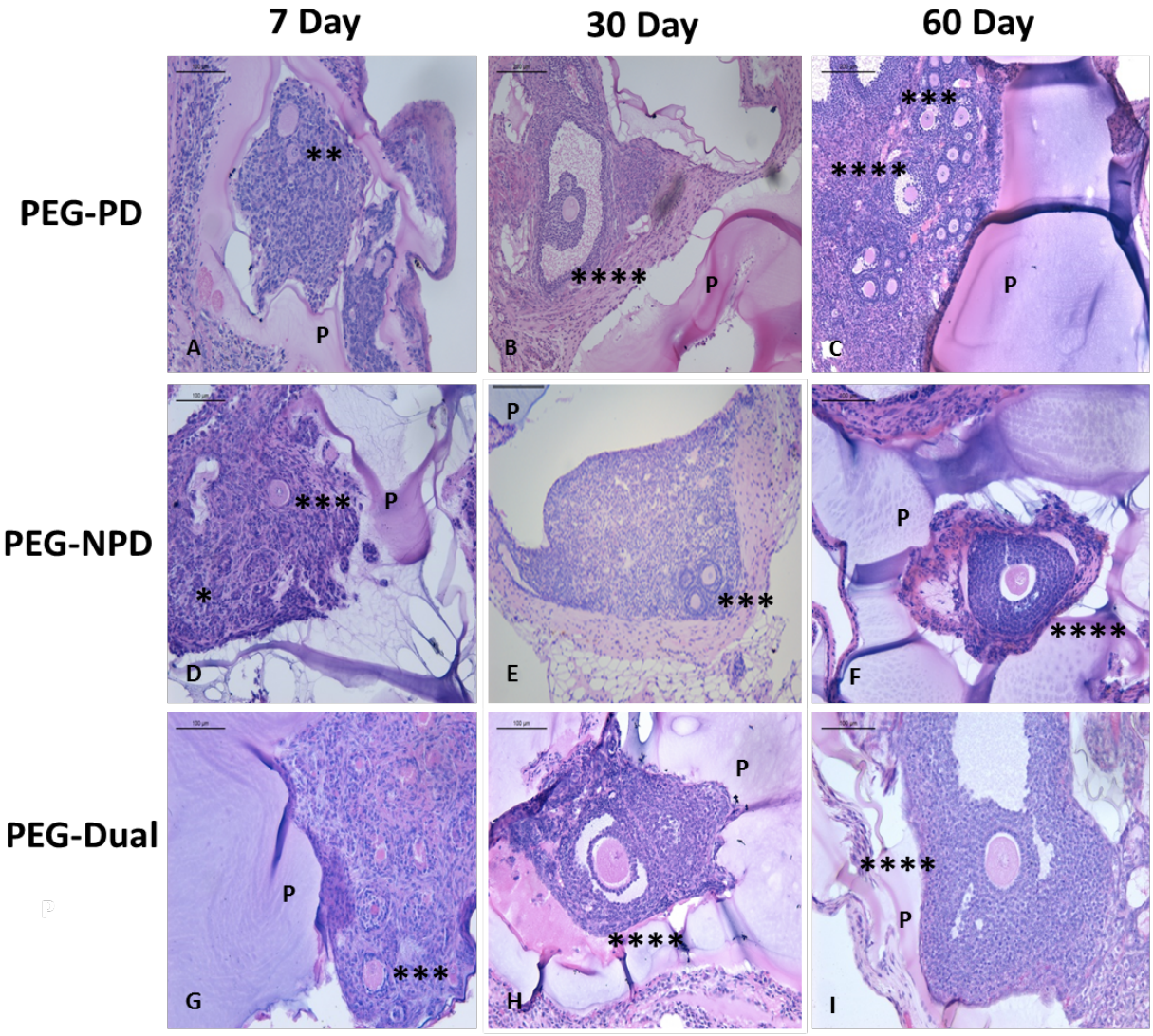

Figure 3.4: Histological image of ovarian tissue encapsulated: in PEG-PD (**A**) showing primordial (*) and primary follicles (**) in 7 day implants (n=3 mice), (**B**), (**C**) showing secondary (***) and antral follicles (****) in 30 (n=4 mice) and 60 day (n=7 mice) implants respectively, PEG-NPD implants showing primordial and secondary follicles (**D, E, F**) after 7 (n=8 mice), 30 (n=4 mice) and 60 (n=6 mice) days respectively and PEG-Dual implants showing secondary (**G**) and antral (**H,I**) follicles in 7 (n=3 mice), 30 (n=4 mice) and 60 (n=11 mice) day implants respectively. (P) indicates the encapsulating PEG hydrogel. “ac” indicates antral cavity. Magnification 10X (**B,C,E**), 20X (**A,D,F,G,H,I**).

3.4.4 Restoration of ovarian endocrine function

In adult mice with healthy functioning ovaries the levels of circulating FSH is below 20 ng/mL. After ovariectomy the lack of negative feedback of estradiol, normally produced in the ovarian follicles, results in increased levels of FSH that can reach 100 ng/mL. Mice in all groups had the average FSH level of 4-8 ng/mL before ovariectomy (n=16 for PEG-NPD, n=11 for PEG-PD, n=18 for PEG-Dual). After a bilateral ovariectomy, FSH levels rose significantly ($p<<0.05$) to an average of 55-71 ng/mL (n=15 for PEG-NPD, n=12 for PEG-PD, and n=16 for PEG-Dual). The rise in FSH levels is the result of low levels of circulating estradiol, confirming that the ovaries were removed and the hypothalamus-pituitary-gonad axis was disrupted. 60 days after mice received ovarian tissue encapsulated in PEG-NPD (n=6), PEG-PD (n=7), or PEG-Dual hydrogel (n=11), FSH levels decreased significantly from an average of 64 ng/mL to an average of 34.8 ($p=0.0004$), 30.5 ($p=0.028$), and 34.3 ng/mL ($p=0.01$), respectively (**Figure 3.5A**), indicating the HPG axis was restored upon implantation in all the groups.

3.4.5 Estrous Cycle Restoration

Estrous cycle correlates with ovulation and lasts 4-5 days in rodents. After ovariectomy the estrous cyclicity ceases, which is determined by the absence of cornified cells in the vaginal secretions. Implantation of ovarian tissue in PEG-PD restored cyclicity in 90% of the mice one week post implantation, and in 100% by the second week (**Figure 3.5B**). Restoration of cyclicity was delayed in mice that received the implants in PEG-NPD and PEG-Dual with 60% of the mice cycling 1 week after implantation, and reaching 100% cyclicity by week 4. However, while 90% of the mice that received ovarian implant in PEG-Dual capsule continued cycling for 9 weeks, only 67% of the mice that received the PEG-NPD capsule continued cycling after 7 weeks, which correlates with the histological analysis and suggests that the follicle growth was restricted in the non-degradable capsules.

A

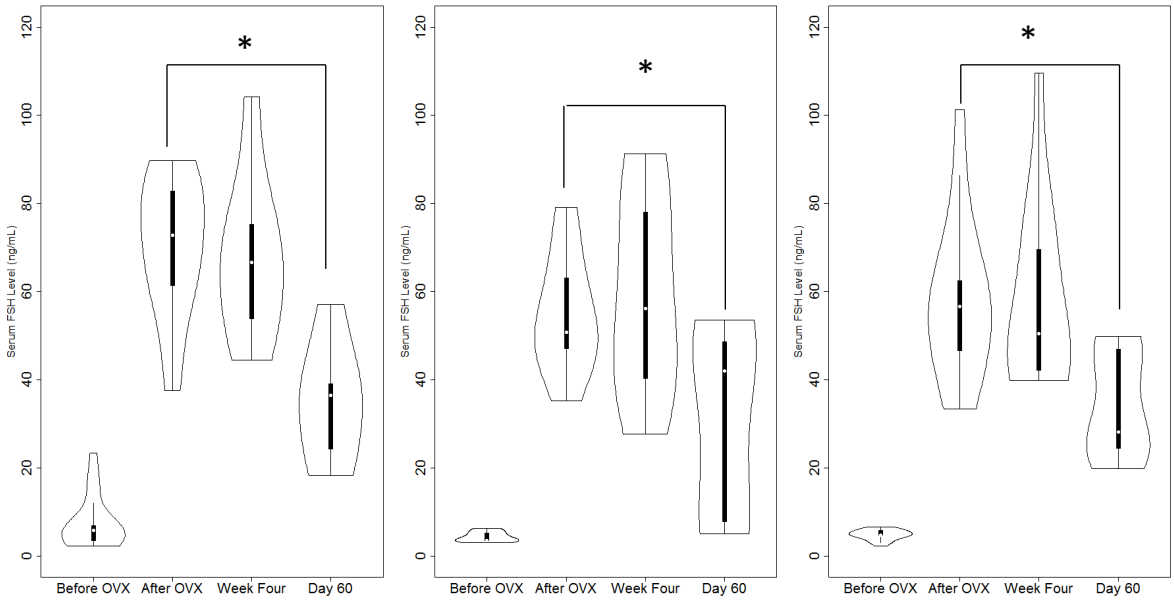

B

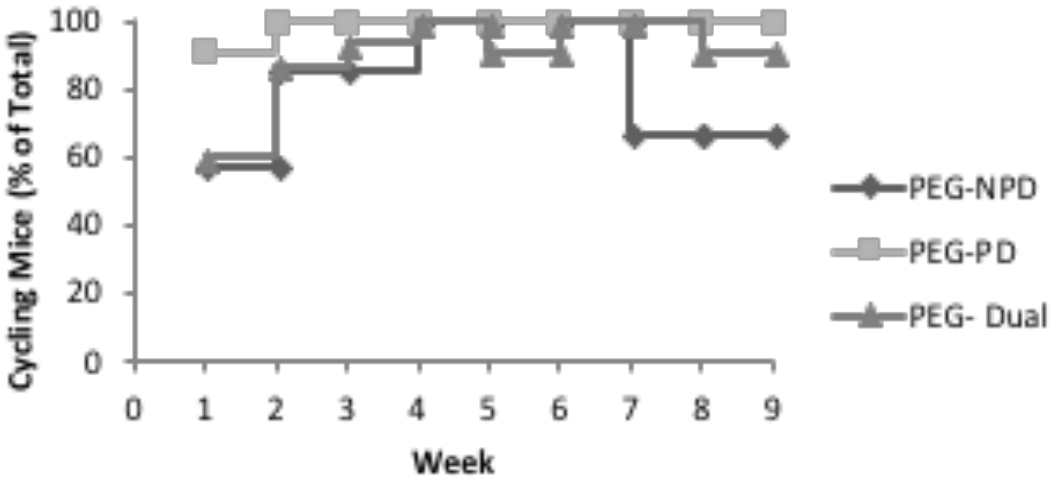

Figure 3.5: A) FSH levels of mice receiving ovarian tissue encapsulated in PEG-NPD, PEG-PD, and PEG-Dual before ovariectomy, after ovariectomy, four weeks post-implantation, and sixty days post-implantation. An asterisk (*) denotes a significant difference ($p<0.05$) between pre-ovariectomy levels and the designated group. Significance was determined by a two-sample T-test. (**B**) Cyclicity observed in mice implanted with D-PEG, ND-PEG and PEG-Dual in the syngeneic model. Presence of a change between leukocytes and cornified cells at least once per week was deemed continuation of estrous cycles.

3.4.6 Collagen Deposition

After implantation for 30 and 60 days, PEG-PD, PEG-NPD, and PEG-Dual exhibited a thin fibrotic capsule around the respective hydrogel (**Figure 3.6A-F**). There was no significant difference in the fibrotic capsule thickness around the immuno-isolating capsules (**Figure 3.6G**). When comparing fibrotic capsule thickness from 30 to 60 days post-implantation, there was no significant difference in collagen deposition ($p<0.05$), indicating the absence of a chronic inflammatory response. Cell infiltration from the host or cell migration from the encapsulated ovarian follicles was not observed in the implants. Interestingly, cells were present throughout the fibrotic capsule around the degradable hydrogel (PEG-PD) (**Figure 3.6A**), but in the case of non-degradable PEG, cells were concentrated in the narrow space between the gel and the fibrotic capsule. This finding may indicate that a degradable gel induced a different reaction with the innate immune cells compared to a non-degradable gel.

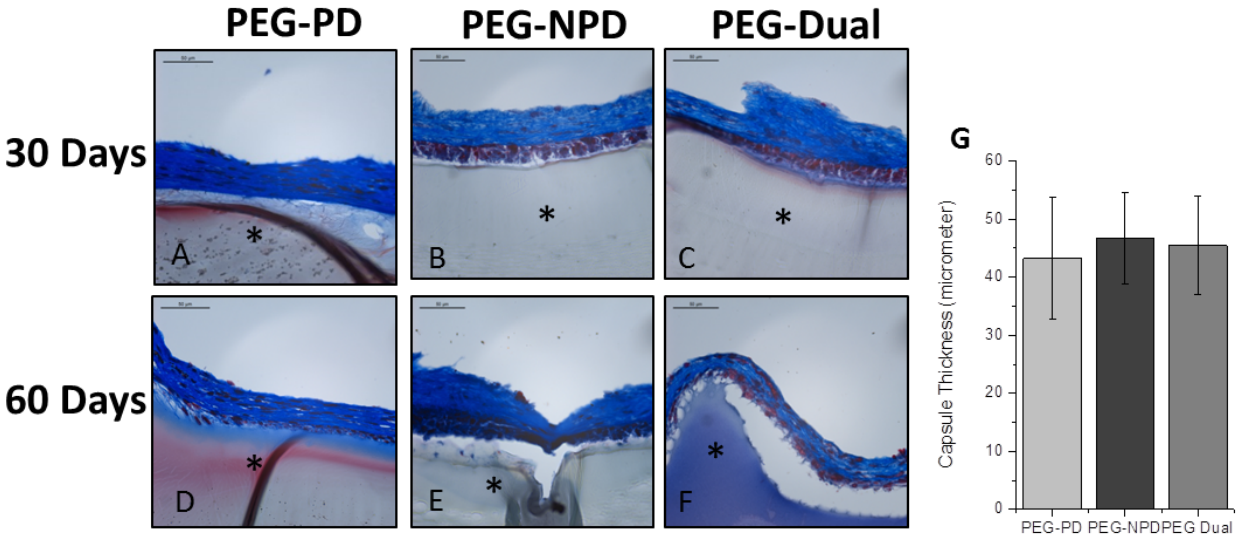

Figure 3.6: Trichrome staining of fibrotic capsule around PEG-NPD, PEG-PD, and PEG-Dual after 30 days (**A, B, C**) and 60 days (**D, E, F**) subcutaneous implantation in mice. An asterisk (*) indicates the PEG hydrogel. Magnification 40X. (**G**) Quantification of fibrotic capsule thickness around immuno-isolating devices after 30 and 60 days using Image J. n=10 for PEG-PD, PEG-NPD, and PEG-Dual.

3.5 Discussion

This study investigated whether the PEG-based immuno-isolating capsules support the viability and function of encapsulated and implanted ovarian tissue for the purpose of restoration of ovarian endocrine function in ovariectomized mice. The results show for the first time the development and characterization of novel photo-polymerized and dual PEG based hydrogel systems. We found that PEG-VS based hydrogels support ovarian tissue and restore endocrine function for at least 60 days. Future allogeneic studies in mice and higher species will confirm whether PEG-PD and PEG-Dual constructs protect the tissue from being recognized and/or destroyed by allo-immunity.

We designed the immuno-isolating capsule by tuning the physical properties of the PEG hydrogels and combining degradable and non-degradable layers to meet the numerous requirements for immuno-isolation of ovarian tissue. For example, the diffusion of nutrients was achieved with low solid concentration and efficient crosslinking density of the network. The non-degradable layer of the PEG hydrogel created a physical barrier between the host and the implant. The proteolytic degradation in response to the cell-secreted proteases from the encapsulated follicles allowed the volumetric expansion of ovarian tissue. Lastly, the intermediate stiffness and inertness of the PEG hydrogel caused minimal inflammatory response at the interface of the capsule and the host.

The strategy of encapsulating the tissue grafts in encapsulating devices allows oxygen and nutrients delivery via diffusion through the hydrogel without the risk of exposure to the immune cells. These properties may be useful to prevent rejection of tissue allografts which inevitably occur when the tissue is directly transplanted. The tunability of PEG hydrogels allows excellent control over pore size of the network formed around the encapsulated tissue. Ovarian tissue encapsulated in PEG-PD, PEG-NPD and the PEG-Dual capsule survived the encapsulation and the implantation for 60 days. The histological sections of the retrieved tissue demonstrated no evidence of necrosis and appeared normal with phenotypically healthy follicles. Further, in the dual capsule we matched the swelling ratio and storage moduli of each layer, which allowed us to co-encapsulate several layers of hydrogels having similar properties. The degradable core

around the encapsulated ovarian tissue surrounded by a non-degradable shell interfacing with the host isolated the tissue from the host environment, while still allowing diffusion and promoting survival of the tissue.

Ovarian follicles exhibit dynamic growth during the hormonal phases, necessitating a need for a material with viscoelastic properties that either degrades in response to follicle secreted proteases or can mechanically withstand the follicle expansion. Our previous study using alginate as an immuno-isolator for ovarian tissue demonstrated that the viscous properties of alginate were insufficient to support the follicle expansion, and either excessively compressed the tissue or failed to maintain the protective layer [144]. Shikanov et al. demonstrated that a proteolytically degradable PEG-VS hydrogel system was conducive for the development of ovarian follicles as they can grow, mature, and respond to circulating gonadotropins in culture [146]. Here, we proposed to encapsulate the ovarian tissue in viscoelastic PEG hydrogel and determine whether the proteolytic degradation of the matrix was essential for ovarian tissue survival and function. When implanted in mice for 7, 30, and 60 days, all PEG constructs supported ovarian tissue survival and secondary and antral follicles were present in the retrieved implants. FSH levels in mice with ovarian tissue encapsulated in PEG-NPD, PEG-PD, and PEG-Dual significantly decreased 60 days post-implantation compared to pre-implantation levels ($p<0.05$), indicating the reversal of the ovariectomized phenotype and restoration of the ovarian endocrine function. The restoration of the estrous cycle and the decrease in FSH levels proved that the tissue encapsulated in the construct responded to the circulating gonadotropins and the encapsulated follicles secreted estradiol creating a negative feedback loop in the HPG axis. The histological evaluation of the encapsulated tissue indicated that PEG-PD was superior in terms of supporting tissue viability and function compared to PEG-NPD. PEG-PD degraded in response to the secreted proteases from cells, providing a supporting network without exerting a compressive force back on the tissue in a way PEG-NPD does. However, PEG-PD cannot solely serve as an efficient immunoisolator and eventually would degrade exposing the tissue to the host immune system. Co-encapsulation of a degradable PEG-PD core in a non-degradable PEG-NPD shell demonstrated successful restoration of ovarian endocrine function similar to PEG-PD alone with the possibility for no risk of rejection. As PEG-PD degrades over time, the outer layer

of PEG-NPD is crucial to protect the implanted tissue for allogeneic implantations. The inclusion of a degradable core provides the biomimetic microenvironment for the encapsulated ovarian tissue while the PEG-NPD outer shell provides protection from the immune cells in the host. In the current study, we demonstrated that the ovarian tissue encapsulated in PEG-Dual hydrogel remains healthy long-term and restoration of endocrine function occurs as indicated by the continuation of the estrous cycle. Corresponding to this observation we observed a significant decrease in FSH levels compared to the pre-implantation levels.

Synthetic biomaterials, such as PEG hydrogels, are an attractive platform for protein and cell delivery because of their low inflammatory index [85,106]. PEG hydrogels are one of the most commonly used synthetic materials for islet immuno-isolation, for example. Multiple reports demonstrated that islets encapsulated in PEG remained viable and maintained normoglycemia[50-52,162]. PEGylated membranes also protected islets from cytokine induced inflammation and destruction in vitro [64]. Similarly, the implanted PEG-based capsules with encapsulated ovarian tissue described here did not cause an excessive inflammatory reaction. Our in vivo studies demonstrated a thin collagen capsule formation, which correlates with a minimal inflammatory response characteristic to the inert properties of PEG hydrogels. Importantly, we did not observe infiltration of cells or blood vessels from the host, which further confirmed the efficiency of the tested hydrogels as establishing a barrier between the tissue and the host environment.

3.6 Materials and Methods

3.6.1 Hydrogel Preparation

To form the PEG-NPD hydrogel network, 4-arm poly (ethylene glycol) vinyl sulfone (PEG-VS, 20kDa, JenKem Technology, Beijing, China) is dissolved in a solution containing sterile D-PBS (pH 7.4) and 0.4 mg/100 µL Irgacure 2959 (Ciba, Switzerland, MW=224.3) to create a concentration of 5% w/v. Irgacure 2959 is the photo-initiator of choice as it has been demonstrated to be

biocompatible across multiple cell lines [130]. Further, N-vinyl-2-pyrrolidone (NVP) (Sigma-Aldrich, St. Louis, USA) is added at a final concentration of 0.1%, as NVP has been demonstrated to enhance gelation without impacting cytocompatibility [140]. To induce cross-linking, the precursor solution is exposed to UV light at a constant intensity (1090 µW/cm2 at a distance of 4 cm).

The PEG-PD hydrogels are formed via Michael-type addition through the inclusion of a plasmin sensitive tri-functional peptide sequence (Ac-GCYK↓NSGCYK↓NSCG, MW 1525.69 g/mol, >90% Purity, CelTek, ↓ indicates the cleavage site). Briefly, to prepare the gels, 8-arm PEG-VS (40kDa, JenKem Technology, Beijing, China) is dissolved in an isotonic HEPES buffer (HEPES 0.05M, pH=7.4) to create a final concentration of 5 or 10% w/v and YKNS was added, such that the molar ratio of –SH and –VS groups was 1:1.

The PEG-Dual hydrogel construct contains a proteolytically degradable core with a non-degradable outer shell. To manufacture the dual PEG hydrogel, a 4 µL degradable core (5% w/v PEG-VS) is formed via the aforementioned technique for the degradable 8-arm PEG-VS hydrogel. Immediately after 5 minutes of gelation, the degradable hydrogel bead is transferred over and placed in the center of a 10 µL bead of the non-degradable precursor solution. The PEG-Dual construct is then exposed to a constant intensity (1090 µW/cm^2 at a distance of 4 cm) for 6 minutes creating the non-degradable outer shell of the hydrogel (**Figure 3.1**).

3.6.2 Swelling Ratio

5% w/v PEG-NPD and PEG-PD hydrogels were tested. The PEG-NPD gels were exposed to UV light for 6 minutes and were submerged in DPBS for 24 hours. Similarly, the PEG-PD gels formed for 5 minutes after the introduction of YKNS; thereafter the reaction was quenched by submerging the gels in DPBS and remained there for 24 hours. After 24 hours, excess DPBS was removed and the swollen mass of the hydrogels was obtained. Gels were then removed from solution and allowed to dry at room temperature. Larger volumes were used to minimize error from weighing. The mass swelling ratio (Q_m) was determined by dividing the mass of the swollen gels (M_s) by the mass of the dry gels (M_d) [120].

3.6.3 Rheology

The storage modulus (G') and loss modulus (G") was investigated for two PEG constructs—5% PEG-NPD and 5% PEG-PD. The gels were prepared and swollen in DPBS overnight. A TA HR-2 rheometer (TA Instruments, USA) equipped with 20 mm parallel plates and a Peltier stage was used for this purpose. To ensure the hydrogel was the same size as the geometry, 1 mm thick hydrogel slabs were made and a 20mm diameter disc was punched out. A constant strain rate of 5% was kept for all samples and the storage modulus was obtained by performing an angular frequency sweep from 0.1 to 10 rad/s.

3.6.4 Ovariectomies in recipient mice

Before any surgical procedure, preemptive analgesics were administered. To induce infertility, bilateral ovariectomies were performed on 12-16 week old adult female mice (B6CBAF1). All procedures (PRO00005750) followed the IACUC guidelines for survival surgery in rodents and the IACUC Policy on Analgesic Use in Animals Undergoing Surgery. Briefly, the female was anesthetized by isoflurane, Carprofen (Rimadyl, Zoetis, USA) was administered, and a midline incision was made in the abdominal wall. Using an abdomen retractor, the intraperitoneal space was exposed, and the ovaries were removed, leaving the remainder of the reproductive tract. The muscle and skin layer of the abdominal wall were closed with 5/0 absorbable sutures (AD Surgical, USA). The animal recovered in a clean warmed cage. Post-surgery, animals received analgesia for at least 24 hours or as needed.

3.6.5 Ovarian tissue encapsulation in PEG hydrogels

Ovaries were collected from 6-8 days old B6CBAF1 female pups. These pups are genetically matched to the receiving host. The collected ovaries were transferred to Leibovitz L-15 media (Sigma-Aldrich, USA) and dissected into 2 pieces. The ovarian tissue pieces were then transferred into maintenance media (α-MEM) and placed into incubator set to 5% CO_2. For encapsulation in PEG-NPD, the ovarian tissue was transferred into a 10uL droplet of the precursor solution (5% w/v PEG-VS, .4% Irgacure 2959, .1% NVP) and exposed to UV light. For encapsulation in the PEG-PD, the ovarian tissue was transferred into a 10 µL droplet of the plasmin sensitive tri-functional

peptide and PEG-VS precursors' solution. The droplet was allowed to crosslink for 5 minutes and then was quenched in maintenance media. For the PEG-Dual hydrogel encapsulation, the tissue was first encapsulated in a 4 µL PEG-PD gel and was then placed in the center of a 10 µL bead of PEG-NPD and exposed to UV light. All constructs were imaged immediately after encapsulation of the tissue.

3.6.6 Implantation of immuno-isolating capsules in mice

To investigate the survival and function of the ovarian tissue encapsulated in immuno-isolation capsules we implanted subcutaneously immuno-isolating capsules in the ovariectomized mice. Briefly, a small incision was made on the dorsal side of the anesthetized mice and two constructs (PEG-NPD, PEG-PD, or PEG-Dual) with encapsulated ovarian tissue were implanted subcutaneously and the skin was closed using 5/0 absorbable sutures. The mice received analgesia for at least 24 hours after surgery or as needed. Mice were euthanized at pre-determined end time points (7, 30, and 60 days post-operation).

3.6.7 Serum Hormone analysis

Blood was collected from the lateral tail vein at designated time points with a 5 **3/4"** glass Pasteur pipette up to the time of sacrifice. After collection, all samples were stored at 4°C overnight, then centrifuged for 10 minutes at 10,000 rpm and the collected serum was stored at -20°C. The samples were analyzed for mouse FSH using a radio-immunoassay (Ligand Assay and Analysis Core Facility, University of Virginia Center for Research in Reproduction). The core at the University of Virginia used mouse FSH reference preparation AFP5308D for assay standards and mouse FSH antiserum (guinea pig; AFP-1760191) diluted to a final concentration of 1:400,000 as primary antibody. The secondary antibody is from Equitech-Bio, Inc. and was diluted to a final concentration of 1:25. The radio-immunoassay has a sensitivity of 2.0 ng/ml and less than 0.5% cross-reactivity with other pituitary hormones. When needed, the samples were diluted 5-10 fold.

3.6.8 Evaluation of the regularity of estrous cycle

To assess estrous cycle cessation, vaginal cytology was performed seven days after ovariectomy. After transplantation, vaginal cytology was resumed seven days post-operation and was performed daily until sacrifice. The transition from leukocytes to cornified cells at least once a week was counted as a resumed or continued cycle.

3.6.9 Histological analysis of the retrieved capsules and the encapsulated tissue

Immediately after retrieval of the immunoisolating capsules from mice, the capsules were fixed in Bouin's fixative at 4°C overnight and transferred and stored in 70% ethanol at 4°C. Constructs encapsulating ovarian tissue were then processed, embedded in paraffin, serially sectioned at a 5 µm thickness, and stained with hematoxylin and eosin. To determine the stage of follicular development, follicles were classified as follows: follicles with one layer of squamous granulosa cells around the oocyte were classified as primordial follicles, a single layer of cuboidal granulosa cells - primary follicles, two or more layers of granulosa cells - a secondary follicle, and follicles with an antral cavity were classified as antral follicles.

3.6.10 Trichrome Staining

After retrieval of the PEG constructs from the mice, the capsules were fixed in Bouin's fixative at 4°C overnight and transferred and stored in 70% ethanol at 4°C. Hydrogels were then processed, embedded in paraffin, serially sectioned at a 5 µm thickness, and stained with Masson's Trichome 2000 Stain Kit (American Mastertech, Inc., USA.). Capsule thickness was quantified via Image J software.

3.6.11 Statistics

Statistical analysis was performed using the R software. Two-sample t-tests were used to evaluate changes in hormone levels and differences in swelling ratio and storage modulus between PEG constructs. The results were considered statistically significant when $p < .05$.

CHAPTER IV

Encapsulation of ovarian allograft precludes immune rejection and promotes restoration of endocrine function in immune-competent ovariectomized mice

4.1 Authors

James Ronald Day, Anu David, Mayara Garcia de Mattos Barbosa, Margaret Ann Hammersley, Marilia Cascalho, Ariella Shikanov

4.2 Abstract

Premature ovarian insufficiency (POI) is a significant complication of cytotoxic treatments due to extreme ovarian sensitivity to chemotherapy and radiation. POI is particularly devastating for young girls reaching puberty, because it irreversibly affects their physical and cognitive development. Changes occurring during puberty determine their height, bone health, insulin responsiveness, lipid metabolism, cardiovascular health and cognition. The only available treatment for POI during puberty is hormone replacement therapy (HRT), which delivers non-physiological levels of estrogen, lacks other ovarian hormones and pulsatility, and is not responsive to feedback regulation. Here we report that ovarian allografts encapsulated in a hydrogel-based capsule and implanted in ovariectomized mice restore ovarian endocrine

function in immune competent mice. Ovarian tissue from BALB/c mice was encapsulated in poly(ethylene-glycol) (PEG) hydrogels, with a proteolytically degradable core and a non-degradable shell. The dual capsules were implanted subcutaneously in immune competent ovariectomized C57BL/6 mice for a period of 60 days. Non-encapsulated ovarian allografts implanted in a control group sensitized the recipients as confirmed with donor-specific IgG in the serum, which increased 26-fold in the 3 weeks following transplantation ($p=0.02$) and infiltration of the graft with CD8 T cells consistent with allo-immunity. In contrast, encapsulation in the Dual PEG capsules prevented sensitization to the allograft in all the recipients with no evidence of lymphocytic infiltration. In summary, the approach of hydrogel-based immuno-isolation presents a minimally invasive and a robust cell-therapy to restore hormonal balance in ovarian insufficiency. This report is the first to demonstrate the application of a tunable PEG-based hydrogel as an immuno-isolator of allogeneic ovarian tissue to restore endocrine function in ovariectomized mice and prevent cell-mediated immune rejection in immune competent mice.

4.3 Introduction

Childhood cancer survival rates have significantly increased reaching over 80% in 2017 due to improved cancer therapies; however, the same life-saving anticancer treatments have led to profound health complications in the young survivors [8, 46,47 163-165. One of the most significant side effects of the anticancer therapy is ovarian toxicity, leading to impaired gonadal function and premature ovarian insufficiency (POI) [19,166]. POI is particularly devastating for young girls reaching puberty, because it irreversibly affects their physical and cognitive development. Changes occurring during puberty promote the physical and psychologic

development into adulthood determining height, bone health, insulin responsiveness, lipid metabolism, cardiovascular health and cognition[9-11]. These changes are initiated before puberty and orchestrated by the pulsatile secretion of gonadotropin releasing hormone (GnRH) and growth hormone (GH) from the hypothalamus, which in turn regulate the release of gonadotropins, luteinizing (LH) and follicle-stimulating (FSH) hormones from the pituitary. FSH and LH stimulate the ovaries to produce estradiol, androstenedione, progesterone, inhibins A and B, activin and follistatin which have systemic effects in many organs and tissues including endocrine glands and the regulation of reproductive functions.

Hormones secreted from the ovary create a negative feedback loop by inhibiting the production of GnRH and FSH in the brain, resulting in dynamic oscillating levels of circulating hormones and gonadotropins [12-14]. The pulsatility and the circadian rhythm of the hypothalamic-pituitary-gonadal (HPG) axis are crucial for the development and regulation of a multitude of systems including the reproductive, fat, musculoskeletal, cardiovascular, and immune systems [15,16] (**Figure 1.1**). Deficiency of gonadal hormones, as occurs in POI, leads to irreversible imbalance in bone development and metabolic abnormalities. Thus, POI inhibits normal puberty causing stunted bone growth, abnormal fat distribution and deposition and metabolic changes [19-21].

The only available treatment to initiate puberty in girls with POI is hormone replacement therapy (HRT). HRT was originally designed to treat postmenopausal symptoms in women and long-term safety data in children are scant [44]. For puberty induction HRT is usually initiated with low levels of estrogen, followed by increasing doses of estrogen and progesterone combination as a life-long treatment, until menopause [167]. Unfortunately, HRT delivers only a fraction of ovarian hormones, e.g. estrogen and progesterone, at higher doses and at a constant and non-pulsatile

rate, which is inadequate to reproduce physiological puberty [45]. Achieving an optimal pharmaceutical delivery of all the ovarian hormones is challenging due to the complexity of the regulation of the HPG axis. As a result, HRT-mediated puberty in girls with POI results in premature closure of the bone growth plate, cessation of bone growth and long-term metabolic imbalances [44,46-48].

On the other hand, cryopreservation of ovarian tissue prior to gonadotoxic treatments followed by auto-transplantation is a promising novel experimental approach, which restores fertility and ovarian endocrine function. This practice has already resulted in more than 70 babies born to identical twin sisters and cancer survivors who cryopreserved their ovaries [31-36]. However, in patients with hematological malignancies, this procedure cannot be performed because of the risk of introducing malignant cells present in the ovarian tissue, nor would it be helpful for patients who did not cryopreserve their tissue before the anti-cancer treatments, which by far is the most common case [39,40].

To mitigate the limitations of HRT and to avoid the risk of cancer recurrence associated with auto-transplantation of ovarian tissue from subjects with hematologic cancers, we have developed a novel strategy to restore ovarian endocrine function. In this study we investigated whether a synthetic viscoelastic poly(ethylene glycol vinyl sulfone) (PEG-VS) hydrogel sustains survival and function of allogeneic ovarian tissue while preventing rejection. The capsule provides a supportive environment for the encapsulated and implanted tissue, allows diffusion of oxygen and nutrients, and physically prevents cell migration. Our earlier studies demonstrated that ovarian follicles encapsulated in proteolytically degradable PEG-VS hydrogels developed to the antral stages *in vitro* [146] and *in vivo* [168]. By keeping the follicular structure intact we

attempted to mimic the physiological interactions between the follicular cells and to maintain the follicle symphony [169-171]. Additionally, non-degradable PEG-VS matrices conducive for tissue encapsulation evoked minimal inflammatory response after implantation in a syngeneic mouse model [172-173]. The objective of this study was to investigate whether PEG-VS-based capsules support the survival and function of ovarian allografts and protect them from rejection, in absence of immune-suppression, in immune competent mice with POI.

4.4 Results

4.4.1 Macroscopic Evaluation of the Ovarian Implants

To determine physical integrity, all the encapsulating devices were macroscopically inspected at the time of retrieval after 60-day implantation period. The PEG-VS hydrogel-based capsules were easily identified and removed from the subcutaneous space. The ovarian tissue was visible at the center of the hydrogels. The PEG-based hydrogel capsules with ovarian allografts demonstrated minimal interaction with the host tissues at the implantation site (**Figures 4.1C, D, G, and H**). Similar to our findings from the syngeneic implantation[44], macroscopically the capsules appeared intact and transparent, with no or minimal tissue attached and with no visible blood vessels or capillaries growing around or in the capsule.

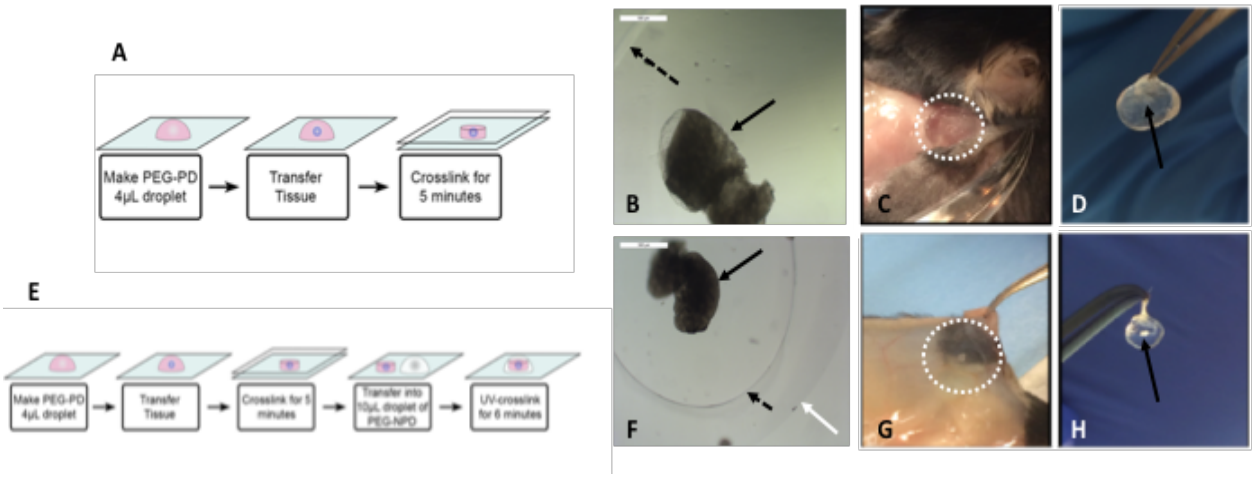

Figure 4.1: A) Schematic of ovarian tissue encapsulation in PEG-PD. (**B**) Ovarian tissue encapsulated in PEG-PD before implantation, (**C**) at time of sacrifice, and (**D**) after removal. (**E**) Schematic of ovarian tissue encapsulation in Dual PEG. (**F**) Ovarian tissue encapsulated in Dual PEG before implantation, (**G**) at time of sacrifice, and (**H**) after removal. Black arrow indicates ovarian tissue, dotted black arrow points to PEG-PD core, white arrow points to the non-degradable PEG-based shell of the Dual PEG, and white dotted circle in **C** and **G** indicates area of gel. Drawings used to depict the encapsulation process were created using Adobe Illustrator (23.0.3 2019).

In contrast, the TheraCyte device, although intact, was firmly embedded in the subcutaneous space of the host. Multiple visible blood vessels surrounded the TheraCyte capsule. These findings are consistent with known properties of the PTFE surface promoting protein adsorption, interactions with cells and inflammatory changes in the surrounding tissues [101]. Ovarian allografts implanted without a device lasted less than 3 weeks after implantation and were completely destroyed leaving only intense vascularization due perhaps to immunity and inflammation (**Supplemental Figure 4.1**).

4.4.2 Restoration of Ovarian Endocrine function

We evaluated restoration of ovarian endocrine function by measuring the regularity of estrous cycles and circulating levels of FSH. In mice of reproductive age (starting at 4 weeks old) regular estrous cyclicity corresponds with normal ovarian function and ovulation. Each estrous cycle lasts 4-5 days and is easily identified by the type of cells present in the vaginal cytology sample. The estrous cycle corresponds to four stages: metestrus, estrus, proestrus and diestrus. After bilateral ovariectomy mice experience persistent diestrus and consistent with absence of ovarian function we found no cornified cells in the samples of vaginal cytology for a 2-week period.

After implantation of allogeneic ovarian tissue encapsulated in PEG-PD, TheraCyte, and Dual PEG mice demonstrated an average of 8, 11, and 12 cycles, respectively, over the 60-day implantation period (**Figure 4.2**). All the mice (n=9/9) implanted with non-encapsulated ovarian allograft (control group), resumed cyclicity one week after implantation. However, four weeks after the implantation all the control mice stopped cycling and returned to the continuous diestrus phenotype characteristic of POI, averaging at 5.75 cycles over a 60-day implantation period (**Figures 4.2A and B**). In the PEG-PD group 90% of mice resumed cyclicity in the first week, however the rate of cyclicity continuously decreased and at the end of the experiment (60 days), only 50% of the mice were still cycling. Implantation of ovarian allograft encapsulated in TheraCyte restored cyclicity in 80% of the mice by the first week of implantation. The percentage of cycling mice steadily increased and and reached 100% after 4 weeks and remained steady up to day 60. Mice that received ovarian allograft encapsulated in Dual PEG experienced a delay in resumption of cyclicity compared to other mice, with only 50% of the mice cycling in the first week of implantation, 80% by the second and 100% by week 4. By the end of the implantation period, 80% of the mice receiving the Dual PEG implants were still cycling (**Figures 4.2B, C, D, and**

E). Mice receiving allogeneic tissue encapsulated in Dual PEG exhibited the highest degree of estrous cycle resumption indicated by an average of 12 cycles over the 60 day implantation period (**Figure 4.2A**), which is the expected amount of cycles for a non-menopausal mouse over that time span given the observed delay to resume estrous activity.

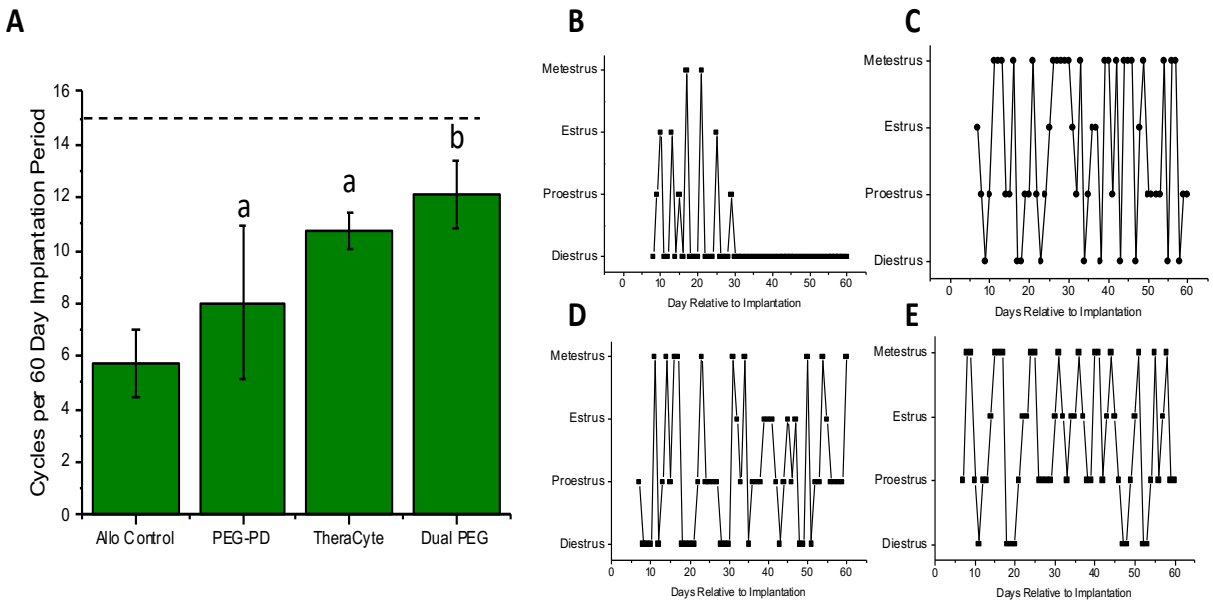

Figure 4.2: Restoration of estrous cycle in mice receiving encapsulated ovarian tissue. (**A**) Average number of cycles over the 60-day implantation period in mice receiving encapsulated ovarian tissue in PEG-PD, TheraCyte, and Dual PEG. Dashed line indicates the expected average number of cycles over 60 days, and "a" and "b" indicate significant differences, $p<0.05$. Representative cycles of mice receiving (**B**) non-encapsulated ovarian tissue, (**C**) ovarian tissue encapsulated in PEG-PD, (**D**) ovarian tissue encapsulated in TheraCyte, and (**E**) ovarian tissue encapsulated in Dual PEG.

Circulating FSH and estradiol levels in healthy mice are inversely proportional and fluctuate during the estrous cycle because estradiol inhibits the production and secretion of FSH via negative feedback loop. Circulating FSH levels, serve as reliable surrogates for ovarian endocrine

function. Before ovariectomies, mice in all the groups had an average FSH level of 9 ng/mL (n=9 for the controls, n=10 for the TheraCyte, n=10 for the PEG-PD and n=10 for Dual PEG). Following ovariectomies, FSH levels rose significantly to an average of 53 ng/mL, confirming the disruption of the HPG axis in all these mice (**Figure 4.3**). In the control group, where mice received the non-encapsulated allogeneic ovarian tissue, FSH levels remained elevated during the 60-day implantation period, confirming insufficient production and secretion of ovarian hormones (**Figure 4.3B**). In the PEG-PD group, five out of ten mice exhibited a significant decrease of FSH levels from 53 ng/mL to 23 ng/mL (p=0.003) by day 60 and were deemed the "functional group" (**Figures 4.3A and D**). The remaining five mice had an average FSH level of 56 ng/mL at day 60 similar to the levels before implantation (54 ng/mL) indicating absence of ovarian endocrine function, e.g. the "non-functional group" (**Figures 4.3A and E**). In the TheraCyte implant group, seven out of ten mice were "functional" and had an average FSH level of 34 ng/mL after implantation compared to 50 ng/mL before implantation, (p=0.02) (**Figures 4.3A and H**). In three mice with TheraCyte implants, however, FSH levels did not decrease and reached an average of 63 ng/mL at 60 days indicating tissue failure. (**Figures 4.3A and I**). The Dual PEG group had the greatest number of mice demonstrating estrous cyclicity and decreased levels of FSH. Based on estrous activity, the encapsulated tissue in Dual PEG was functional in eight of ten mice after 60 days of implantation. In these eight mice, we observed a significant decrease of FSH levels from 48 ng/mL to 28 ng/mL (p=0.002) (**Figures 4.3A and L**). The remaining two mice with the Dual PEG implants that stopped cycling by day-60 had an average FSH level of 68 ng/mL at day 60 indicating tissue failure (**Figures 4.3A and M**).

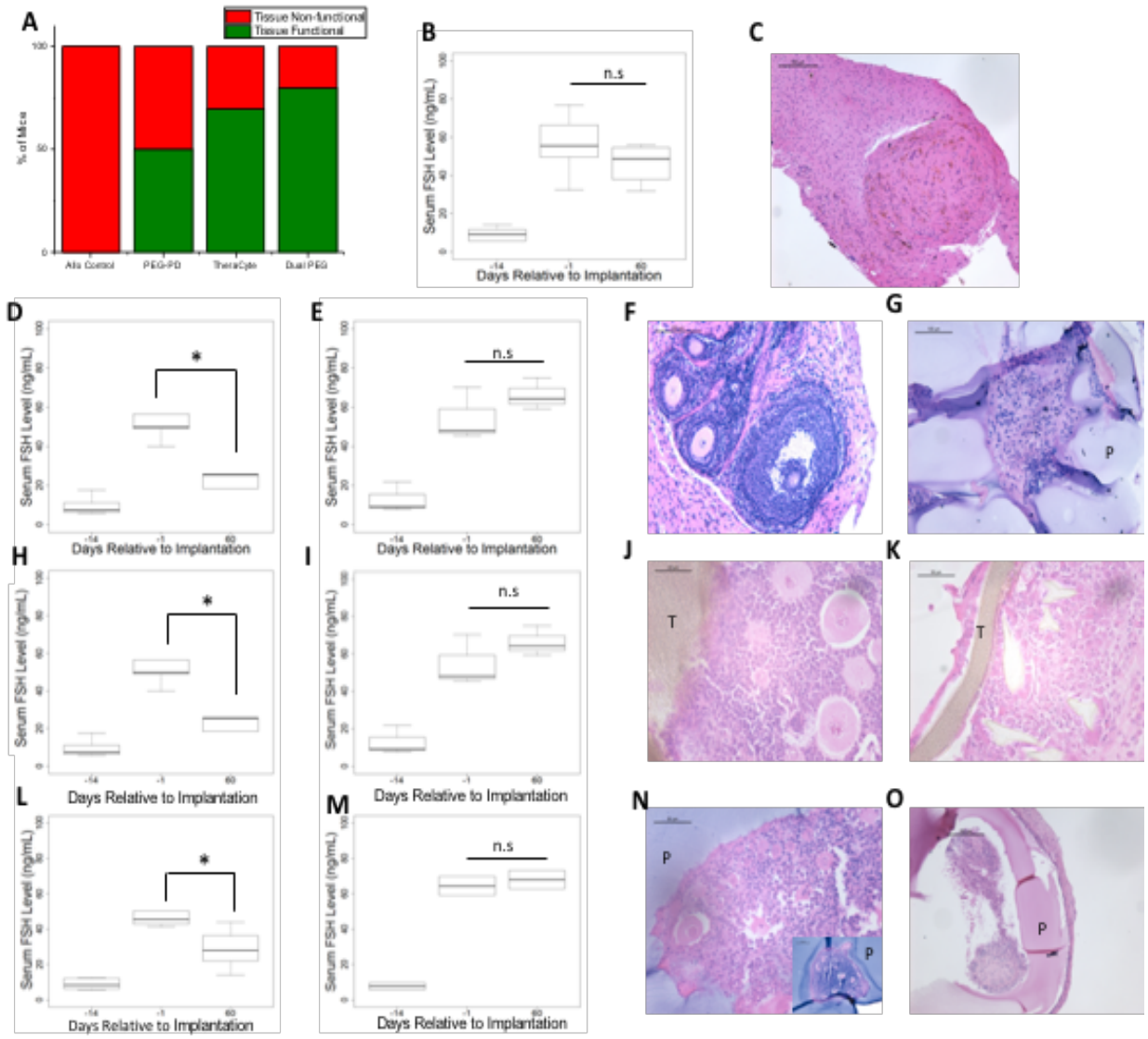

Figure 4.3: Percentage of non-encapsulated ovarian tissue and encapsulated ovarian tissue in PEG-PD, TheraCyte, and Dual PEG that remained functional throughout the time course of the implantation or became non-functional. Consistent estrous cyclicity and decrease in circulating FSH levels qualified as "functional grafts", while absence of cycles and/or FSH levels similar to levels in ovariectomized deemed as "non-functional". (**B**) FSH levels of mice receiving non-encapsulated allogeneic ovarian tissue. (**C**) Histological image of non-encapsulated allogeneic ovarian tissue after 28 days post implantation. Serum FSH levels of (**D, H, L**) encapsulated ovarian tissue that remained functional or (**E, I, M**) became non-functional during the time course of the implantation in PEG-PD, TheraCyte, and Dual PEG, respectively. * indicates statistical significance, $p<0.05$, and n.s. represents not significant. Histological images of “functional” (**F,J, N**) or (**G, K, O**) “non-functional” encapsulated ovarian allografts in PEG-PD, TheraCyte, and Dual PEG,

respectively, and retrieved 60 days after implantation. '-14' corresponds to one day before ovariectomy and 2 weeks prior to implantation. '-1' corresponds to two weeks after ovariectomy and 1 day prior to implantation. (**N inset**) Ovarian allografts containing healthy ovarian follicles were completely encapsulated in PEG through 60 days implantation. (P) indicates PEG, and (T) represents TheraCyte. Scale bars: 500µm(F), 200µm (**C, O**), 100µm (**G, N inset**), 50µm (**J,K, N**).

To evaluate the follicular development of the implanted ovarian tissue we analyzed tissue sections explanted at 60 days after implantation by histological analysis. In controls transplanted with non-encapsulated ovarian allografts we observed no ovarian follicles at the site of implantation, consistent with graft rejection (**Figure 4.3C**). In contrast, we observed all stages of ovarian follicle development (*up to the antral stage*) in sections obtained from the functional PEG-PD, TheraCyte and Dual PEG encapsulated allografts (**Figures 4.3F, J, and N**) indicating that those devices support follicle development. Multiple antral follicles were not observed in any of the groups. As expected, there were no structurally healthy-looking ovarian follicles in sections from non-functional PEG-PD, TheraCyte and Dual PEG implants (**Figures 4.3G, K, and O**).

4.4.3 Ovarian Allograft Immunity

Efficacy of encapsulation to sustain ovarian allograft function depends on preventing host sensitization and/or destruction by allo-immunity effectors. Allo-specific immunity is manifested by the production of specific-antibodies and by infiltration of grafts by lymphocytes. To determine if encapsulated ovarian allografts evoked immunity we measured circulating allo-specific IgM and IgG by flow cytometry. Figures 4.4A and 4.4B demonstrate that donor-specific IgG increased 26 fold in the 3 weeks following transplantation ($p=0.02$) of non-encapsulated

ovarian allografts. As hypothesized, all of the ovarian allografts evoked allo-specific immunity (n=9/9) (**Figures 4.4A and B**). Immuno-pathology examination of the grafts revealed infiltration with CD8 T cells consistent with allo-immunity **(Figure 4.4C)**. In contrast, encapsulation of the ovarian tissue in Dual PEG hydrogels blocked sensitization in all the recipient mice. None of the mice receiving ovarian allograft encapsulated in Dual PEG devices (n=10/10 immunoisolating) produced allo-specific IgG up to 60 days after transplantation, at explant(**Figures 4.4D and E**). Consistent with the absence of allo-immunity, immunopathology analysis of the ovarian allografts encapsulated in the Dual PEG device showed no evidence of lymphocytic infiltration. (**Figure 4.4F**). These results indicate that the Dual PEG device has immune-isolating properties and suggests non-immunologic reasons, such as primary tissue-driven failure, for the absence of ovarian function in two Dual PEG device encapsulated allografts.

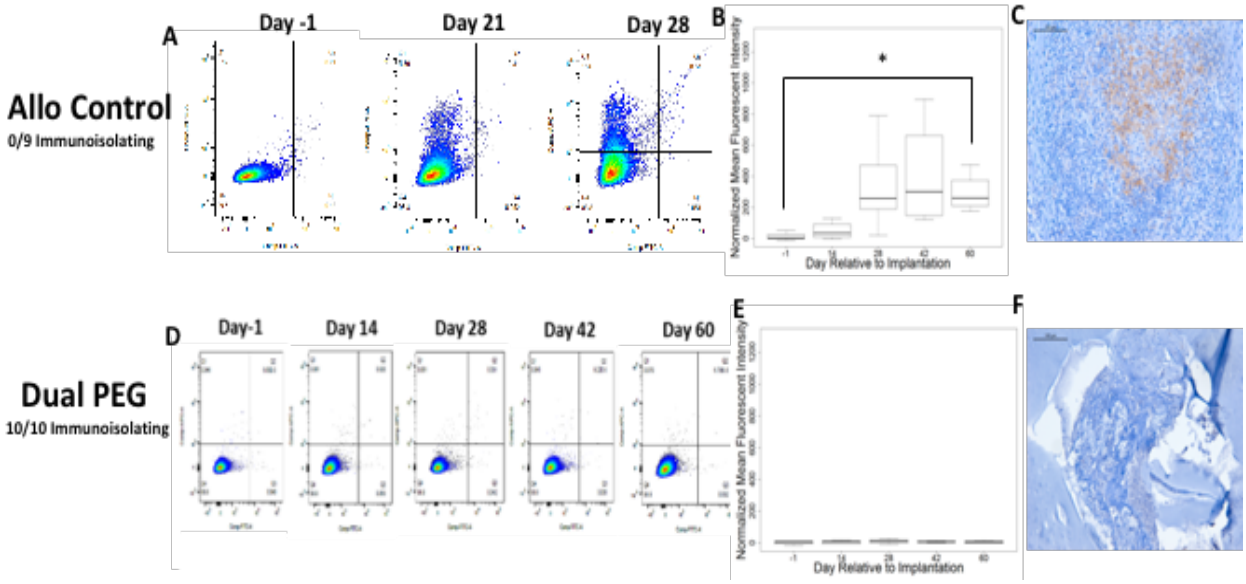

Figure 4.4: A) Representative flow cytometry plots reflecting binding of serum allo-specific antibodies from recipients of non-encapsulated grafts, to donor cells. Y-axis, donor-specific IgG; X-Axis, donor-specific IgM. The mean fluorescence intensity (MFI) for donor specific IgG reflects the average of values read on the Y-Axis; the MFI for donor specific IgM reflects the average of values read on the X-Axis (**B**) Graph depicts the average MFI±SD of allo-specific IgG in mice receiving non-encapsulated allogeneic ovarian tissue. * indicates statistical significance ($p<0.05$)

(**C**) Immunohistochemical staining of CD8+ cells present in the non-encapsulated allograft. (**D**) Representative flow cytometry plots reflecting binding of serum allospecific antibodies, obtained from recipients of dual PEG-encapsulated grafts, to donor cells; and (**E**) Average MFI±SD of allo-specific IgG in mice receiving allogeneic ovarian tissue encapsulated in Dual PEG. (**F**) Immunohistochemical staining of CD8+ cells in the dual PEG-encapsulated allograft. Scale bars: 100 µm(**C**), 200 µm(**F**). Inability to detect circulating allo antibodies and absence of CD8+ T cells in the allografts were deemed the capsules "immunoisolating".

Ovarian allografts encapsulated in degradable capsules, PEG-PD, and Theracyte produced mixed results in terms of ovarian function and allo-immunity (**Figure 4.5**). Encapsulation in PEG-PD hydrogels was less effective at preventing sensitization than encapsulation with in Dual PEG hydrogels. Three out of 10 mice with allografts encapsulated in PEG-PD hydrogels had allo-specific IgG and CD8 T lymphocytes were detected in the excised graft. (**Figures 4.5D, E and F**). In these mice, follicles were not observed and little viable tissue remained after 60 days, corroborating the tissue was not functional. Of the 10 mice implanted with ovarian allografts encapsulated in TheraCyte, three mice developed a an allo-specific IgM-IgG response and had CD8 lymphocytes in the graft (**Figures 4.5J, K and L**). In summary we show that Dual PEG devices allow long-lived function of ovarian allographs while blocking sensitization of the host. Dual PEG devices were superior to TheraCyte or PEG-PD at maintaining function of the enclosed tissue (**Figure 4.3A**).

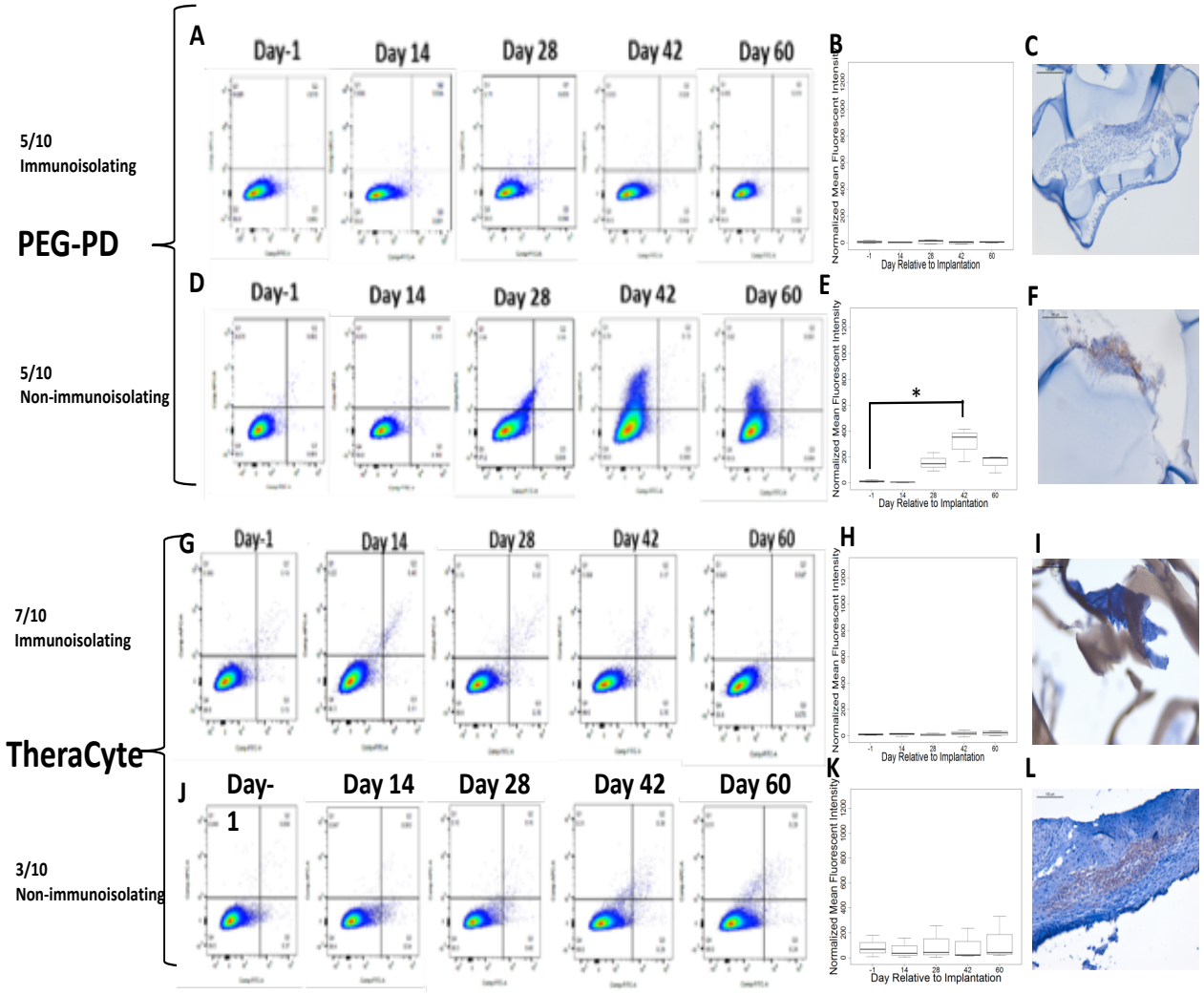

Figure 4.5: Representative flow cytometry plots reflecting binding of serum allo-specific antibodies from recipients of allogeneic ovary tissue encapsulated in PEG-PD or TheraCyte where the tissue (**A,G**) remained functional or (**D,J**) failed during the implantation period. Average MFI±SD of allo-specific IgG levels in mice receiving PEG-PD and TheraCyte where the tissue (**B,H**) remained functional or (**E,K**) failed during the implantation period. Immunohistochemical staining of CD8+ cells present in mice receiving PEG-PD and TheraCyte where the tissue (**C,I**) remained functional or (**F,L**)failed. Scale bars: 100µm (**C,F,I,L**)

4.5 Discussion

In this study, we used PEG based hydrogel capsules to enclose and implant ovarian allografts in immune competent ovariectomized mice to restore the ovarian endocrine function in the hosts. We had demonstrated earlier that the proteolytically degradable synthetic PEG hydrogels (PEG-PD) cross-linked with protease sensitive peptides promote the survival and growth of encapsulated murine primordial ovarian follicles in a syngeneic mouse model of POI [146, 168]. Our results show that encapsulation with PEG-PD and Dual PEG hydrogel sustain physiological development of ovarian allograft tissue in vivo. Dual PEG implants proved to be superior at maintaining function in the long run because they maintain structural integrity for longer that PEG-PD.

While the degradable PEG-PD hydrogels sustain ovarian follicle growth in a syngeneic model, we hypothesized that degradation of these hydrogels cannot support long-term survival and function of ovarian allografts because the immune cells from the host would eventually reach the allograft causing rejection. In fact, 60 days post implantation, 50% of PEG-PD ovarian allografts were “non-functional” similar to non-encapsulated allografts with elevated levels of circulating allo-specific IgG. We hypothesize the degradable matrix of PEG-PD resulted in larger pores over time, which allowed sensitization to occur and allowed host immune cells to infiltrate the hydrogel and cause further damage to the encapsulated tissue. Interestingly, only 50% of the hydrogels degraded enough to allow infiltration of the immune cells while the other 50% remained functioning with no detectable sensitization. These findings suggest that the kinetics

of degradation of the PEG-PD hydrogels determines variable host responses and may introduce variability.

To combine the benefits of hydrogels at sustaining ovarian function and a more robust shell to avoid sensitization and early graft demise, we developed a Dual PEG hydrogel encapsulating system with a proteolytically degradable core to allow follicular development and a non-degradable outer shell to act as a barrier against the host immune system. In a syngeneic study, Dual PEG hydrogels implanted with ovarian tissue caused minimal inflammatory response and supported ovarian follicle survival and development, and promoted restoration of endocrine function in ovariectomized mice for at least 60 days [172]. In the current study, we investigated whether Dual PEG hydrogels protected the encapsulated ovarian allograft from the host immune system and restored ovarian endocrine function. The dual capsule was compared to TheraCyte, a commercially available immunoisolator experimentally used for allogeneic islet transplantation. Encapsulated islets have been shown to survive in TheraCyte in allogeneic models, however in human clinical trials, insulin independence was not achieved [174]. Recently, we showed that TheraCyte supports implantation of ovarian allograft for 21 days and protects the tissue from rejection [144]. TheraCyte immuno-isolating properties depend on a specialized construction involving two membranes: the outer membrane promotes vascularization and the inner membrane prevents infiltration of immune cells. In accord, we found the retrieved TheraCyte devices to be significantly more vascularized compared to Dual PEG hydrogels that presented with minimal interactions with the host. However, the design of the TheraCyte device and the augmented vascularization did not improve the survival or function of ovarian allograft compared to Dual PEG hydrogels, suggesting that vascularization of the device plays a less

significant role for ovarian follicles compared to other tissues, such as islets, which are more sensitive to hypoxia. Importantly, the modular design of the Dual PEG capsule can support significantly greater number of tissue constructs, compared to the TheraCyte's rigid pouch. Lastly, Dual PEG capsules shielded the allogeneic ovarian tissue against sensitization. Inclusion of the non-degradable shell adds immune-protection, which is not observed with the PEG-PD alone. Of those mice that did not experience rejection, a significant decrease in the levels of FSH compared to the preimplantation FSH levels was observed. This decrease in FSH levels is due to the implants' ability to produce estrogen thereby restoring the HPG axis in the ovariectomized mice. We used ovaries from 6-8 days old BALB/c mice due to the presence of a higher proportion of primordial/primary follicles, which could withstand the initial hypoxic environment post-transplantation. Following transplantation, a restoration of estrous activity could be due to the activation of the implanted follicles and recruitment into the growing pool with every estrous cycle. Growing follicles were consistently present in the histological analysis of the encapsulated ovarian implants in mice showing decreased FSH levels.

Sittadjody et al [175, 176] reported that multilayered constructs prepared with cells isolated from ovarian tissues and encapsulated in alginate secreted sex hormones in vitro and restored HPG axis in syngeneic studies in rats. Importantly, this study demonstrated superior short- and long-term outcomes from delivery of ovarian cells compared to pharmacological HRT (pHRT) in ovariectomized rats, which may have important clinical implications. In the current study we investigated whether the allogeneic ovarian tissue was immune-protected by measuring allo-specific antibodies and T-cell infiltration of grafts. In contrast to the non-encapsulated or failed ovarian allografts that presented with elevated levels of allo-specific IgG and CD8+ lymphocyte

graft infiltration, allo-specific IgG in the sera of mice receiving the dual encapsulated ovarian tissue were undetectable and there was no lymphocyte infiltration of the implants. Mice with elevated allo-specific IgG and CD8 T cells corresponded with the failure to restore HPG axis. These mice had elevated FSH levels indicating that the implanted allogeneic ovarian tissue was rejected by the host immune system.

In summary, the approach of hydrogel-based immuno-isolation presents a minimally invasive and a robust way to restore hormonal balance in mice. The basic biology and the factors regulating folliculogenesis are similar in mouse and humans, however further comprehensive and mechanistic studies in large animals will establish the importance of vascularization and the advantages over pharmacological regimens currently available. Because, this cell-based therapy delivers hormones in a pulsatile self-regulating manner, adverse side effects observed with pharmacological treatments can be avoided. This report is the first to demonstrate the feasibility and application of a tunable PEG-based hydrogel to encapsulate allogeneic ovarian tissue and to restore endocrine function in ovariectomized mice preventing rejection. Future non-human primate studies will be conducted to assess the ability of the Dual PEG capsule to support corpus luteum formation; capsule modification may be required to promote vasculature formation and greater diffusion of necessary metabolites and nutrients without the risk of immune rejection.

4.6 Materials and Methods

4.6.1 Experimental Design

Adult cycling female mice (C57BL/6) underwent bilateral ovariectomies to induce POI. Ovaries from BALB/c 6-8 days old mice were encapsulated in (i) a proteolytically degradable PEG-VS

hydrogel (PEG-PD) (**Figure 4.1A**), (ii) a dual PEG-VS hydrogel (Dual PEG) containing a proteolytically degradable PEG-VS core with a non-degradable shell and subcutaneously implanted for 60 days (n=10 recipient mice) (**Figure 4.1E**) and (iii) TheraCyte, a commercially available poly-terephthalate-ethylene (PTFE) pouch. TheraCyte was used as a control for immune-protective capabilities as it has been used towards islet transplantation. All the encapsulated ovarian allografts were implanted subcutaneously for 60 days (n=10 recipient mice). In the control group, non-encapsulated allogeneic ovaries from 6-8 days old BALB/c mice were subcutaneously implanted in C57BL/6 mice (n=9) for 28 or 60 days. The number of donor mice matched the number of recipient mice with each recipient mouse receiving 2 BALB/c ovaries.

4.6.2 Ovariectomies in Recipient Mice

The IACUC guidelines for survival surgery in rodents and the IACUC Policy on Analgesic Use in Animals Undergoing Surgery were followed for all the procedures. Animal experiments for this work were performed in accordance with the protocol approved by the Institutional Animal Care and Use Committee (IACUC) at the University of Michigan (PRO00007716).

Bilateral ovariectomies were performed on adult female mice (C57BL/6) aged 12–16 weeks. The mice were anesthetized by isoflurane. Carprofen (5mg/kg. body weight, Rimadyl, Zoetis) was administered subcutaneously for analgesia. The intraperitoneal space was exposed through a midline incision in the abdominal wall secured using an abdominal retractor. The ovaries were removed, and the muscle and skin layer of the abdominal wall were closed with 5/0 absorbable

sutures (AD Surgical). The mice recovered in a clean warmed cage and received another dose of Carprofen 12 hours post recovery or as needed.

4.6.3 Collection of Donor Ovaries

Ovaries from 6 to 8 days old BALB/c mice were collected and transferred to Leibovitz L-15 media (Sigma-Aldrich, USA). The ovaries were dissected into 2–4 pieces and transferred in the maintenance media (α-MEM, Gibco, USA) and placed in the CO_2 incubator for further manipulation.

4.6.4 Hydrogel Preparation and Ovarian Tissue Encapsulation

To prepare PEG-PD hydrogels, 8-arm PEG-VS (40kDa, Jenkem Technology, Beijing, China) was cross-linked with a plasmin sensitive tri-functional peptide sequence (Ac-GCYK↓NSGCYK↓NSCG, MW 1525.69 g/mol, >90% Purity, CelTek, ↓ indicates the cleavage site of the peptide). Dual PEG hydrogels were prepared using 4-arm PEG-VS 20kDa, Jenkem Technology) with Irgacure 2959 (Ciba, Switzerland, MW=224.3) and 0.1% N-vinyl-2-pyrrolidone (Sigma-Aldrich, St. Louis, USA). The detailed protocol is described in Day et al. [172] donor ovaries were collected from 6-8 days old BALB/c mice. The collected ovaries were transferred to Leibovitz L-15 media (Sigma-Aldrich, USA) and dissected open. The ovarian tissue was then transferred into maintenance media (α-MEM; Gibco, USA), kept at 37˚C and 5% CO_2. For encapsulation in the PEG-PD, the ovarian tissue was transferred into a 10 μL droplet of the plasmin sensitive tri-functional peptide and PEG-VS precursors' solution. The droplet was allowed to crosslink for 5 minutes and then was quenched in maintenance media (**Figure 4.1A**). For Dual PEG hydrogel encapsulation, the tissue was first

encapsulated in a 4 μL PEG-PD hydrogel and was then placed in the center of a 10 μL bead of PEG-VS precursor solution (5% w/v PEG-VS, .4% Irgacure 2959, 0.1% NVP) and exposed to UV light for 6 minutes(**Figure 4.1E**). All constructs were imaged immediately after encapsulation of the tissue (**Figures 4.1B and F**).

4.6.5 Ovary Encapsulation in TheraCyte

The port of the TheraCyte was widened using a Hamilton syringe without compromising the integrity of the TheraCyte wall. Using a mouth pipette, the ovarian pieces were aspirated into the pipette and inserted into the TheraCyte. To verify whether all the ovarian pieces were in the TheraCyte, the transparent plastic port and the pipette were inspected under the stereo microscope. The long port tube was shortened and sealed by melting the plastic to prevent leakage of the ovarian pieces and invasion of the host cells. Each TheraCyte contained ovarian tissue from two ovaries, and each recipient (C57BL/6) was implanted with one TheraCyte.

4.6.6 Subcutaneous Implantation

A small incision was made on the dorsal side of the anesthetized mice (C57BL/6) and the immunoisolators (PEG-PD, Dual PEG and TheraCyte) with the ovarian tissue were implanted subcutaneously. The skin was closed using 5/0 absorbable sutures. The mice received Carprofen for analgesia for at least 24 hours after surgery or as needed. Mice were monitored for two months and euthanized at the end of the experiment. Control mice received empty PEG-VS hydrogels or non-encapsulated ovarian tissue (BALB/c, without a capsule) that were implanted subcutaneously for 28 days.

4.6.7 Serum Hormone analysis

Every two weeks blood was collected from the lateral tail vein at set time points, up to 1% of the total volume of the blood with a 5 $^{3/4"}$ glass Pasteur pipette. At the time of sacrifice, blood was collected via cardiac puncture. Following blood collection, samples were stored at 4°C overnight, then centrifuged for 10 minutes at 10,000 rpm and the separated serum was stored at -20°C. The samples were analyzed for mouse FSH using a radio-immunoassay (Ligand Assay and Analysis Core Facility, University of Virginia Center for Research in Reproduction).

4.6.8 Vaginal Cytology

Daily vaginal cytology was used to establish presence of estrous cycle following ovariectomies and restoration of ovarian endocrine function after implantation of ovarian allografts. The loss of estrous cycle as a result of ovariectomies was confirmed by a persistence of leukocytes, which also correlated with elevated levels of circulating follicle stimulating hormone (FSH). The cyclical transition of cells from leukocytes to cornified and then to nucleated cells signaled resumption of normal estrous cyclicity and restoration of ovarian endocrine function.

4.6.9 Histological analysis of the retrieved devices and the encapsulated ovarian tissue

Following sacrifice, the immunoisolating devices were retrieved from mice, fixed in Bouin's fixative at 4°C overnight, transferred and stored in 70% ethanol at 4°C. After processing, samples were embedded in paraffin, serially sectioned at 5 µm thickness, and stained with hematoxylin and eosin.

4.6.10 Flow Cytometry

Serum allo-antibody titer measurements were performed using flow cytometry before and after implantation and reported as mean fluorescence intensities (MFI) for the highest dilution showing fluorescence detectable above background (non-immune serum from a non-implanted mouse) in immunized mice (positive controls implanted with allogeneic ovaries without a device). Thymocytes were isolated from BALB/c mice and incubated with serially diluted recipient serum for 30 minutes at 4˚C. Antibodies bound to the thymocytes were detected by Cy5-conjugated goat anti-mouse IgG (1:250 dilution, 1030-15, Southern Biotech) and Alexa Fluor 488-conjugated goat anti-mouse IgM (1:250 dilution, 1020-30, Southern Biotech) for 30 minutes at 4˚C and analyzed in a BD FACSCanto II (BD Biosciences, Franklin Lakes, NJ). The mean fluorescence intensities (MFI) in the APC-channel (measuring bound IgG) and FITC channel (measuring bound IgM) were determined with FlowJo 10 software (FlowJo, LLC, Ashland, OR).

4.6.11 Immunohistochemistry for T cells

To analyze T cell infiltration following subcutaneous implantation with PEG-PD, Dual PEG, and TheraCyte, paraffin-sectioned slides were stained to identify CD4 and CD8+ cells. First, sections were deparaffinized with Xylene and rehydrated. The slides were incubated in antigen retrieval buffer, pH9.0 (ab94681, Abcam) for 20 minutes at 97°C and additional 20 minutes at room temperature to cool down. Next, the slides were incubated with KPL Universal Block (5560-0009, Sera-Care) to block non-specific binding sites for 30 minutes at room temperature. The sections were incubated at room temperature for 1 hour with primary antibodies: rabbit monoclonal anti-

mouse CD4 antibody (1:1000 dilution, ab183685, Abcam), rabbit polyclonal anti-mouse CD8 antibody (1:500 dilution, ab203035, Abcam). The slides were subsequently incubated at room temperature with secondary antibodies: goat anti-rabbit Ig (1:100 dilution for 15 minutes, 4010-05, Southern Biotech) for CD4 and goat anti-rabbit (1:50 dilution for 30 minutes, 4010-05, Southern Biotech) for CD8. Diaminobenzidine (BDB2004L, Betazoid DAB Chromogen kit, BioCare Medical) was used as a chromogen for 10 minutes at room temperature. Hematoxylin (220-102, Fischer Scientific) was used as a counterstain. For negative-controls, paraffin sections were incubated without the primary antibody. To assess presence or absence of CD8+ cells, 12 sections from the front, middle, and end of each specimen were examined, to represent the full thickness of the implant.

4.6.12 Statistics

Statistical analysis was performed using the R software. R version 3.1.2 (2014) was utilized. Significance was determined by Welch's two-sample t-test. To determine whether there was a significant difference between the ability of capsule to prevent rejection or not compared to controls, Pearson's Chi-squared test was used. The two main outcomes of the test were 1) functionality of the tissue and 2) the ability of the capsule to minimize the exposure of the allograft to the recipient's immune system and minimize infiltration of the immune cells into the capsule. 1) Consistent estrous cyclicity and decrease in circulating FSH levels qualified as "functional grafts", while absence of cycles and/or FSH levels similar to levels in ovariectomized deemed as "non-functional". 2) Inability to detect circulating allo-antibodies and absence of CD8+ T cells in the allografts were deemed the capsules "immunoisolating". Mice that presented with

elevated levels of FSH, yet had undetectable levels of circulating allo-antibodies were classified as having a primary failure of the ovarian tissue for non-immunological reasons.

4.7 Supplemental Figures

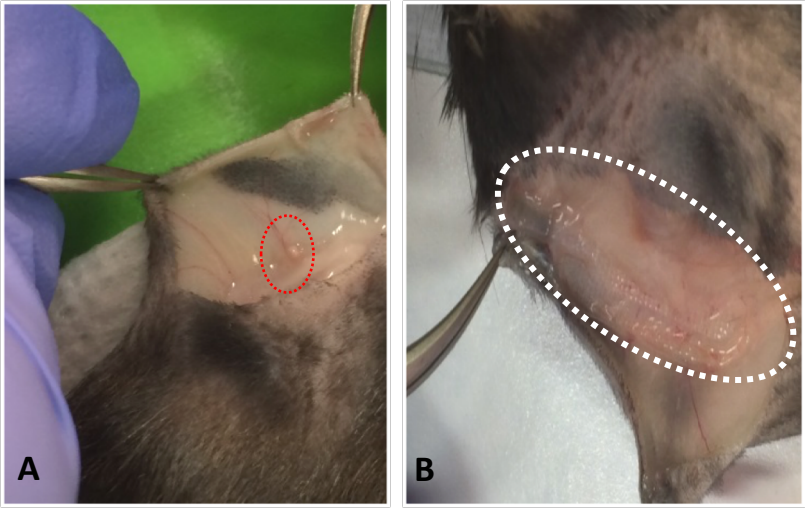

Supplemental Figure 4.1: (A) Non-encapsulated allogeneic ovarian tissue and **(B)** TheraCyte after 60 days of subcutaneous implantation in ovariectomized mice

Chapter V

Immuno-isolating Dual Poly(ethylene glycol) Capsule Prevents Cancer Cells from Spreading Following Mouse Ovarian Tissue Auto-transplantation

5.1 Authors

James R. Day, Anu David, Catherine Long, Grace G. Bushnell, Teresa K. Woodruff, Lonnie D. Shea, Ariella Shikanov

5.2 Abstract

For female cancer survivors, premature ovarian insufficiency (POI) is a common complication of anticancer treatments. Ovarian tissue cryopreservation before treatment, followed by auto-transplantation after remission is a promising option to restore fertility and ovarian endocrine function. However, auto-transplantation is associated with the risk of re-introducing malignant cells harbored in the stroma of the ovarian autograft. To mitigate this risk, we investigated in this pilot study whether an immuno-isolating dual-layered poly(ethylene glycol) (PEG) capsule can retain cancer cells, while supporting folliculogenesis. The dual PEG capsule loaded with 1,000 4T1 cancer cells retained 100% of the encapsulated cells *in vitro* for 21 days of culture. However, a greater cell load of 10,000 cells/capsule led to capsule failure and cells' release. To assess the

ability of the capsule to retain cancer cells, prevent metastasis, and support folliculogenesis *in vivo* we co-encapsulated cancer cells with ovarian tissue in the dual PEG capsule and implanted subcutaneously in mice. Control mice implanted with 2,000 non-encapsulated cancer cells had tumors formed within 14 days and metastasis to the lungs. In contrast, no tumor mass formation or metastasis to the lungs was observed in mice with the same number of cancer cells encapsulated in the capsule. Our findings suggest that the immuno-isolating capsule may prevent the escape of the malignant cells potentially harbored in ovarian allografts and, in the future, improve the safety of ovarian tissue autho-transplantation in female cancer survivors.

5.3 Introduction

Premature ovarian insufficiency (POI) is a common complication of anticancer treatments, such as chemo- and radio therapy, due to ovarian sensitivity to these treatments [164, 166]. In recent years, the survival rate of children with cancer has increased to over 85% due to the development of modern anticancer therapies; however, these patients experience long-term health problems far after they're cancer-free [177,178]. Female cancer survivors with POI suffer from sterility and a myriad of problems associated with ovarian hormone deficiencies, such as premature osteopenia, muscle wasting, and cardiovascular disease [179]. Fertility preservation options, such as oocyte and embryo cryopreservation, are available for post-pubertal adolescent girls and young women. However, these options are not available for prepubertal patients [180].

For prepubertal patients, an experimental option of cryopreservation of ovarian tissue before exposure to toxic treatments, and subsequent auto-implantation after remission would restore both fertility and ovarian endocrine function [38,161,181-189]. Ovarian tissue auto-

transplantation has resulted in close to 100 births to date [190]. Importantly, ovarian tissue auto-transplantation is associated with a significant risk of re-introducing malignant cells harbored in the autologous transplant, particularly in the case of hematologic malignancies, which is common in children [39-41, 161]. A few patient cases of ovarian auto-transplantation in Europe resulted in relapse and multiple experiments in mice further confirmed the risks associated with this approach [39-43]. A potential option for these patients that would provide minimize the risk of cancer re-introduction is allotransplantation of donor ovarian tissue [144,172,173], however this option would solely provide ovarian endocrine function restoration and not provide an option for biologic fertility preservation.

To date, there is no standard universal protocol to ensure the absence of malignant cells in ovarian autografts removed from the patient prior to anti-cancer treatments. Several groups attempted to identify and quantify cancerous cells present in ovarian tissue using histology or PCR [19,21-22]. However, challenges in identifying cancer cells harbored in the tissue prevent clinical translation of this approach, especially in the case of hematologic malignancies, such as acute lymphoblastic leukemia, acute myeloid leukemia, and non-Hodgkin's lymphoma, where ovarian involvement can be high. For example, even when histological analysis showed no evidence of malignant cells, an increase in cancer biological markers was shown through PCR analysis [39,41,42]. It's recommended that the use of molecular markers be used to detect malignant cells, because solely histology is not sufficient; however, not all cancers display specific genetic markers that can be detected via PCR making tissue characterization very difficult [43]. Additionally, there is no consensus as to which markers are most sufficient to detect malignant

cells present in ovarian tissue, dependent on the strain of cancer [42], further complicating the classification of the ovarian tissue as safe.

We hypothesized that immuno-isolation may mitigate the risk of re-introducing malignant cells during ovarian tissue auto-transplantation. Immuno-isolation uses a semi-permeable membrane to encapsulate foreign allogeneic tissue and allow free diffusion of nutrients and metabolites, while preventing the infiltration of immune cells attenuating the immune response. Previously, we have shown that an immuno-isolating multilayered poly(ethylene glycol) (PEG) capsule supports ovarian tissue *in vivo* and did not elicit a measurable inflammatory response [172,173]. The immuno-isolating capsule contains a degradable core that is conducive for ovarian tissue survival and a non-degradable shell, which acts as the immuno-protective barrier. We have demonstrated that allogeneic ovarian tissue does not elicit a host immune response when encapsulated in the Dual PEG capsule, and the capsule prevents lymphocytic infiltration, allowing for allogeneic transplantation of ovarian tissue. Because the immuno-isolating capsule prevents infiltration of immune cells from the host towards the allograft through the barrier, we hypothesized that the capsule will contain cancer cells harbored in the ovarian tissue and will prevent their escape. Thus, encapsulating ovarian autografts in the immuno-isolating capsule mitigates the risk of cancer relapse or metastasis. Here we investigated the ability of the immuno-isolating capsule to prevent spreading of the cancer cells *in vitro* and *in vivo*, preventing tumor mass formation and metastasis, while maintaining the function of ovarian tissue. BALB/c derived 4T1 breast cancer cells originate from an invasive cancer line and were chosen to investigate the effectiveness of the capsule to retain cancerous cells and detect metastasis in a scenario when cancer cells escape the capsule and invade the host. This work aims to mitigate the risk of ovarian

tissue auto-transplantation and provide female cancer survivors experiencing POI with safer options to restore fertility and hormonal balance.

5.4 Results

5.4.1 Encapsulation of cancer cells in Dual PEG prevents cancer cell escape in culture

First, we evaluated the ability of the immuno-isolating capsule to retain cancer cells and prevent their migration and/or proliferation in the respective capsule. To determine whether cancer cells escaped from the gels, the cell-containing capsules were placed in non-tissue treated well plates and imaged every other day. One thousand and 10,000 cells per gel were encapsulated in both PEG-MT, a degradable capsule, and Dual PEG, a capsule containing a degradable core and non-degradable shell. For Dual PEG, cells were only encapsulated in the degradable core component of the capsule, which would mimic the clinical scenario where only the ovarian tissue surrounded by a degradable hydrogel contains cancer cells. Cells encapsulated in PEG-MT escaped the capsule by Day 6 in 100% of the gels for both the 1,000 and 10,000 cell/gel groups (n=5) (**Figure 5.1 A-C,H**).

With the inclusion of the non-degradable shell in the case of Dual PEG, cell escape out of the capsule significantly decreased ($p<0.05$). Dual PEG gels with 1000 cells encapsulated in its core showed 0% escape through 21 days culture (**Figure 5.1 D-H**). When the cell concentration was increased and 10,000 cells were encapsulated in PEG-Dual, cells did escape with 80% of gels showing some extent of cell escape by day 21. However, the kinetics of cell escape was attenuated compared to PEG-MT, as at day 2, 100% of Dual PEG gels containing 10,000 retained the cells in the core and at day 6, 80% showed complete retention (**Figure 5.1H**). This

demonstrated that the inclusion of the non-degradable shell greatly hinders cell migration and proliferation out of the gel, leading to the retention of cells in the capsule through 21 days *in vitro* culture.

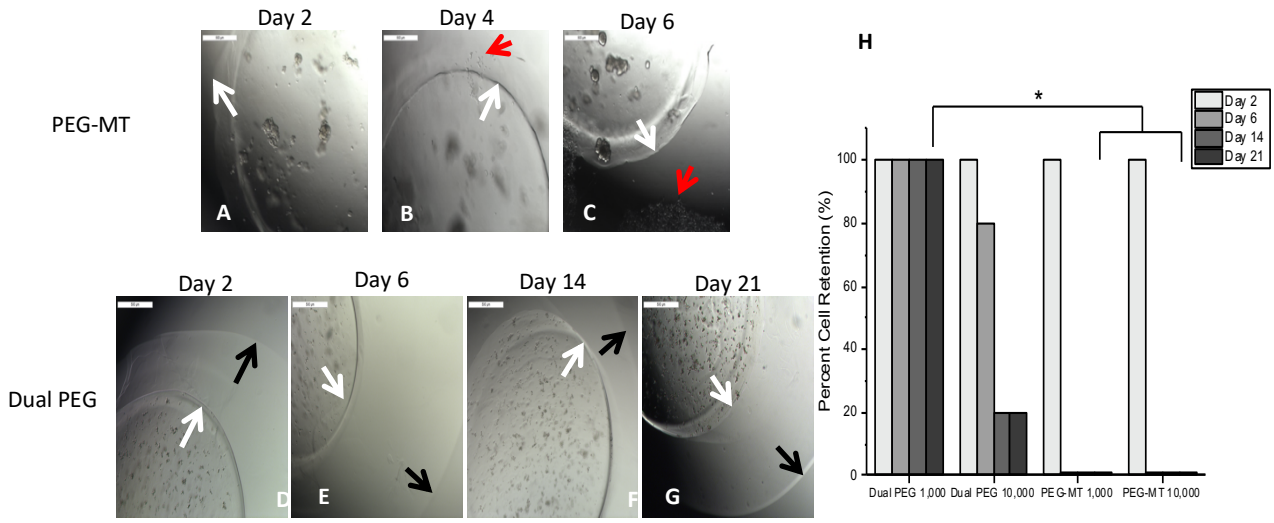

Figure 5.1: *in vitro* encapsulation of 1000 4T1 cells in (**A–C**) PEG-MT and (**D–G**) Dual PEG. (**H**) Percentage of hydrogels (n = 5) for each group that retained encapsulated cancer cells through 21 days of culture. White arrow indicates border of PEG-MT hydrogel, red arrow indicates escaped cancer cells, and black arrow indicates border of non-degradable shell in Dual PEG. * indicates statistical significance ($p < 0.05$).

5.4.2 Encapsulation of cancer cells in Dual PEG prevents spreading and metastasis in vivo

To evaluate the Dual PEG capsule's ability to retain cancerous cells *in vivo*, cells were co-encapsulated with mouse ovarian tissue and implanted subcutaneously in a BALB/c mouse model. The cancer cell line, mouse ovarian tissue, and recipient mouse strain were all the same

to negate any possible immune response. Either, 1,000 or 10,000 cells, were encapsulated in Dual PEG with 6-8 day old ovarian tissue (**Figure 5.2A,B**). Each mouse (n=5 per group) received two identical capsules. For positive controls, a cell suspension containing either 2,000 or 20,000 4T1 cells was injected subcutaneously. When 2,000 cells were injected, proliferation was exhibited in 5/5 mice with radiance increasing from 3.56E4 to 6.02E9 photons/sec from day 0 to 14 (**Figure 5.2C-E,O**). By Day 14, all mice had to be sacrificed as a tumor mass had formed on the dorsal side and ulceration started to occur (**Figure 5.3A**). In the mice receiving 20,000 non-encapsulated cancer cells, proliferation and tumor mass formation was observed in 4/5 mice (**Figure 5.2F-H, O**). Similar to the 2,000 cell group, the mice exhibited ulceration by day 14 and had to be sacrificed. The cells proliferated as shown by the significant increase of radiance from day 0 to day 14 (**Figure 5.2O**). To confirm the extracted tumor masses were in fact the labeled 4T1 cells, bioluminescence imaging was used. All tumors exhibited bioluminescence indicating the mass was cancerous and derived from the injected 4T1 cells (**Figure 5.3B**).

When 1,000 cells were encapsulated in Dual PEG and two capsules were implanted per mouse (total of 2,000 cells per mouse), 0 out of 5 mice exhibited a tumor mass formation through 28 days as shown through a non-significant change in radiance from day 0 to day 28 (**Figure 5.2I-K, O**). From IVIS imaging, it appeared that all cancer cells were retained within the capsule. To confirm, when hydrogels were extracted, the capsules as well as the surrounding tissue were imaged via bioluminescence and only the inner core of the hydrogels showed luminescent signal (**Figure 5.3E**). Additionally, upon macroscopic evaluation, the hydrogels containing cancer cells and ovarian tissue looked exactly as they did when implanted on day 0 and no tumor mass was present (**Figure 5.3D**). For the mice receiving 10,000 cancer cells co-encapsulated with ovarian

tissue in Dual PEG (2 devices, 20,000 cancer cells total per mouse), 4/5 mice demonstrated tumor formation as shown through a significant increase in radiance over the 28 day implantation period (**Figure 5.2 L-O**). Upon extraction, a tumor mass localized to the hydrogels was evident as the hydrogel appeared cloudy in appearance (**Supplemental Figure 5.1**). However, although the 10,000 cancer cells proliferated over the 28 day implantation period, the cells remained localized to the hydrogel, as the hydrogel showed a high level of radiance, indicating the cancer cells were present within the capsule, itself (**Supplemental Figure 5.1**).

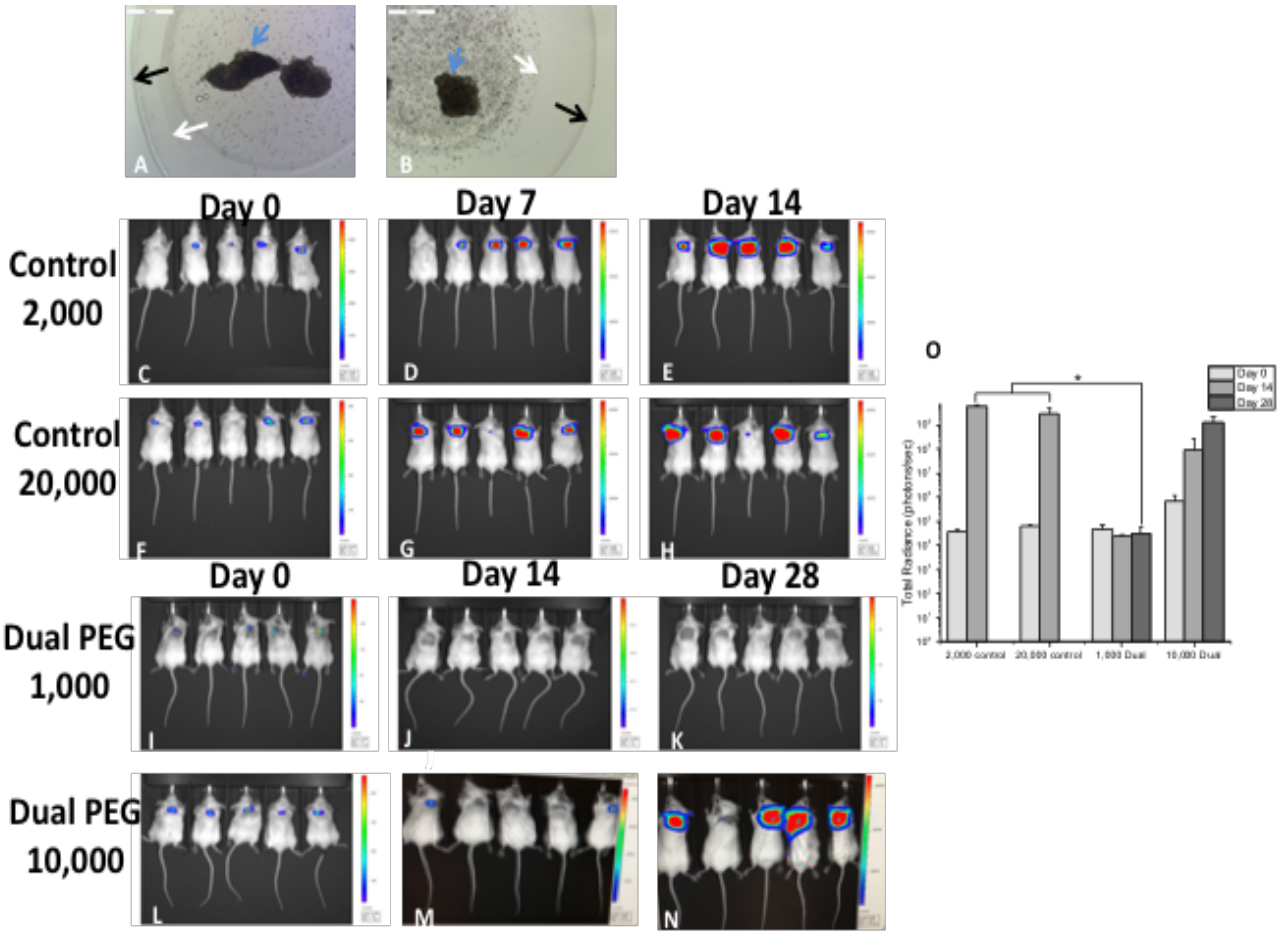

Figure 5.2: Microscopic image of (**A**) 1000 and (**B**) 10,000 4T1 cells co-encapsulated with BALB/c ovarian tissue in Dual PEG. Magnification 5×. Bioluminescent imaging of mice receiving (**C–E**)

2000 non-encapsulated 4T1 cells, (**F–H**) 20,000 non-encapsulated 4T1 cells, (**I–K**) 2 Dual PEG capsules both encapsulating 1000 4T1 cells and ovarian tissue and (**L–N**) 2 Dual PEG capsules both encapsulating 10,000 4T1 cells and ovarian tissue. (**O**) Average radiance of mice receiving control non-encapsulated cells or cells encapsulated in Dual PEG (n = 5 per group). White arrow indicates border of degradable PEG-PD core, black arrow indicates border of non-degradable shell in Dual PEG, and blue arrow indicates ovarian tissue. * indicates statistical significance ($p < 0.05$).

To assess metastasis, organs such as the brain, ovaries, lungs, spleen, blood, and liver were explanted and examined for the presence of cancerous cells through bioluminescent imaging. In the 2,000 and 20,000 cell control groups, radiance was exhibited in all the lungs, indicating cancerous cells metastasize to the lungs, which is expected for this cell line (**Figure 5.3C**). When 4T1 cells were encapsulated in Dual PEG, none of the extracted organs in any animal exhibited bioluminescence indicating the encapsulation prevented metastasis of cancerous cells to the lungs (**Figure 5.3F**) contrary to the non-encapsulated control.

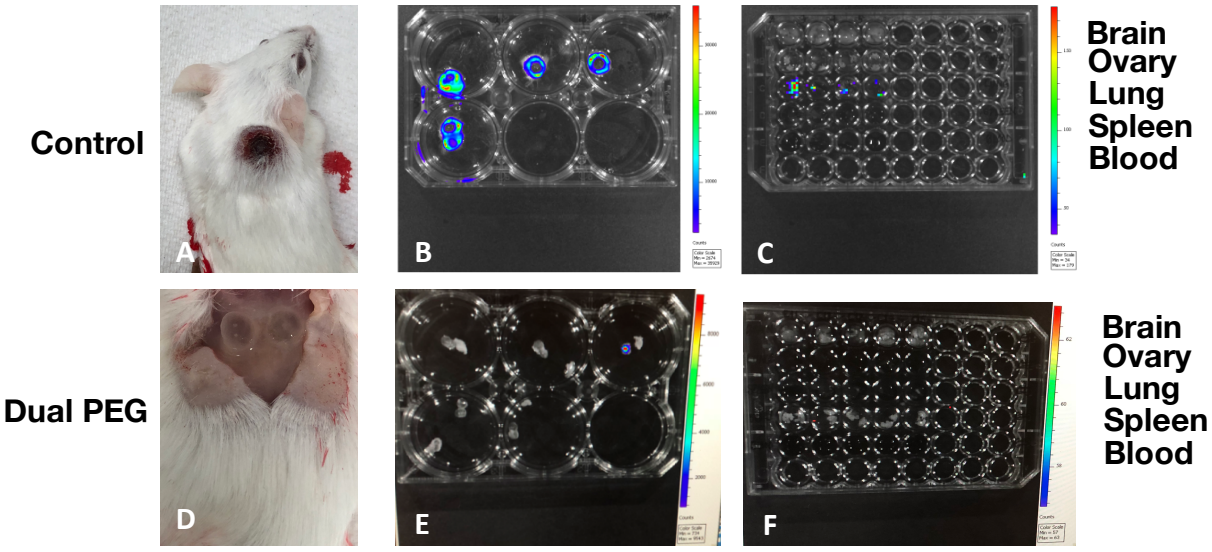

Figure 5.3: A) Macroscopic image of mice receiving non-encapsulated 4T1 cells and ovarian tissue. Bioluminescent imaging of (**B**) resected tumors and (**C**) organs following sacrifice 14 days after injection. Organs removed include brain, ovary, lung, blood, and spleen. (**D**) Macroscopic

image of mice receiving Dual PEG containing 1000 4T1 cells and ovarian tissue. Bioluminescent imaging of (**E**) resected capsules and (**F**) organs following sacrifice 28 days after implantation. White circle indicates location of hydrogels.

Lastly, to assess the ability of ovarian tissue to survive and develop in the presence of cancer cells, histological analysis was performed after explantation of the Dual PEG capsules to investigate the degree of folliculogenesis. Healthy, developing primary and secondary follicles were seen in ovarian tissue co-encapsulated with 1,000 and 10,000 cancerous cells (**Figure 5.4**) demonstrated folliculogenesis was supported. Interestingly, a higher number of follicles were observed in the ovarian tissue encapsulated with 1,000 cancer cells compared to 10,000 cells, which could be due to damage to ovarian tissue by the cancerous cells [191]. Multiple primordial follicles are present in capsule with 1,000 and 10,000 cancer cells (**Figure 5.4B and D**).

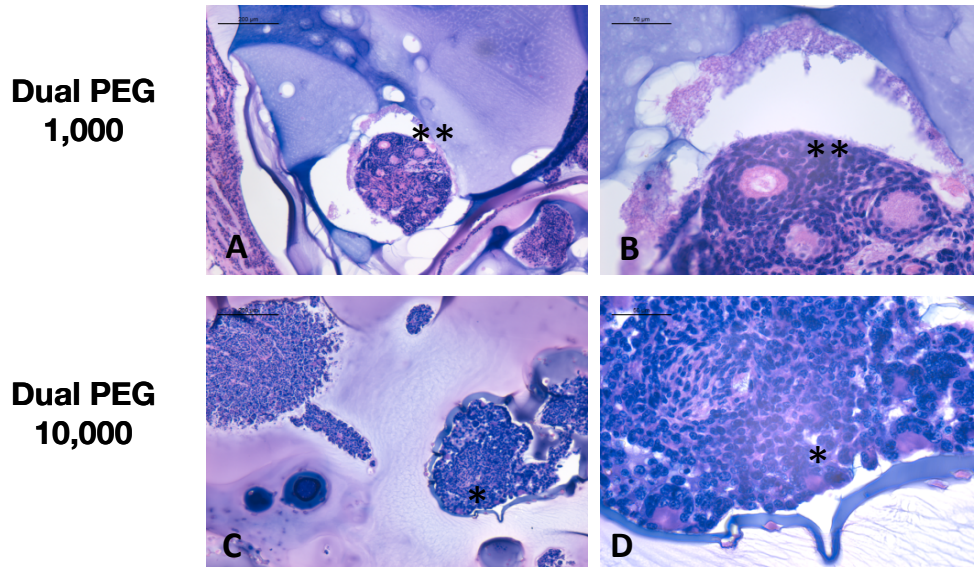

Figure 5.4: Histological image of ovarian tissue encapsulated in Dual PEG with (**A,B**) 1000 4T1 cells and (C,D) 10,000 4T1 cells. Scale bars: 200 µm (**A,C**) and 50 µm (**B,D**). * indicates primordial follicles, ** indicates primary follicles, and *** indicates secondary follicles.

5.5 Discussion

Cryopreservation and subsequent auto-transplantation of a patient's own tissue would be an optimal option for young female cancer survivors, as it gives patients the option to have biological children long after treatment and restores their natural hormone function [179-184]. However, auto-transplantation presents the patients with a risk of re-introducing malignant cells, as the ovarian tissue was resected before treatment leading to the possibility of malignant cells being stored in the stroma of the tissue. In hematological cases, which is a high percentage of childhood cancers, this risk and ovarian involvement is very high [38-42]. Previous studies have been conducted to identify cancerous cells present in resected ovarian tissue from cancer patients. Due to discrepancies in characterization methodology, molecular marker criteria, and tissue heterogeneity, no universal protocol has been established to characterize ovarian tissue as safe [39-42]] creating a risk of re-seeding malignant cells for female cancer survivors following ovarian tissue auto-transplantation.

This work describes a method to mitigate this risk by retaining cancerous cells in a capsule which is also conducive for ovarian tissue survival and development. Previously, we developed a multilayered immuno-isolating capsule, Dual PEG, which contains a degradable core that is conducive for ovarian tissue development and a non-degradable shell that acts as an immunoprotective barrier [172]. We demonstrated that when encapsulating allogeneic ovarian tissue and using an allogeneic mouse model, larger immune cells such as cytotoxic T cells are unable to penetrate the capsule. If cells are unable to penetrate the capsule from the outside immune environment, we hypothesized the Dual PEG capsule could retain encapsulated cancerous cells present in ovarian tissue and not let cells escape.

First, we tested Dual PEG's ability to retain cancerous cells *in vitro* in comparison to a degradable PEG-MT capsule. We demonstrated that by adding the non-degradable photopolymerized PEG layer, the ability of the capsule to retain cancer cells significantly increases. Through 21 days of culture, we showed 100% effectiveness of cancer cell retention when 1,000 cells were encapsulated in Dual PEG, compared to 0% cancer cell retention through 2 days when encapsulated in PEG-MT. This difference is due to the nature of the crosslinks in the respective capsules. In PEG-MT, the crosslinks are formed via a protease-sensitive peptide, so when the cancer cells grow and proliferate, they secrete proteases, which break down the bonds of the hydrogel. This opens up the pores and network of the hydrogel, allowing the cells to escape from the gel. The photopolymerized layer is not susceptible to proteolytic or hydrolytic degradation as the crosslinks are formed via free radicals reacting with double bonds. We observed that when the amount of cancer cells was increased to 10,000 per Dual PEG capsule, cancer cells did escape in a portion of the gels. This may be due to incomplete encapsulation of the cancer cell-containing core or the core being broken down and swelling past the outer shell's capabilities. However, this cell concentration of 2.5 million cells/mL is far above what would be present in a clinical situation and was used to test the upper limits of Dual PEG.

Next, we tested the ability of Dual PEG to retain cancer cells and prevent tumor mass formation and metastasis *in vivo* in a syngeneic mouse model. Previous studies have suspended 100-200 cancerous cells in a fibrin or alginate matrix, and when implanted into mice, did not reintroduce leukemic cell contamination [192,193]. Here, we encapsulated BALB/c mouse ovarian tissue with BALB/c derived 4T1 cancer cells (1,000 or 10,000 cells per capsule) in Dual PEG and implanted two devices subcutaneously in BALB/c mice. A syngeneic model was used to mimic auto-

transplantation of cancer cell-containing ovarian tissue. We compared the controls of injections containing cell suspensions of 2,000 or 20,000 4T1 cells to match the total amount of encapsulated cells in the mice receiving Dual PEG. When non-encapsulated cancer cells were injected subcutaneously, we observed rapid cell proliferation via luminescent imaging as well as tumor mass formation. By Day 14, we had to sacrifice all control mice as the tumors resulted in ulceration. Additionally, luminescent signal was observed in the lungs, indicating the 4T1 cells metastasized to the lungs, which is expected for this cancer cell line. When encapsulating 1,000 cancer cells (250,000 cells/mL) in Dual PEG, we observed no change in luminescent signal in all mice through 28 days indicating the absence of tumor mass formation. Additionally, there were no cancer cells present in any of the surrounding tissue or organs of interest, indicating cancer cells were retained within the capsule and metastasis had not occurred. All observed luminescent signal was concentrated in the capsule, further confirming that all cancer cells present were retained in the capsule throughout the whole implantation period. When the amount of cell in each capsule was increased in 10,000 (2.5 million cells/mL), an increase in luminescent signal was observed over the 28 day implantation period indicating cell proliferation and tumor mass formation was taking place; however, all the cells were maintained in the gel as indicated by the lack of cells in surrounding tissues and susceptible organs. Macroscopically, we were able to see the tumor mass within the gel itself and upon IVIS imaging, the hydrogel was shown to be the only entity that contained cancer cells. At a high cell density of 10,000 cells/capsule, the Dual PEG gel is able to retain those cells and prevent metastasis, unlike the non-encapsulated control. When the capsules were explanted and histological analysis was performed, we observed the presence of healthy primary and secondary follicles. This is vital to a successful encapsulation

strategy for auto-transplantation, as this shows the tissue is capable of surviving within the capsule, potentially restoring fertility and ovarian endocrine function.

This work demonstrated the capability of using an immuno-isolating capsule to retain cancer cells that may be present in an ovarian tissue autograft. Previously, we have shown that Dual PEG can support ovarian tissue survival and development, leading to the restoration of ovarian endocrine function. We have also demonstrated the capsule's ability to protect encapsulated ovarian tissue from an immune response. By using this capsule to encapsulate a patient's ovarian autograft, the risk of re-introducing malignant cells present in that tissue is mitigated. Given there is no protocol by which clinical investigators can be absolutely certain ovarian autografts do not contain cancerous cells, girls that had hematologic malignancies, and showed zero to a low concentration (250,000 cells/mL) of cancerous cells in their ovarian biopsy, could potentially use of an immuno-isolating capsule to decrease the risk of cancer re-introduction. Through this work, the option of auto-transplantation is potentially safer, which, although experimental, is the only option for pre-pubescent female cancer survivors to retain, both, future fertility and ovarian endocrine function. Future work will be done to assess the ability of encapsulated mouse ovarian tissue to produce viable eggs once encapsulated in the dual PEG capsule. To this end, developing new methods to create a capsule using alternatives to photopolymerization may be necessary. Limitations of this study include the use of mouse ovarian tissue and a short in vivo transplantation period. For this reason, future studies encapsulating human ovarian tissue will be conducted to investigate the ability of the PEG capsules and other biocompatible materials to accommodate the large volumetric expansion of human follicles during development and the ability for capsule to support ovulation and corpus luteum formation.

5.6 Materials and Methods

5.6.1 Gel Preparation

Degradable poly(ethylene glycol) hydrogels (PEG-MT) were formed via Michael-type addition. To prepare degradable PEG-MT hydrogels for the core, 8-arm PEG-VS (40kDa, Jenkem Technology, Beijing, China) was cross-linked with a plasmin sensitive tri-functional peptide sequence (Ac-GCYK↓NSGCYK↓NSCG, MW 1525.69 g/mol, >90% Purity, CelTek, ↓ indicates the cleavage site of the peptide). The non-degradable shell for Dual PEG hydrogels were prepared using 4-arm PEG-VS 20kDa, Jenkem Technology) with Irgacure 2959 (Ciba, Switzerland, MW=224.3) and 0.1% N-vinyl-2-pyrrolidone (Sigma-Aldrich, St. Louis, USA). The detailed protocol is described in Day et al [172].

5.6.2 Collection of murine donor ovaries

Donor ovaries were collected from 6-8 days old BALB/c mice. The collected ovaries were transferred to Leibovitz L-15 media (Sigma-Aldrich, USA) and dissected open. The ovarian tissue was then transferred into maintenance media (α-MEM; Gibco, USA), kept at 37C and 5% CO_2 until encapsulated.

5.6.3 4T1 cell and ovarian tissue encapsulation

BALB/c derived 4T1 cancer cells were encapsulated at a concentration of 250,000 cells/mL (1,000 cells/gel) or 2.5 million cell/mL (10,000 cells/gel). For encapsulation in the PEG-MT, the cancer cells and/or ovarian tissue were transferred into a 4 μL droplet of the plasmin sensitive tri-functional peptide and PEG-VS precursors' solution. The droplet was allowed to crosslink for 5 minutes and then was quenched in maintenance media. For Dual PEG hydrogel encapsulation, the tissue was first encapsulated in a 4 μL PEG-MT hydrogel and was then placed in the center of a 10 μL bead of PEG-VS precursor solution (5% w/v PEG-VS, .4% Irgacure 2959, 0.1% NVP) and exposed to UV light. All constructs were imaged immediately after encapsulation of the cells and tissue to verify complete encapsulation.

5.6.4 Subcutaneous injection and implantation

For controls, a cell suspension containing 2,000 or 20,000 cancer cells was injected subcutaneously on the dorsal side of the anesthetized mice (BALB/c). For animals receiving the cancer cells/ovarian tissue encapsulated in Dual PEG, a small incision was made on the dorsal side of the anesthetized mice (BALB/c) and 2 capsules per mouse were placed subcutaneously containing either 1,000 or 10,000 cancer cells in each capsule making each mouse receive a total of 2,000 or 20,000 cancer cells to compare to controls. The skin was closed using 5/0 absorbable sutures. The mice received Carprofen for analgesia for at least 24 hours after surgery or as needed. Mice were monitored for two weeks to one month and euthanized at the end of the experiment. Control mice were sacrificed at 14 days and mice receiving Dual PEG were sacrificed after one month. N=5 for each group.

The IACUC guidelines for survival surgery in rodents and the IACUC Policy on Analgesic Use in Animals Undergoing Surgery were followed for all the procedures. Animal experiments for this work were performed in accordance with the protocol approved by the Institutional Animal Care and Use Committee (IACUC) at the University of Michigan (PRO00007716).

5.6.5 IVIS imaging

Bioluminescent imaging via the IVIS (In vivo Imaging System) was utilized to

to track cell growth during the implantation period. Implanted 4T1 cells were labeled with firefly luciferin. Briefly, on the day of implantation and every 7 days during the time course of the study, 150 μL of 63mM substrate (Xenolight D-Luciferin-K+ Salt Bioluminscent substrate, PerkinElmer) was injected intraperitoneally. After 10 minutes of incubation, mice were imaged. Similarly, to assess metastasis, collected organs and tumors on day of sacrifice were imaged by adding 28uL of 63mM substrate per mL of culture media. Images were processed and analyzed using LivingImage software.

5.6.6 Tumor, gel, and organ collection

At the time of sacrifice, tumors or gels were collected, imaged via IVIS, and fixed in Bouin's fixative. Additionally, the brain, liver, lungs, spleen, blood, and ovaries were collected, imaged via IVIS, and fixed in Bouin's fixative.

5.6.7 Histological analysis of retrieved capsules and the encapsulated ovarian tissue

Following sacrifice, the immuno-isolating devices were retrieved from mice, fixed in Bouin's

fixative at 4°C overnight, transferred and stored in 70% ethanol at 4°C. After processing, samples were embedded in paraffin, serially sectioned at 5 µm thickness, and stained with hematoxylin and eosin.

5.6.8 Statistics

A Pearson's (N-1) Chi-squared test was performed. Calculated values were performed using R, and all p-values were evaluated against a significance level (α) of 0.05. To test significance in change in radiance over time, a Welch's t-test was used with $p<0.05$ determined as significant.

5.7 Supplemental Figures

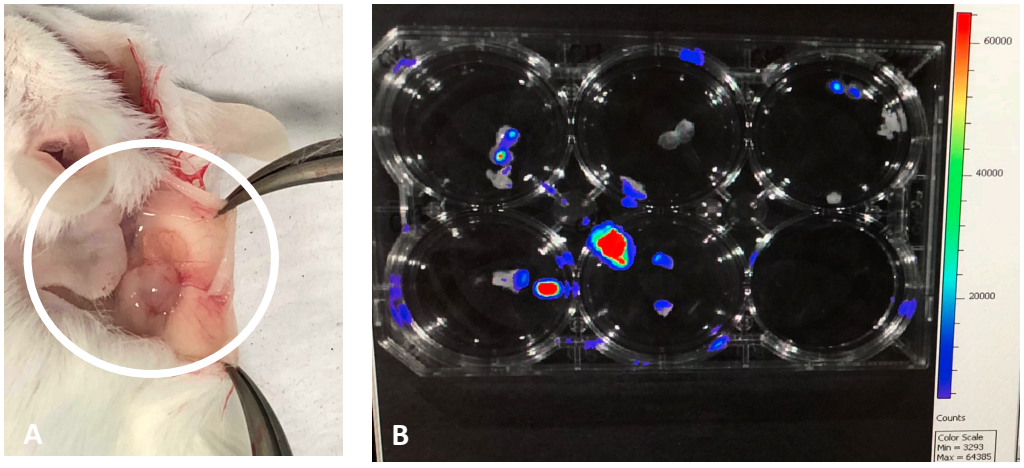

Supplemental Figure 5.1: (A) Macroscopic image of mice receiving Dual PEG containing 10,000 4T1 cells and ovarian tissue. **(B)** Bioluminescent imaging of resected capsules containing 10,000 4T1 cells following sacrifice 28 days after implantation. White circle indicates the location of the capsules and tumor mass

CHAPTER VI

Encapsulation of ovarian allograft precludes sensitization of host immune response in immune-competent ovariectomized mice

6.1 Authors

James R. Day, Anu David, Mayara Garcia de Mattos Barbosa, Jenna Barnes, Evan Farkash, Marilia Cascalho, Ariella Shikanov

6.2 Abstract

Sensitization is an immune memory response in which circulating HLA antibodies in the blood hold the potential for accelerated antibody production. Memory T cells mediate this reaction in the case of allo-transplantation of organs where allo-antigens on the surface are recognized as foreign and presented to T cells for destruction. Immunosuppressive therapies are the only clinically available treatment to prevent graft failure in sensitized recipients. Here we utilized an immuno-isolating hydrogel-based capsule to protect transplanted ovarian allografts without the need for immunosuppressant. For female cancer survivors, allo-transplantation of donor ovarian tissue holds great potential as these patients often experience premature ovarian insufficiency

(POI) due to ovarian cytotoxity to chemo- and radio-therapy. Implantation of encapsulated CBAXC57Bl/6 (F1) ovarian allografts in a Dual PEG capsule, with a degradable core and non-degradable shell, did not sensitize the BALB/c host immune system. When ovarian allografts were implanted in a Dual PEG capsule for 60 days followed by another Dual PEG capsule for another 60 days, allo-antibody levels were significantly lower compared to non-encapsulated controls. We observed the presence of healthy developed antral follicles in the encapsulated graft, indicating folliculogenesis was supported and endocrine function was restored. This is the first report to demonstrate that ovarian tissue encapsulated in Dual PEG does not sensitize the host as shown through subsequent allogeneic implantations.

6.3 Introduction

Sensitization is an immune memory response in which circulating HLA antibodies in the blood are present and the immune system holds the potential for accelerated production of HLA antibodies. Memory T cells mediate this reaction when they interact with antigen-presenting cells, become active lymphoblasts and eliminate allo-antigens at a rapid rate [194]. In the case of allo-transplantation of organs, allo-antigens on the surface are recognized as foreign and presented to T cells for destruction. Clinically, sensitization can result in graft failure and remains a major challenge in organ transplantation as it limits the available donor pool and increases the risk of mortality and morbidity if immunosuppressive therapies are not administered [194-196]. Immunoisolation is a promising approach to allow transplantation of allogeneic tissues without immunosuppression, but it is limited to small tissue fragments that do not require direct vascularization and can be sustained by diffusion. One example of such application is allo-

implantation of ovarian donor tissue to restore ovarian endocrine health in adolescent childhood cancer survivors reaching the age of pubertal development. Over the past few decades the rates of childhood cancer survival have increased significantly, rising to over 85% in some cases, due to advances in anti-cancer therapies. Unfortunately, these therapies exhibit ovarian toxicity, leading to premature ovarian insufficiency (POI). Adolescent patients with POI experience hormonal imbalances which in turn lead to long-term co-morbidities such as decreased height, diminished bone health, muscle wasting, insulin irresponsiveness, poor lipid metabolism, and poor cardiovascular health and cognition [9-11]. The only clinically available option to treat POI is hormone replacement therapy (HRT). However, HRT delivers only a fraction of ovarian hormones—estrogen and progesterone—at higher doses and in a non-pulsatile manner which is essential for proper regulation and does not mimic the physiological hormonal milieu [44,46-48]. Alternatively, another experimental option for these patients is cryopreservation of ovarian tissue prior to gonadotoxic treatments followed by subsequent auto-transplantation. However, there is an associated risk of re-implanting malignant cells present in the ovarian tissue, particularly in patients with hematological malignancies [39-41, 161]. There is no accepted protocol to deem ovarian tissue free of cancerous cells and safe [19,21-22]. Additionally, patients often have to undergo treatments immediately after diagnosis and do not have a chance to cryopreserve their tissue before treatment [146,180,197].

Transplantation of donor ovarian tissue to restore ovarian endocrine function for patients experiencing POI is an experimental option to avoid the risk of cancer recurrence associated with auto-transplantation. Previously, we have developed a novel poly(ethylene glycol)-based (PEG) capsule to support ovarian development and function, while preventing an immune-mediated

rejection in mouse model of allogeneic transplantation. We demonstrated that the capsule prevents infiltration of immune cells and the encapsulated tissue restores ovarian endocrine function and does not elicit the production of allo-specific antibodies. The question remains as to whether the allo-antigens are possibly diffusing from the encapsulated ovarian allograft, even in the absence of rejection, sensitizing the host and as a result preventing future successful implantations. In this study, we investigated whether recipients are sensitized to ovarian allografts encapsulated in a Dual PEG capsule after sequential allogeneic implantations. Mice were implanted with non-encapsulated or Dual PEG encapsulated ovarian allografts and were subsequently implanted with another non-encapsulated or Dual PEG encapsulated ovarian allograft. The two-phased implantation schedule mimics the reality in which a recipient is already sensitized to antigens prior to implantation. The objective of this study was to show that encapsulation of allogeneic ovarian tissue in a Dual PEG capsule, prevents sensitization of the recipient even in the cases when the immune system was primed to allo-antigens present in the encapsulated graft; this would prolong graft survival, and clinically, allow for multiple implantations of encapsulated allogeneic ovarian tissue to restore ovarian endocrine function in patients with POI.

6.4 Results

6.4.1 Non-encapsulated ovarian allograft sensitize the recipient mice

Implantation of non-encapsulated ovarian allografts elicited an immune response when implanted subcutaneously resulting in a 23-fold increase in allo-specific antibody production (**Figure 6.2 A,B**). The number of circulating allo-specific antibodies gradually increased from undetectable 14 days post transplantation to 750 MFI on day 28 and 500 MFI on day 42. On the contrary, after implantation of ovarian allograft encapsulated in Dual PEG the levels of circulating allo-specific antibodies remained consistently low, ranging between 100 to 250 MFI for 60 days after implantation (**Figure 6.2 C,D**). Negative results of immunohistochemical staining of the retrieved grafts confirmed that the graft was isolated and protected from cellular infiltration.

The endocrine activity of the implanted ovarian allografts was consistent with the levels of circulating antibodies and cellular infiltration into the grafts. Ovariectomized mice implanted with non-encapsulated ovarian allografts briefly resumed estrous activity after 1 week, and stopped in all mice after 4 weeks, correlating with the increasing levels of circulating allo-antigens. The estrous activity in ovariectomized mice implanted with encapsulated ovarian allo-grafts resumed in all mice after 2 weeks and persisted for 9 weeks until the end of the study (**Figure 6.2 E-G**).

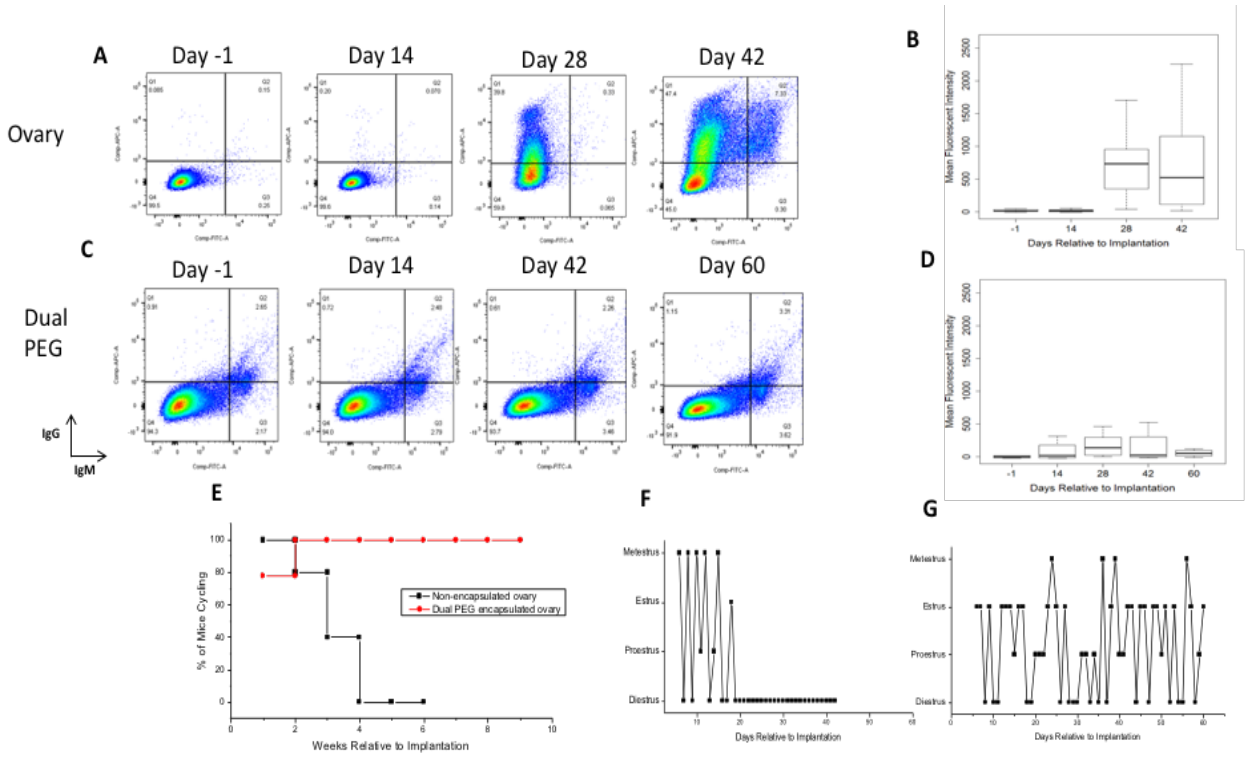

Figure 6.2: Representative flow cytometry plots of binding of serum allo-specific antibodies from recipients of **(A)** non-encapsulated allogeneic ovary tissue for 42 days and (**C)** tissue encapsulated in Dual PEG for 60 days. Y-axis, donor-specific IgG; X-Axis, donor-specific IgM. Graph depicts the average MFI±SD of allo-specific IgG in mice receiving **(B)** non-encapsulated allogeneic ovarian tissue and **(D)** tissue encapsulated in Dual PEG capsules. **(E)** Resumption of estrous cycle of mice receiving non-encapsulated and Dual PEG encapsulated allogeneic ovarian tissue. Representation of estrous activity in mice receiving **(F)** non-encapsulated and **(G)** Dual PEG encapsulated allogeneic ovarian tissue

6.4.2 Encapsulated ovarian tissue functions in sensitized and naïve mice

We demonstrated that encapsulated ovarian allografts implanted in naïve mice are protected from immune rejection. However, the question remained whether the encapsulated ovarian

allografts remained protected in the host that had been previously sufficiently exposed to allo-antigens resulting in sensitized immune system for subsequent implantations. We tested whether encapsulation of ovarian allo-tissue in Dual PEG prevents rejection in a sensitized environment where mice were already sensitized with non-encapsulated ovarian tissue for 60 days and then implanted with ovarian tissue encapsulated in Dual PEG. When we implanted ovarian tissue encapsulated with Dual PEG in mice with elevated levels of circulating allo-specific antibodies after the sensitization period (**Figure 6.3 A,B**) the antibody production in the hosts plateaued and leveled off through 60 days of the second implantation, indicating a memory response was not present. No presence of CD8+ cells was evident in the graft indicating the capsule prevented cellular infiltration (**Figure 6.3 C**). Graft survival was confirmed by the presence of multiple healthy developing follicles in the encapsulated graft (**Figure 6.3 D-F**) and resumption of estrous activity following the implantation of the encapsulated graft (**Figure 6.3 J,K**). By 3 weeks after the initial non-encapsulated implantation, all mice stopped cycling indicating the graft was no longer functional and the mice were sensitized. Once the encapsulated allograft was implanted in the sensitized mice at 60 days, all mice resumed cycling by 2 weeks post-implantation and continued cycling through the entire of the implantation period (**Figure 6.3 J,K**). The presence of healthy developed follicles in the graft once removed from a sensitized host (**Figure 6.3 D-F**) was similar to that observed in a naïve mouse that received Dual PEG encapsulated allograft for a primary implantation (**Figure 6.3 G-I**), confirmed the ovarian allograft was not rejected and remained functional in a sensitized mouse.

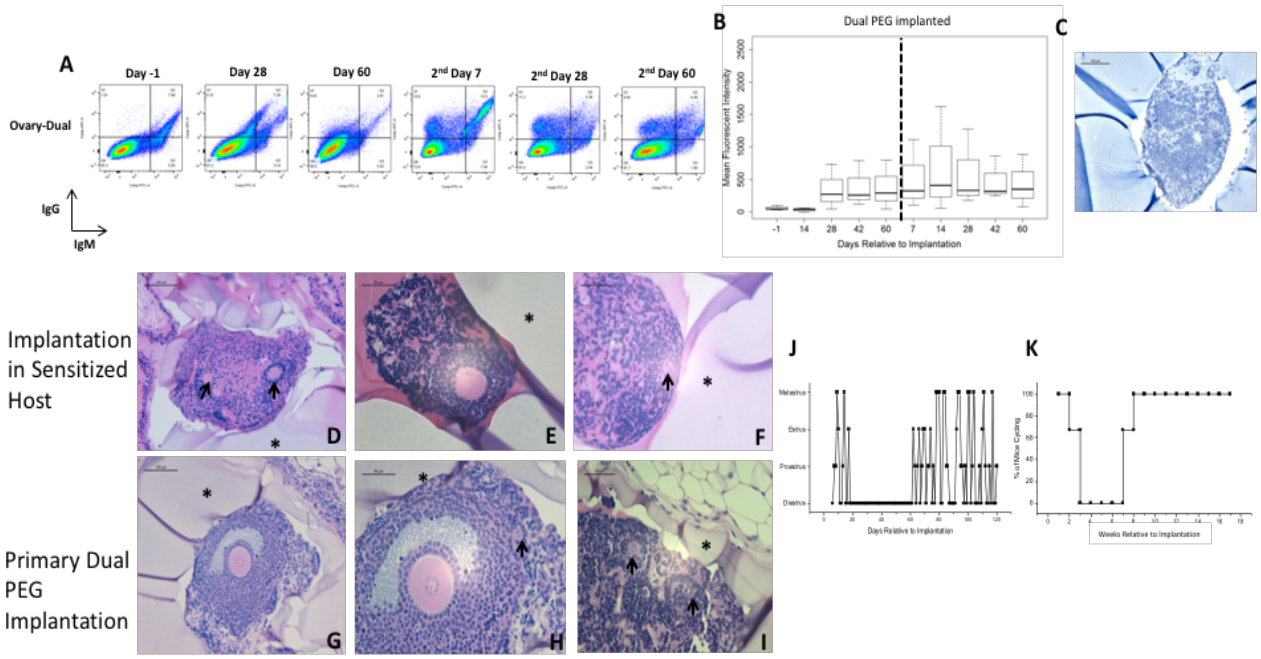

Figure 6.3: A)Representative flow cytometry plots of binding of serum allo-specific antibodies from recipients of Dual PEG encapsulated allogeneic ovary tissue in an already sensitized recipient, implanted with non-encapsulated ovarian tissue 60 days prior. Y-axis, donor-specific IgG; X-Axis, donor-specific IgM. The mean fluorescence intensity (MFI) for donor specific IgG reflects the average of values read on the Y-Axis.(**B**) Graph depicts the average MFI±SD of allo-specific IgG in mice receiving non-encapsulated ovarian tissue for 60 days followed by Dual PEG encapsulated ovarian tissue for 60 days. The mean fluorescence intensity (MFI) for donor specific IgG reflects the average of values read on the Y-Axis. (**C**) Immunohistochemical staining of CD8+ cells in Dual PEG-encapsulated ovarian allograft. Histological images of allogeneic ovarian tissue encapsulated in Dual PEG in a (**D-F**) sensitized host and (**G-I**) primary implantation in a naïve host. Representative plot of estrous activity of mice receiving a **(J)** non-encapsulated ovarian tissue and then Dual PEG encapsulated tissue. **(K)** Resumption of estrous activity in mice receiving a

non-encapsulated ovarian tissue and then Dual PEG encapsulated tissue. * indicates the PEG hydrogel. Black arrows mark supporting primordial and primary follicles. Scale bars: 50 μm (**E,F,H,I**), 100 μm (**C,D,G**).

6.4.3 Dual PEG precludes sensitization compared to non-encapsulated controls

We wanted to mimic the clinic and test allogeneic reaction in a sensitized environment. To confirm that F1 ovaries sensitize the BALB/c host, we implanted non-encapsulated ovarian allografts in naïve BALB/c mice. The first implantation period lasted 42 days, and was followed with another implantation of a non-encapsulated allograft for 14 days. Allo-specific immunity and subsequent sensitization is manifested by the production of allo-specific antibodies and cellular infiltration. **Figure 6.4A** demonstrates that donor-specific IgG increased significantly in recipient mice from undetectable to 742 MFI by 28 days after implantation of non-encapsulated ovaries. When these mice received a subsequent implantation of non-encapsulated allogeneic ovarian tissue, an increase in IgG was observed 7 days after implantation indicating a memory response took place. A memory response is when HLA antibodies are already present and when exposed to the same allo-antigen that the host had previously been exposed to, a rapid production of antibodies occurs resulting in faster kinetics of immune rejection (**Figure 6.4B**). In most cases (n=5 of 7), the graft could not be found in the mouse as rejection had occurred and eliminated the allograft. In a couple cases (n=2) where the grafts were retrieved histological analysis showed necrosis with no evidence of surviving healthy follicles (**Figure 6.4J**). The

presence of CD8+ T cells were present in the graft indicating cellular infiltration and subsequent immune rejection had taken place (**Figure 6.4C**).

To test whether ovarian allografts encapsulated in Dual PEG led to sensitization, we implanted mice with Dual PEG encapsulated ovarian allografts for 60 days followed by another ovarian allograft encapsulated in Dual PEG for an additional 60 days. Similar to our previous results, encapsulation of ovarian tissue in Dual PEG elicited minimal donor-specific antibodies as through 60 days IgG increased to 65 MFI, which is significantly lower than what is observed when the allogeneic ovarian tissue is not encapsulated (**Figure 6.4G**,**H**). When mice were implanted with ovarian tissue encapsulated in Dual PEG after an initial implantation of 60 days with Dual PEG, minimal allo-specific IgG was produced indicating the mice were not sensitized from the initial implantation and the ovarian tissue was immuno-isolated. When the encapsulated grafts were removed, we observed the presence of healthy developing follicles up to the antral stage (**Figure 6.3 G-I, Figure 6.4 L-M**), indicating the graft was protected against a host response and folliculogenesis was supported. Secondary and antral follicles are capable of producing estradiol in response to circulating gonadotropins, restoring ovarian endocrine function. All mice resumed estrous activity by 2 weeks following the initial implantation and continued cycling through the 120 day implantation period (**Figure 6.40,P**)

Additionally, no presence of CD4+ and CD8+ cells were present within the graft and capsule, indicating the Dual PEG capsule did not allow for cellular infiltration during both implantation periods (**Figure 6.4I**).

To confirm the lack of sensitization after implantation of ovarian tissue encapsulated in Dual PEG, mice were implanted with Dual PEG for 60 days and followed by an implantation of non-

encapsulated ovarian tissue. Non- sensitized mice by the ovarian tissue encapsulated in Dual PEG should respond similarly to the first implantation of the ovary-ovary group, as if it is the first time the host is the allo-antigens. As expected, during the 60 days of implantation period of encapsulated allograft, the production of IgG was minimal and remained below 100 MFI. Once the mice received non-encapsulated tissue following the 60 day Dual PEG implantation, allo-specific IgG rose to 666.6 MFI (**Figure 6.4 D,E**). Importantly, the kinetics and levels of the allo-specific IgG was very similar to the first implantation of the ovary-ovary group (**Figure 6.4A,B**) indicating the mice were not sensitized to the F1 ovarian tissue that had been in present in the mice in Dual PEG for 60 days. Interestingly, while the dual PEG immunoisolating capsule protected the ovarian allograft the host did not develop tolerance towards the allogeneic tissue, which was rejected when implanted without the immunoisolating capsule. No presence of CD8+ cells were observed (**Figure 6.4F**) and healthy developing follicles were found in the encapsulated tissue retrieved from the Dual PEG graft after 120 days indicating long-term graft survival was supported (**Figure 6.4K**).

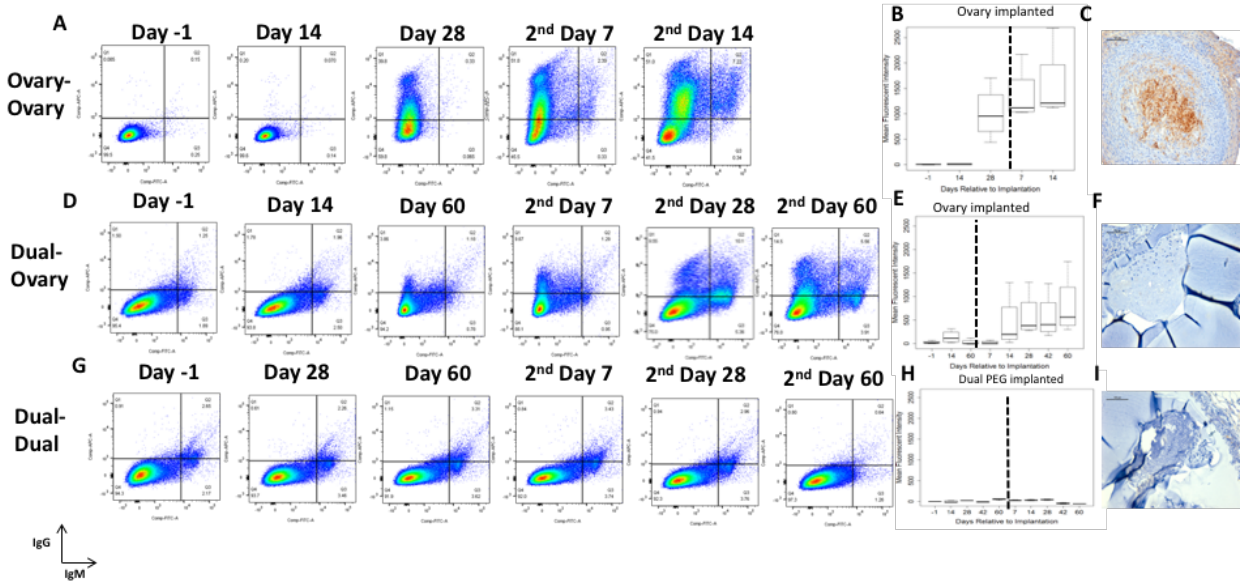

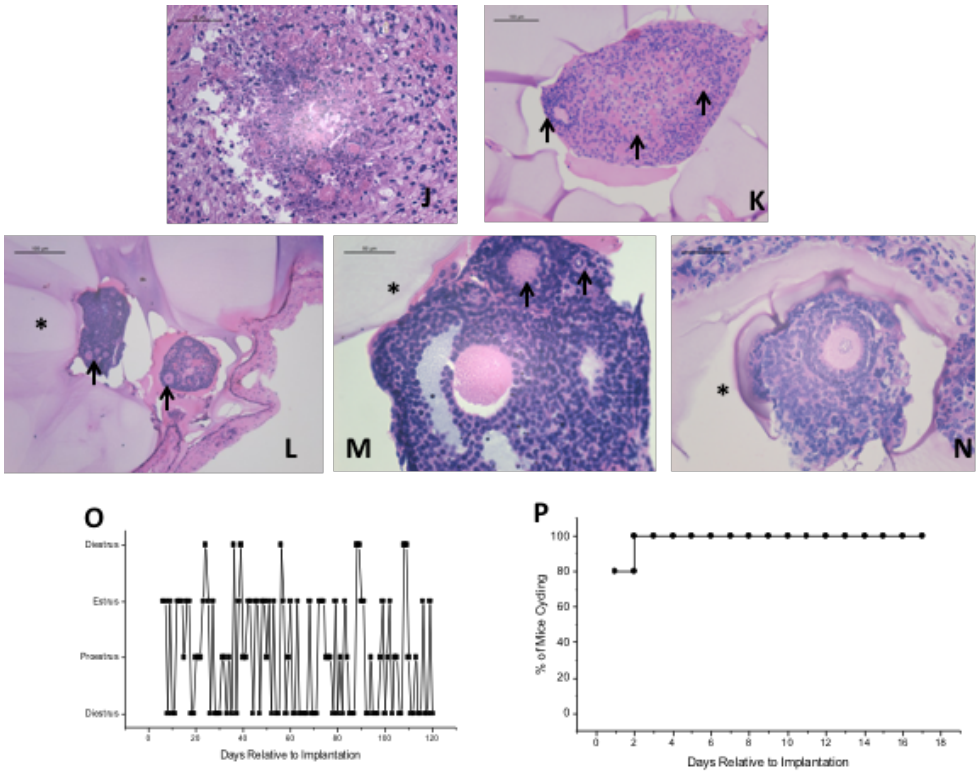

Figure 6.4: Representative flow cytometry plots of binding of serum allo-specific antibodies from recipients of (**A**) non-encapsulated allogeneic ovary tissue first for 42 days and then again received non-encapsulated ovarian tissue , (**D)** Dual PEG encapsulated ovarian tissue and then non-encapsulated ovarian tissue, and **(G)** consecutive Dual PEG encapsulated ovarian tissue, to donor cells. Y-axis, donor-specific IgG; X-Axis, donor-specific IgM. The mean fluorescence intensity (MFI) for donor specific IgG reflects the average of values read on the Y-Axis; the MFI for donor specific IgM reflects the average of values read on the X-Axis Graph depicts the average MFI±SD of allo-specific IgG in mice receiving (**B**) non-encapsulated allogeneic ovarian tissue followed by another non-encapsulated tissue implantation, **(E)** Dual PEG encapsulated ovarian tissue followed by non-encapsulated ovarian tissue, and **(H)** two consecutive Dual PEG encapsulated ovarian allografts. Immunohistochemical images of CD8+ cells in (**C**) non-

encapsulated ovarian tissue, (**F**) Dual PEG encapsulated tissue, and (**I**) Dual PEG encapsulated tissue following an initial Dual PEG implantation. Histological images of (**J**) non-encapsulated ovarian tissue and (**K**) Dual PEG encapsulated ovarian tissue in mice receiving both encapsulated and non-encapsulated tissue, and (**L-N)** Dual PEG encapsulated ovarian tissue following a primary Dual PEG implantation. Representative plot of estrous activity of mice receiving a **(O)** Dual PEG encapsulated tissue and then another Dual PEG encapsulated tissue. **(P)** Resumption of estrous activity in mice receiving consecutive Dual PEG encapsulated tissue implantations. * indicates the PEG hydrogel. Black arrows mark supporting primordial and primary follicles. Scale bars: 50 µm (**J,M,N**), 100 µm (**C,F,I,K,L**).

6.5 Discussion

In this study, we investigated whether encapsulating ovarian allografts in PEG based capsules protects against sensitization of the host immune system in an immune competent ovariectomized murine model. If encapsulation precludes sensitization, ovarian graft survival is prolonged and ovarian endocrine function is restored. Previously, we have demonstrated that the Dual PEG capsule containing a degradable core with a non-degradable shell supports ovarian survival and development leading to restoration of ovarian endocrine function [172]. Additionally, we've shown that in an immune competent model, encapsulation of allogeneic ovarian tissue in Dual PEG did not result in elevated allo-antibodies or allow cellular infiltration, resulting in the graft surviving and restoring endocrine function. While we have shown that allogeneic tissue encapsulated in Dual PEG survives in an immune competent mouse, the question remained whether the host is exposed to allo-antigens during the implantation period

resulting in sensitization and the host immune system being primed to reject any subsequent implantations that may follow. This would be crucial to answer in the application of ovarian tissue allotransplantation as we hypothesize patients would receive numerous implantations through their treatment to maintain ovarian endocrine function.

We tested whether consecutive implantations of non-encapsulated allogeneic ovarian tissue resulted in sensitization of the host, measured by allo-specific antibody levels in the recipient's serum. As hypothesized, the introduction of an ovarian allograft, followed by another ovarian allograft resulted in sensitization of the host and rapid rejection of the secondary implantation. This was indicative by the increase in IgG by 7 days after the second implantation, which is much more rapid than the kinetics of antibody production if the host's B cells had never seen the F1 allo-antigens before. Rejection was confirmed by no presence of follicles in the grafts.

Conversely, we compared these results to encapsulated allogeneic ovarian tissue. When implanting mice with ovarian allografts encapsulated in Dual PEG, followed by another ovarian allograft encapsulated in Dual PEG, we observed no levels of elevated allo-specific antibodies in the first or second implantation, indicating encapsulation precludes sensitization. We hypothesize that this is based on size exclusion and the inability for antigen presenting cells to come in contact with allo-antigens and propagate a subsequent humoral and cellular response. Precluding sensitization is vital for ovarian tissue survival in allotransplantation as patients will receive multiple grafts throughout their treatment. The fact that the encapsulated ovarian tissue was not rejected was confirmed by the presence of healthy developing follicles present in the graft, up to the antral stage. The presence of secondary and antral confirms the graft was

immuno-isolated from the outside immune environment, leading to the restoration of endocrine function.

Previous studies have studied sensitization in transplantation through skin or kidney transplants [198. 199], where tissue/organs is transplanted in the recipient and the immune system is exposed to allo-antigens resulting in sensitization to that strain of animal. For the application of ovarian tissue allo-transplantation, we used a similar concept to test whether the Dual PEG capsule precludes sensitization utilizing allogeneic ovarian tissue. To confirm encapsulation of ovarian allografts in Dual PEG precludes sensitization, we implanted mice with encapsulated ovarian allografts and either followed that with a subsequent non-encapsulated ovarian allograft or implanted the capsule in previously sensitized mice. As hypothesized, when implanting encapsulated ovarian tissue, elevated IgG levels were not observed through 60 days. The tissue was functional as healthy follicles were observed via histological analysis. When following that implantation with a non-encapsulated ovarian allograft, interestingly, allo-antibody levels did rise significantly, indicating an immune response, but at the kinetics similar to that of the first implantation in the mice receiving two ovarian allografts consecutively. This indicates that the host immune system had not been exposed to the allo-antigens present in the non-encapsulated ovarian allografts even though encapsulated allogeneic ovarian tissue was present in the Dual PEG capsule for 60 days. When encapsulated ovarian allografts were implanted in previously sensitized mice, we demonstrated that allo-antibody levels did not rise following that implantation and in fact, plateaued; indicating the sensitized mice were not further being exposed to allo-antigens and a memory response was not mounted.

Previously, we have shown changing the degradability of the capsule impacts the ability to protect allogeneic ovarian tissue against an immune response. Day et al demonstrated ovarian tissue encapsulated in a proteolytically degradable PEG matrix crosslinked via Michael-type addition (MT PEG) resulted in some grafts being rejected, resulting in elevated IgG, cellular infiltration and failure to restore endocrine function; while some grafts were protected and rejection was not observed similar to Dual PEG. We hypothesize that this is due to the degradable nature of the capsule and as the cells secrete proteases, the pores of the network become larger leading to the encapsulated allogeneic tissue being more susceptible to interaction with the host immune system. This led us to hypothesize that antigen presentation may also be impacted and the interaction with the immune system may be completely different than in Dual PEG. To test this, we implanted mice with ovarian allografts encapsulated in MT PEG for 60 days followed by a subsequent non-encapsulated ovarian allograft. Following the initial implantation of MT PEG, we did not observe a significant increase in IgG production. Healthy follicles were present in the graft following explantation indicating the encapsulated tissue was functional. Interestingly, when we followed the initial 60-day implantation with non-encapsulated allografts, we demonstrated elevated IgG production, but it was slightly lower than when a non-encapsulated allograft followed a Dual PEG implantation. Previous, studies have shown that a slow delivery of antigens may induce a tolerogenic effect on the host immune system. Further studies must be conducted to test whether encapsulating ovarian allografts in MT PEG induces tolerance by manipulating the kinetics of exposure to allo-antigens. This however demonstrates that antigen presentation may be different based on nature of the network the tissue is encapsulated in as the accessibility of the antigens is altered.

In summary, encapsulating allogeneic ovarian tissue in an immune-isolating capsule precludes sensitization of the host immune system, protecting the tissue and resulting in ovarian endocrine function restoration. For patients experiencing POI, this allogeneic cell-based therapy delivers hormones in a pulsatile self-regulating manner, potentially avoiding adverse side effects observed with pharmacological treatments and the risk of re-introducing cancerous cells. The ability for Dual PEG to preclude sensitization is vital as we envision patients receiving multiple grafts as some patients who experience POI as a child or adolescent have a treatment period spanning decades. This is the first report to demonstrate that the Dual PEG capsule completely hides the ovarian tissue from the host immune response and the encapsulated tissue does not sensitize the host. Future non-human primate and xenogeneic models using human tissue must be conducted as the genetic makeup of these animals is much more diverse than inbred mice and the kinetics of growth of ovarian tissue is different, which may impact the ability to immuno-isolate tissue and preclude sensitization.

6.6 Materials and Methods

6.6.1 Experimental Design

Adult cycling female mice (BALB/c) underwent bilateral ovariectomies to induce POI. As a positive control for sensitization, BALB/c mice were implanted subcutaneously with a non-encapsulated ovary from 6-8 day old CBAXC57Bl/6 (F1) mice for 42 days and followed by a subsequent implantation of another non-encapsulated F1 ovary for 14 days. For experimental groups, BALB/c mice were (i) implanted with non-encapsulated F1 ovarian tissue for 60 days followed by an implantation of ovarian tissue encapsulated in Dual PEG for 60 days (ii) implanted with

encapsulated ovarian tissue in Dual PEG for Dual PEG for 60 days followed by ovarian tissue encapsulated in Dual PEG for another 60 days (iii) implanted with F1 ovarian tissue encapsulated in Dual PEG for 60 days followed by an implantation of non-encapsulated F1 ovarian tissue for another 60 days (**Figure 6.1**).

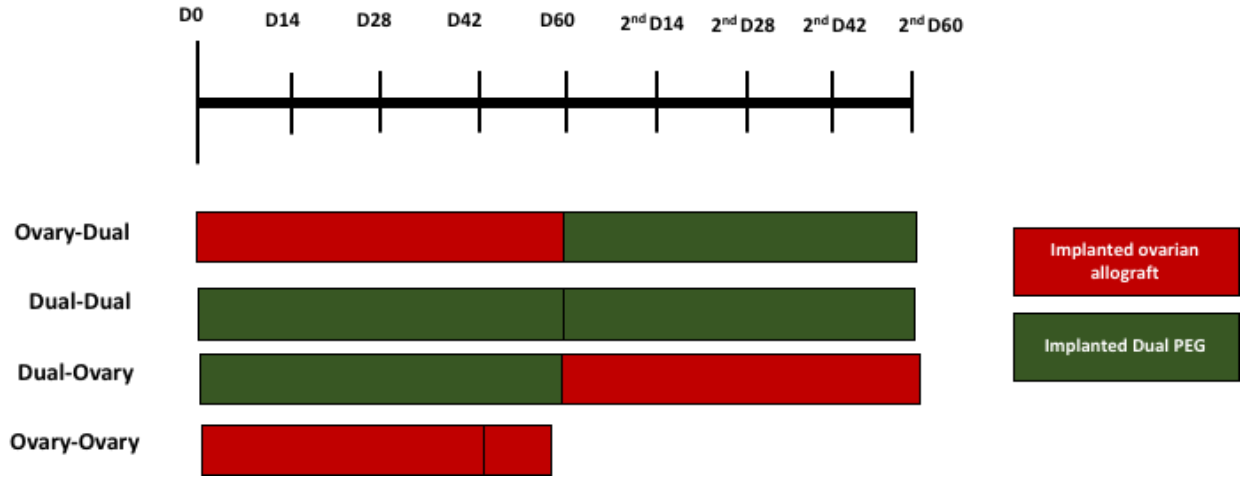

Figure 6.1: Experimental design to test sensitization in mice.

6.6.2 Ovariectomies in Recipient Mice

The IACUC guidelines for survival surgery in rodents and the IACUC Policy on Analgesic Use in Animals Undergoing Surgery were followed for all the procedures. Animal experiments for this work were performed in accordance with the protocol approved by the Institutional Animal Care and Use Committee (IACUC) at the University of Michigan (PRO00007716).

Bilateral ovariectomies were performed on adult female mice (BALB/c) aged 12–16 weeks. The mice were anesthetized by isoflurane. Carprofen (5mg/kg. body weight, Rimadyl, Zoetis) was administered subcutaneously for analgesia. The intraperitoneal space was exposed through a

midline incision in the abdominal wall secured using an abdominal retractor. The ovaries were removed, and the muscle and skin layer of the abdominal wall were closed with 5/0 absorbable sutures (AD Surgical). The mice recovered in a clean warmed cage and received another dose of Carprofen 12 hours post recovery or as needed.

6.6.3 Collection of Donor Ovaries

Ovaries from 6 to 8 days old CBAXC57Bl/6 (F!) or BALB/c mice were collected and transferred to Leibovitz L-15 media (Sigma-Aldrich, USA). The ovaries were dissected into 2–4 pieces and transferred in the maintenance media (α-MEM, Gibco, USA) and placed in the CO_2 incubator for further manipulation.

6.6.4 Hydrogel Preparation and Ovarian Tissue Encapsulation

To prepare MT PEG hydrogels, 8-arm PEG-VS (40kDa, Jenkem Technology, Beijing, China) was cross-linked with a plasmin sensitive tri-functional peptide sequence (Ac-GCYK↓NSGCYK↓NSCG, MW 1525.69 g/mol, >90% Purity, CelTek, ↓ indicates the cleavage site of the peptide). Dual PEG hydrogels were prepared using 4-arm PEG-VS 20kDa, Jenkem Technology) with Irgacure 2959 (Ciba, Switzerland, MW=224.3) and 0.1% N-vinyl-2-pyrrolidone (Sigma-Aldrich, St. Louis, USA). The detailed protocol is described in Day et al. [172] donor ovaries were collected from 6-8 days old BALB/c mice. The collected ovaries were transferred to Leibovitz L-15 media (Sigma-Aldrich, USA) and dissected open. The ovarian tissue was then transferred into maintenance media (α-MEM; Gibco, USA), kept at 37˚C and 5% CO_2. For encapsulation in the MT PEG, the ovarian tissue was transferred into a 10 μL droplet of the plasmin sensitive tri-functional peptide and PEG-VS

precursors' solution. The droplet was allowed to crosslink for 5 minutes and then was quenched in maintenance media (**Figure 4.1A**). For Dual PEG hydrogel encapsulation, the tissue was first encapsulated in a 4 μL MT PEGhydrogel and was then placed in the center of a 10 μL bead of PEG-VS precursor solution (5% w/v PEG-VS, .4% Irgacure 2959, 0.1% NVP) and exposed to UV light for 6 minutes(**Figure 4.1E**). All constructs were imaged immediately after encapsulation of the tissue.

6.6.5 Subcutaneous Implantation

A small incision was made on the dorsal side of the anesthetized mice (BALB/c) and the immunoisolators (MT PEG, Dual PEG) with the ovarian tissue or non-encapsulated ovarian tissue were implanted subcutaneously. The skin was closed using 5/0 absorbable sutures. The mice received Carprofen for analgesia for at least 24 hours after surgery or as needed.

6.6.6 Histological analysis of the retrieved devices and the encapsulated ovarian tissue

Following sacrifice, the immuno-isolating devices were retrieved from mice, fixed in Bouin's fixative at 4°C overnight, transferred and stored in 70% ethanol at 4°C. After processing, samples were embedded in paraffin, serially sectioned at 5 μm thickness, and stained with hematoxylin and eosin.

6.6.7 Vaginal Cytology

To assess for resumption of estrus activity, daily vaginal cytology was performed. To assess estrous cycle cessation after ovariectomy, vaginal cytology was performed seven days post-

surgery. After transplantation, vaginal cytology was resumed seven days post-operation and was performed daily until sacrifice. The transition from leukocytes to cornified cells at least once a week was counted as a resumed or continued cycle.

6.6.8 Flow Cytometry

Serum allo-antibody titer measurements were performed using flow cytometry before and after implantation and reported as mean fluorescence intensities (MFI) for the highest dilution showing fluorescence detectable above background (non-immune serum from a non-implanted mouse) in immunized mice (positive controls implanted with allogeneic ovaries without a device). Thymocytes were isolated from CBAXC57Bl/6 mice and incubated with serially diluted recipient serum for 30 minutes at 4˚C. Antibodies bound to the thymocytes were detected by Cy5-conjugated goat anti-mouse IgG (1:250 dilution, 1030-15, Southern Biotech) and Alexa Fluor 488-conjugated goat anti-mouse IgM (1:250 dilution, 1020-30, Southern Biotech) for 30 minutes at 4˚C and analyzed in a BD FACSCanto II (BD Biosciences, Franklin Lakes, NJ). The mean fluorescence intensities (MFI) in the APC-channel (measuring bound IgG) and FITC channel (measuring bound IgM) were determined with FlowJo 10 software (FlowJo, LLC, Ashland, OR).

6.6.9 Immunohistochemistry for T cells

To analyze T cell infiltration following into non-encapsulated or encapsulated ovarian allografts, paraffin-sectioned slides were stained to identify CD4 and CD8+ cells. First, sections were deparaffinized with Xylene and rehydrated. The slides were incubated in antigen retrieval buffer, pH9.0 (ab94681, Abcam) for 20 minutes at 97°C and additional 20 minutes at room temperature

to cool down. Next, the slides were incubated with KPL Universal Block (5560-0009, Sera-Care) to block non-specific binding sites for 30 minutes at room temperature. The sections were incubated at room temperature for 1 hour with primary antibodies: rabbit monoclonal anti-mouse CD4 antibody (1:1000 dilution, ab183685, Abcam), rabbit polyclonal anti-mouse CD8 antibody (1:500 dilution, ab203035, Abcam). The slides were subsequently incubated at room temperature with secondary antibodies: goat anti-rabbit Ig (1:100 dilution for 15 minutes, 4010-05, Southern Biotech) for CD4 and goat anti-rabbit (1:50 dilution for 30 minutes, 4010-05, Southern Biotech) for CD8. Diaminobenzidine (BDB2004L, Betazoid DAB Chromogen kit, BioCare Medical) was used as a chromogen for 10 minutes at room temperature. Hematoxylin (220-102, Fischer Scientific) was used as a counterstain. For negative-controls, paraffin sections were incubated without the primary antibody. To assess presence or absence of CD8+ cells, 12 sections from the front, middle, and end of each specimen were examined, to represent the full thickness of the implant.

6.6.10 Statistics

Statistical analysis was performed using the R software version 3.1.2 (2014). Significance was determined by Welch's two-sample t-test.

CHAPTER VII

Ovarian Allograft Encapsulated in Immuno-isolating Dual PEG Restores Ovarian Endocrine Function in an Ovariectomized Adolescent Rhesus Monkeys

7.1 Authors

James R. Day, Anu David, Dennis J. Hartigan-OConnor, Mayara Garcia de Mattos Barbosa, Michele L. Martinez, Charles Lee, Jenna Barnes, Evan Farkash, Marilia Cascalho, Alice Tarantal, Ariella Shikanov

7.2 Abstract

A common complication of life-saving chemo and radiotherapy treatments is premature ovarian insufficiency (POI) due to being gonadotoxic. POI can lead to a multitude of life long co-morbidities and is particularly devastating in patients who experience it prior to puberty; possibly resulting in deleterious effects to bone health, cardiovascular health, cognition, and metabolic balance. The only available treatment for POI during puberty is hormone replacement therapy (HRT), which delivers non-physiological levels of estrogen, lacks other ovarian hormones and pulsatility, and is not responsive to feedback regulation. We have previous shown that the use of an immuno-isolating capsule can support allogeneic ovarian tissue, restoring ovarian endocrine function without causing an immune response in a murine model. Here, we report non-human primate ovarian tissue encapsulated in immune-isolating capsules survives and develops, restoring ovarian endocrine function without evoking an immune response in a syngeneic and allogeneic non-human primate model of POI. Ovariectomized monkeys implanted with

encapsulated either syngeneic and allogeneic ovarian tissue demonstrated pulsatile levels of estradiol (E1C) and progesterone (PdG) throughout the 4 and 5 month implantation period with levels rising to up to 50 and 70ng/mg Cr, respectively. Healthy developed follicles up the antral stage were observed following explantation of the capsule. Importantly, a minimal immune response was provoked by the encapsulated allogeneic tissue as a low percentage of recipient CD4+ and CD8+ cells divided when exposed to the allogeneic donor cells. This demonstrates the immuno-isolating capsule can support the large volumetric expansion present during NHP folliculogenesis without compromising its immuno-isolating capabilities, leading to long term graft survival and restoration of ovarian endocrine function. This is the first report to demonstrate an immuno-isolating capsule can be used to allow for ovarian tissue allo-transplantation, restoring ovarian endocrine function and preventing an immune response in an allogeneic non-human primate model.

7.3 Introduction

Over the past decades, childhood cancer survival rates have increased substantially reaching over 85% due to advances in cancer therapies. However, the same cancer therapies can potentially lead to a myriad of health complications in childhood cancer survivors [8,24,46,47,163,165]. One of the most common complications for female cancer survivors is premature ovarian insufficiency (POI) as the treatments are gonadotoxic. POI leads to depletion of the follicular pool, resulting in infertility and disruption of ovarian endocrine function. POI is particularly detrimental in children that experience it prior to undergoing puberty, as the puberty is one of the most important physiological events in a female's life and the effects are irreversible. Changes occurring during

puberty promote the physical and psychologic development into adulthood determining height, bone health, insulin responsiveness, lipid metabolism, cardiovascular health and cognition [9-11]. These changes are initiated before puberty and orchestrated by the pulsatile secretion of gonadotropin releasing hormone (GnRH) and growth hormone (GH) from the hypothalamus, which regulates the release of gonadotropins, luteinizing (LH) and follicle-stimulating (FSH) hormones from the pituitary. FSH and LH stimulate the ovaries to produce ovarian hormones and peptides including estradiol, androstenedione, progesterone, inhibins A and B, activin and follistatin. All of these hormones have a systemic effect in many organs and tissues downstream. This process is extremely regulated and ovarian hormones create a negative feedback loopy by inhibiting the production of GnRH and FSH in the brain and pituitary [12-14]. This creates a dynamic and pulsatile system known as the hypothalamic-pituitary-gonadal (HPG) axis, and the correct regulation of this axis is crucial for the development of reproductive, musculoskeletal, cardiovascular, and immune systems [15-16]. In young patients with POI, the HPG axis and the negative feedback is disrupted due to deficiencies in ovarian hormones, which leads to imbalances throughout the endocrine system resulting in comorbidities such as irregular bone development, metabolic changes, and abnormal fat deposition [19-21].

The only clinically available option to treat POI in adolescent girls and initiate puberty is hormone replacement therapy (HRT), HRT is the exogeneous delivery of hormones, specifically low levels of estrogen followed by progesterone replacement [44,45,167]. HRT was originally designed to treat postmenopausal systems in women and the impact on children using this methodology for a span of decades is not known [44]. Additionally, HRT delivers only a fraction of ovarian hormones in a non-pulsatile manner which does not mimic physiological puberty due to the

complexity of the HPG axis. In turn, HRT induced puberty in girls with POI can lead to premature closure of bone growth plates, cessation of bone growth, and metabolic imbalances [44,46-48]. Another experimental option to induce puberty in girls with POI is cryopreservation of ovarian tissue prior to anti-cancer treatments followed by auto-transplantation. This option could potentially restore both fertility and endocrine function and has led to more than 100 babies born to identical twin sisters and cancer survivors who cryopreserved their ovaries [29-35]; however; this option is associated with the risk of re-introducing malignant cells harbored in the stroma of ovarian tissue, particularly in patients with hematological malignancies which is common in childhood cancers [38-40]. There has been no universal protocol established to screen ovarian tissue for cancer cells and deem it as safe, which adds to the risk of re-implanting cryopreserved autologous ovarian tissue. Further, auto-transplantation cannot be performed if the patient did not cryopreserve their tissue prior to treatment, which is the most common case [180,197].

To provide physiological delivery of hormones and mitigate the risk of cancer re-implantation, we hypothesize an option for these patients is allo-transplantation from a donor. To avoid the use of immunosuppressive treatments, which have complications of their own, the concept of immuno-isolation must be utilized. Immuno-isolation is the use of a semi-permeable membrane to encapsulate allogeneic cells/tissue, which allows for free diffusion of necessary metabolites and nutrients but does not allow the infiltration of host immune cells preventing rejection. Previously, we have developed a novel synthetic poly(ethylene glycol) (PEG) hydrogel that sustains survival and function of allogeneic mouse ovarian tissue while preventing rejection. The proteolytically degradable core of the capsule provides a supportive environment for the

encapsulated and implanted tissue, while the non-degradable shell allows for diffusion of oxygen and nutrients, but physically prevents immune cell infiltration. Our earlier studies in mice have demonstrated that ovarian follicles and tissue encapsulated in the Dual PEG capsule develop and undergo the process of folliculogenesis, producing ovarian hormones in a regulated physiological manner, restoring ovarian endocrine function in a POI model [146, 172]. Additionally, we demonstrated the Dual PEG capsule was able to isolate the encapsulated allogeneic mouse ovarian tissue from the host immune environment preventing immune-mediated rejection by allo-specific antibodies and cellular infiltration [173]. However, to date, these studies have been conducted using a mouse model, which ovarian follicles grow to approximately 300 μm in size at the antral stage. Larger animals such as non-human primate and human follicles grow to greater than 500 microns and 2 centimeters, respectively. The objective of this study was to demonstrate Dual PEG can support non-human primate ovarian tissue restoring ovarian endocrine function in an ovariectomized syngeneic and allogeneic model. Previous groups have investigated the ability of ovarian tissue to restore fertility and normal hormone function in ovariectomized monkeys [200,201]; however, this study used autologous ovarian tissue so no encapsulation was needed as an immune response was not a factor. Here, we investigated whether the Dual PEG capsule can withstand the large volumetric expansion of monkey ovarian tissue present during folliculogenesis restoring ovarian endocrine function, while maintaining immuno-isolating capability in an allogeneic non-human primate model.

7.4 Results

7.4.1 Ovarian Tissue Encapsulated in PEG Capsules Develops and Restores Endocrine Function

We evaluated restoration of ovarian endocrine function by measuring levels of estradiol (E!C) and progesterone (PdG) in the urine daily. E1C and PdG levels were normalized to creatine levels in the urine. Additionally, any signs of menstruation were observed. After implantation of autologous tissue encapsulated in immuno-isolating capsules, the monkey demonstrated cyclic levels of progesterone and estradiol throughout the initial five-month implantation period. Estradiol and progesterone levels fluctuated from 12 to 69 ng/mg Cr and 8 to 55 ng/mg Cr (**Figure 7.2A**), respectively indicating the encapsulated tissue was producing ovarian hormones in a regulated, pulsatile manner. Levels would reach a depression and peak approximately every 7 days . After the other monkey in the first round of implantations received allogeneic ovarian tissue from the other monkey encapsulated in immuno-isolating capsules, pulsatile levels of E1C and PdG were observed as they fluctuated from 10 to 35 ng/mg Cr and 15 to 55 ng/mg Cr, fluctuating approximately every five days (**Figure 7.2C**). No signs of menstruation were observed in either monkey.

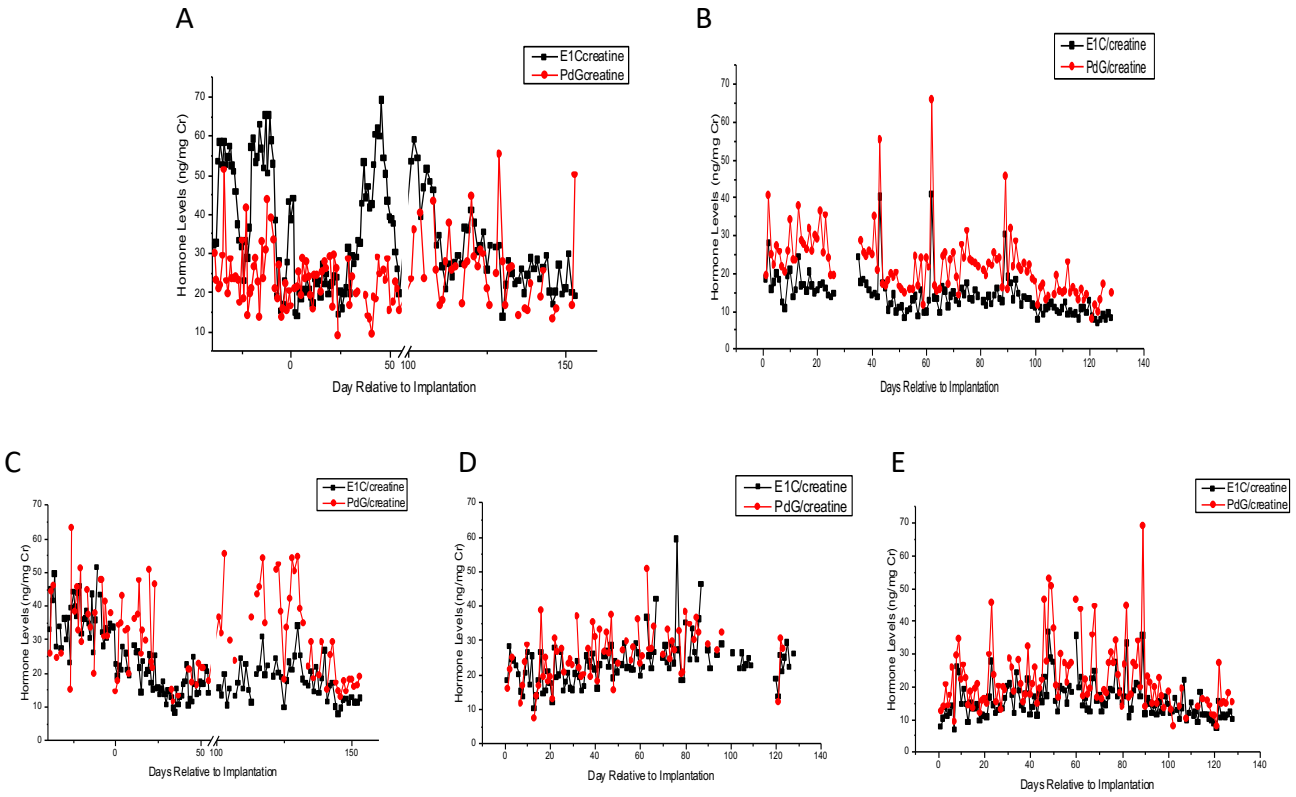

Figure 7.2: Estradiol (E1C) and PdG levels in urine of monkeys that received (**A**) encapsulated autologous tissue for 5 months, (**B**) encapsulated autologous tissue for 4 months, (**C**) encapsulated allogeneic tissue for 5 months and (**D,E**) encapsulated allogeneic tissue for 4 months. Levels are normalized to creatine levels in the urine.

After 5 months implanted subcutaneously, the capsules encapsulating autologous tissue were removed from one of the monkeys. No capsules in the monkey receiving encapsulated allogeneic tissues could be found or retrieved after 5 months. To evaluate the follicular development of the implanted ovarian tissue we analyzed tissue sections explanted after implantation by histological analysis. We observed the presence of healthy developing follicles indicating the process of

folliculogeneis was supported. All stages of follicles ranging from primordial to antral were observed (**Figure 7.3B,C**).

After explantation of the initial capsules, one of the monkeys from the initial implantation period was implanted with allogeneic ovarian tissue encapsulated in Dual PEG for 4 months. Similar to the initial implantation period, fluctuating E1C and PdG were observed for the entirety of the 4 months, although the E1C window of fluctuation was generally tighter and demonstrated more frequent pulsatility. E1C and PdG levels fluctuated from 10 to 59 ng/mg Cr and 5 to 50 ng/mg Cr, respectively, pulsing approximately every 4 days (**Figure 7.2D**). The second monkey was implanted with allogeneic ovarian tissue from another monkey encapsulated in Dual PEG for 4 months. During this time, this monkey demonstrated E1C and PdG levels ranging from 8 to 37 ng/mg Cr and 9 to 67 ng/mg Cr, respectively, pulsing approximately every 7 days (**Figure 7.2E**). When the capsules were removed, we observed the presence of ovarian tissue containing primordial and primary follicles (**Figure 7.3D,E**). Once the additional monkey was ovariectomized, it received its own tissue encapsulated in immuno-isolating capsules for 4 months. E1C and PdG pulsed from 10 to 40 ng/mg Cr and 11 to 68 ng/mg Cr, respectively with 3 very distinct peaks at Day 43, 62, and 89 (**Figure 7.2B**). Between the distinct peaks, the ovarian hormone levels were pulsatile but at a lower amplitude. When the capsules were extracted and sectioned and stained with hematoxylin and eosin, there was little evidence of healthy follicles present in the ovarian tissue.

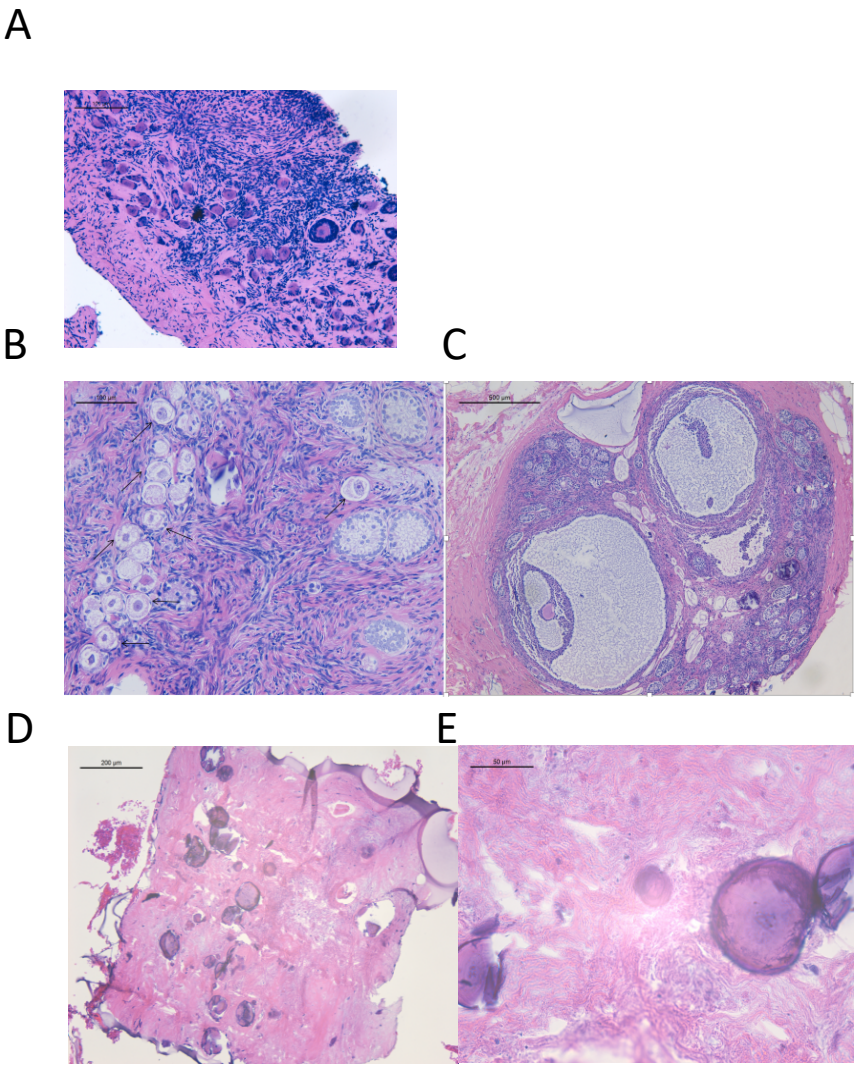

Figure 7.3: Histological analysis of (**A**) non-human primate ovarian tissue at time of implantation, (**B,C**) autologous NHP ovarian tissue encapsulated in immuno-isolating capsules for 5 months, and (**D,E**) allogeneic NHP ovarian tissue encapsulated in immune-isolating capsules for 4 months. Scale bars: 500µm(**C**), 200µm (**D**), 100µm (**A,B**), 50µm (**E**).

7.4.2 Ovarian Tissue Encapsulated in PEG Capsules Elicit Minimal Immune Response

To assess whether animals mounted an immune response against the encapsulated tissue, mixed lymphocyte cultures were performed. Cells from each monkey were tested for reactivity to

autologous cells (negative control) or to cells from the donor of the ovarian allograft. Through the entirety of the four-month implantation time, we observed no significant spike in active CD4+ T cells, with the transient peak being 1.0% of CD4+ cells dividing when cells from a recipient were exposed to cells from an allogeneic donor, which was not significantly higher than negative controls (**Figure 7.4A**). Similarly, there was no significant spike in dividing CD8+ cells in any of the animals when implanted with allogeneic or autologous ovarian tissue; the division was comparable with that seen after mixing responder cells with irrelevant, non-donor stimulators. The peak value observed was 1.5% of CD8+ dividing from a monkey receiving encapsulated allogeneic tissue during the first implantation, which is not significantly different than negative controls. When cells from one of the recipient monkeys were reacted with cells from an allogeneic donor, 0% of CD8+ cells were dividing 4 months after implantation even though allogeneic tissue was encapsulated and present in the recipient (**Figure 7.4B**).

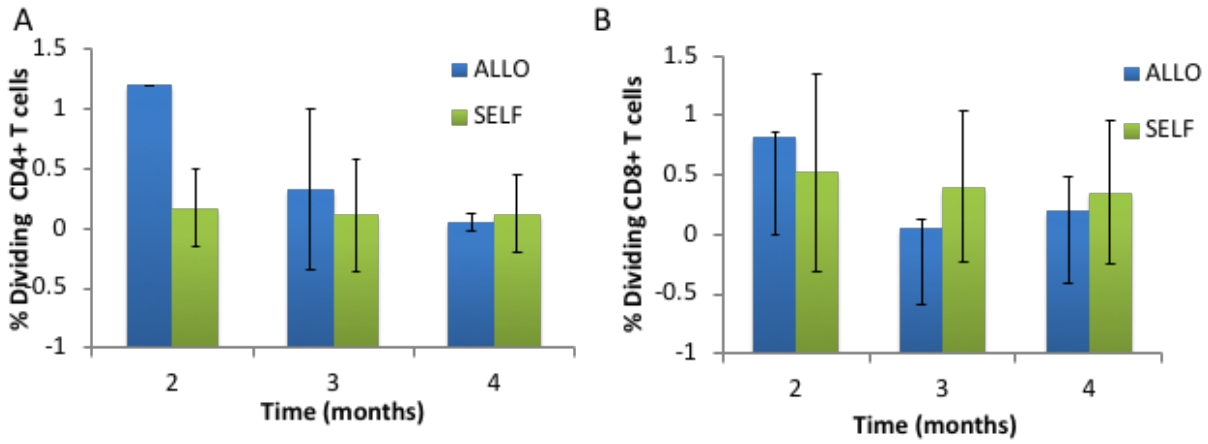

Figure 7.4: Mixed lymphocyte culture of recipient cells reacted with donor cells quantifying dividing (**A**)CD4+ and (**B**) CD8+ cells.(**C**) Immunohistochemical staining of CD8+ cells in encapsulated grafts.

7.5 Discussion

In this study we investigated the ability of a PEG based capsule to support follicular development and protect ovarian allografts from a host immune response, restoring ovarian endocrine function in an ovariectomized syngeneic and allogeneic non-human primate model. Previously, we have developed the Dual PEG capsule to contain a proteolytically degradable PEG core with a non-degradable photo-polymerized PEG shell [173,174]. Day et al demonstrated that the Dual capsule can support folliculogenesis, while protecting encapsulated ovarian allografts from a host immune response [accepted for publication,Scientific reports]. The core cross-linked with protease sensitive peptides supports the growth and development of murine primordial follicles [146, 172]), while the non-degradable shell acts as an immune-protective barrier that elicits a minimal inflammatory response [173]. Here, our results show that the Dual PEG capsule can support non-human primate ovarian allografts, restoring ovarian endocrine function in ovariectomized rhesus monkeys.

While we have previously shown that the Dual PEG capsule can support murine follicular development and protect ovarian allografts from immune rejection, the question remained whether the capsule can support the large volumetric expansion present in non-human primate folliculogenesis while not compromising the capsule's immuno-isolating ability. To measure restoration of endocrine function in a non-human primate POI model, E1C and PdG levels were measured in the urine. Once the monkeys were ovariectomized and implanted with ovarian tissue encapsulated in the respective capsules, they presented with cyclic pulsatile levels of E1C and PdG throughout the entirety of the implantation period. Prior to ovariectomy E1C and progesterone levels were peaking at 65 and 51 ng/mg Cr, respectively. During the implantation

period, E1C levels exceeded 50 ng/mg Cr indicating the HPG axis was restored and ovarian hormones were being produced from the encapsulated ovarian grafts. The presence of cyclic PdG confirmed that ovulation was occurring, although, interestingly, none of the monkeys showed evidence of menstruation upon observation but this may due to the age of the animals. Following transplantation, the presence of pulsatile ovarian hormones could be due to the activation of the implanted follicles and recruitment into the growing pool with pulse. To confirm whether the PEG capsules could support non-human primate folliculogenesis, histological analysis was performed to evaluate tissue morphology. Healthy follicles were consistently present in the histological analysis of the encapsulated ovarian implants in all monkeys. We observed the presence of all stages of follicles (up to the antral stage), indicating non-human primate folliculogenesis can be supported by PEG capsules. The fact that we observed antral follicles indicates that non-human primate ovarian tissue can undergo the massive volumetric expansion during folliculogeneis without being restricted by the Dual PEG capsule. We hypothesize this is due to the viscoelastic properties of the PEG matrix; allowing for a dynamic volumetric change without impacting the network. Upon macroscopic evaluation when explanting the capsules, there also appeared to be minimal inflammation around the implantation site, demonstrating the Dual PEG capsule elicits a minimal foreign body reaction, similar to previous findings [172,173].

Additionally, the presence of ovarian hormones in the transplanted animals and healthy ovarian follicles in the encapsulated ovarian grafts, even in an allogeneic transplantation, indicates the Dual PEG capsule protected encapsulated ovarian allografts from a host immune response. To measure whether implanted monkeys have mounted an immune response against the

encapsulated allografts, mixed lymphocyte cultures were performed. We observed that when cells from any of the monkeys were exposed to cells from the monkey of the respective implanted allograft, a minimal reaction took place (compared to positive controls), indicated by the low percentage of CD4+ and CD8+ that divided upon exposure. In turn, this demonstrates the monkeys were not sensitized to the allo-antigens and the PEG capsules immune-isolated the encapsulated non-human primate ovarian allografts. Importantly, the PEG capsules were able to support folliculogenesis and protect the encapsulated tissue from an immune response, indicating the capsule is able to withstand the 10-fold volumetric change present during non-human primate folliculogenesis without compromising the immuno-isolating capability.

Lee et al have reported the restoration of ovarian endocrine function in ovariectomized non-human primates; however, this study was exclusively in a syngeneic model, necessitating a heterotopic implantation and negating the use of an immune-isolating capsule [201]. This report is the first to demonstrate the use of an immune-isolating Dual PEG capsule can support non-human primate folliculogenesis while protecting the ovarian allograft from an immune response, restoring ovarian endocrine function in an allogeneic model.

In summary, the approach of hydrogel-based immune-isolation presents a minimally invasive and a robust way to restore hormonal balance in non-human primates. We have shown that the Dual PEG capsule can support non-human primate folliculogenesis in an allogeneic model. Further studies testing the ability of the Dual PEG capsule to support human ovarian tissue and promote corpus luteum formation must be conducted. Further capsule modification may be required to promote vasculature formation and greater diffusion of necessary metabolites and nutrients without the risk of immune rejection. Because this cell-based approach delivers hormones in a

pulsatile self-regulating manner, adverse side effects and long-term comorbidities associated with pharmacological treatments can be avoided.

7.6 Materials and Methods

7.6.1 Experimental Design

We performed two rounds of subcutaneous implantations of encapsulated autologous and allogeneic ovarian fragments. In the first round, two animals received 20 encapsulated ovarian fragments (N=1 autologous and N=1 allogeneic). The implants were retrieved after 5 months. In the second round three animals received 20 encapsulated ovarian fragments (N=1 autologous and N=2 allogeneic) (Figure 7.1). The implants were retrieved after 4 months. All animal procedures conformed to the requirements of the Animal Welfare Act and protocols were approved prior to implementation by the Institutional Animal Care and Use Committee (IACUC) at the University of California, Davis. Activities related to animal care (diet, housing) were performed per IACUC approved California National Primate Research Center standard operating procedures (SOPs). Physical signs were monitored daily and body weights assessed each time the animals were sedated for surgery or sample collection.

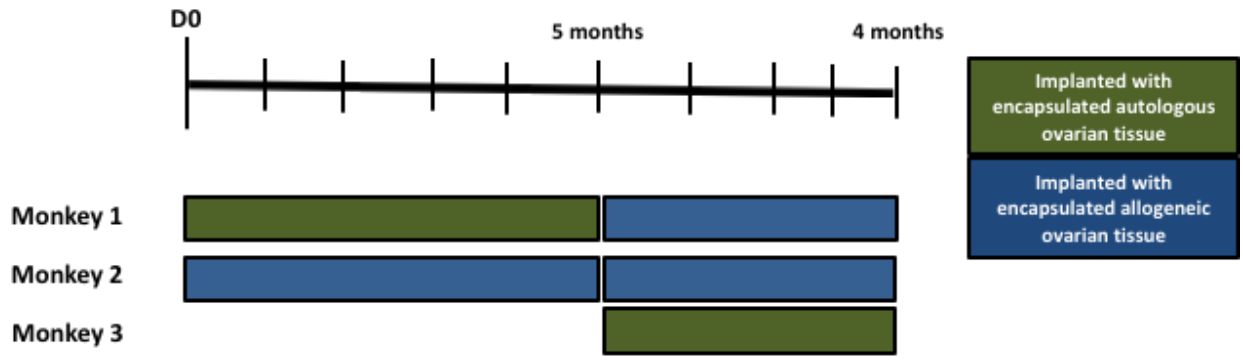

Figure 7.1: Experimental design of encapsulated autologous and allogeneic non-human primate tissue implanted into non-human primates (n=3).

7.6.2 Ovariectomies in Recipient Non-human Primates

Animals were sedated with ketamine (10 mg/kg; IM) and prepared for bilateral ovariectomy according to established protocols. Briefly, atropine was administered (0.04 mg/kg) and the animals intubated and placed on intravenous (IV) fluids and inhaled isoflurane. A small incision was made, and the ovaries exposed and removed individually and placed in a sterile culture dish for processing. During processing the incision was closed according to surgical SOPs. Ovarian tissue from Animal A was encapsulated in hydrogel under aseptic conditions in both Animal A and Animal B. Ovarian tissue from Animal B was processed then cryopreserved using a controlled-rate cryopreservation protocol. Once the encapsulated tissue was ready for Animal A, a small incision (~0.5 cm) was made between the scapulae (right and left). The encapsulated tissue was gently inserted under aseptic conditions then the incisions sutured closed and skin glue added. Animal B received encapsulated tissue from Animal A with insertion and closure as described.

Blood and urine samples were collected regularly as described below. All animals were monitored post-surgery per SOP and administered analgesics post-operatively.

At approximately five months post-surgery all animals were prepared for surgery as described above. The third monkey was ovariectomized and received autologous tissue (right ovary). The initial hydrogels were removed from the initial two animals, and then received encapsulated tissue from the third monkey. At approximately four months post-implantation the encapsulated tissue was collected for analysis.

7.6.3 Collection of Donor Ovaries

Ovaries from rhesus monkeys were collected following ovariectomy and transferred to Leibovitz L-15 media (Sigma-Aldrich, USA). The ovaries were dissected into approximately 60 1X1mm pieces and transferred into maintenance media (α-MEM, Gibco, USA) for encapsulation.

7.6.4 PEG Hydrogel Preparation and Ovarian Tissue Encapsulation

To prepare MT PEG hydrogels, 8-arm PEG-VS (40kDa, Jenkem Technology, Beijing, China) was cross-linked with a plasmin sensitive tri-functional peptide sequence (Ac-GCYK↓NSGCYK↓NSCG, MW 1525.69 g/mol, >90% Purity, CelTek, ↓ indicates the cleavage site of the peptide). Dual PEG hydrogels were prepared using 4-arm PEG-VS 20kDa, Jenkem Technology) with Irgacure 2959 (Ciba, Switzerland, MW=224.3) and 0.1% N-vinyl-2-pyrrolidone (Sigma-Aldrich, St. Louis, USA). The detailed protocol is described in Day et al. [172] for encapsulation in the MT PEG, the ovarian tissue was transferred into a 10 μL droplet of the plasmin sensitive tri-functional peptide and

PEG-VS precursors' solution. The droplet was allowed to crosslink for 5 minutes and then was quenched in maintenance media. For Dual PEG hydrogel encapsulation, the tissue was first encapsulated in an 8 μL MT PEG hydrogel and was then placed in the center of a 20 μL bead of PEG-VS precursor solution (5% w/v PEG-VS, .4% Irgacure 2959, 0.1% NVP) and exposed to UV light for 6 minutes.

7.6.5 Subcutaneous Implantation

Two small incisions were made on the dorsal side of the anesthetized monkey and the immunoisolators (MT PEG, Dual PEG) with the ovarian tissue were implanted subcutaneously. The skin was closed using 5/0 absorbable sutures.

7.6.6 Urine Hormone analysis

Urine samples were collected daily from cage pans according to SOP starting one month prior to surgery and through the post-implantation period. Collected samples were centrifuged at 1,500 g for 10 minutes then supernatant (~2-3 ml) transferred to a cryogenic vial (Caplugs Evergreen, Buffalo, NY) and stored at ≤-20˚C until processed. Urinary estrone conjugates (E1C) and pregnanediol-3-glucuronide (PdG) were determined according to established protocols [202,203]. Urine was not collected and analyzed from day 98 to day 145 in the first four-month implantation.

7.6.7 Histological analysis of the retrieved devices and the encapsulated ovarian tissue

Following sacrifice, the immuno-isolating devices were retrieved from monkeys, fixed in 4%

paraformaldehyde at 4°C overnight, transferred and stored in 70% ethanol at 4°C. After processing, samples were embedded in paraffin, serially sectioned at 5 µm thickness, and stained with hematoxylin and eosin.

7.6.8 Mixed Lymphocyte Culture

PBMC were isolated by centrifugation onto a step gradient of Lymphocyte Separation Medium (LSM; MP Biomedicals, LLC, Solon, OH). Stimulator cells were treated with 40 µg/ml mitomycin C (Sigma) at 37 C for 30 min. CFSE-labeled responder cells were stimulated with an equal number of unlabeled stimulator cells or with plate-bound anti-CD3 antibody (positive control; clone SP34-2). Cells were harvested after 4-6 days of incubation, stained with fluorescently labeled antibodies including those specific for CD4 and CD8 (clones L200 and 3B5, respectively); cytometry data were collected on a BD Fortessa; and the results were analyzed in FlowJo's proliferation platform.

7.6.9 Statistics

Statistical analysis was performed using the R software version 3.1.2 (2014). Significance was determined by Welch's two-sample t-test.

CHAPTER VIII

Conclusions and Future Directions

8.1 Summary of Findings

The aim of the doctoral thesis presented here was to develop means to restore ovarian endocrine function using donor ovarian allogeneic tissue without immunosuppression. We hypothesized that encapsulation of ovarian tissue in immuno-isolating capsule that allows diffusion of nutrients and growth factors while preventing infiltration of immune cells from the host would restore ovarian endocrine function. This dissertation describes the process of identifying the materials, physical characterization of the hydrogels and animal studies to determine survival and function of the implanted grafts and the immuno-isolating abilities of the capsule. We hypothesized that PEG would be an appropriate material for immuno-isolation of ovarian tissue because it is viscoelastic, tunable, inert, robustly functionalized, and can form hydrogels in a physiologically appropriate environments. Variability of the functional end groups on PEG macromolecules supports crosslinking and gelation via a multitude of chemistries. First, we demonstrated that PEG-vinyl sulfone (PEG-VS) was most appropriate to create an immuno-isolating barrier for ovarian tissue in comparison to PEG-acrylate (PEG-Ac) and PEG-maleimide (PEG-Mal) as PEG-VS hydrogels form efficiently, have a network conducive to support ovarian tissue survival and

development, are hydrolytically and proteolytically stable, and elicit a minimal inflammatory response in mice. From here, we developed a Dual PEG hydrogel that is conducive for the dynamic volumetric expansion of ovarian tissue, while protecting the tissue from an immune response. The Dual PEG capsule contains a proteolytically degradable core that supports ovarian tissue growth and development and a non-degradable shell that acts as a protective barrier. We tested in a syngeneic mouse model whether the degradable, non-degradable, and Dual PEG capsules support folliculogenesis in a mouse model of POI. We demonstrated that when ovarian tissue was implanted in these immune-isolating capsules, ovarian endocrine function was restored as demonstrated by resumption of estrous activity, restoration of the HPG axis, and healthy developed follicles present in the graft post-implantation. We next evaluated the Dual PEG capsule's ability to protect encapsulated ovarian allografts in an allogeneic mouse model. We show that compared to controls, ovarian allografts encapsulated in Dual PEG elicit a non-detectable allo-specific antibody response and the Dual PEG does not allow for cellular infiltration, promoting long-term graft survival and restoration of ovarian endocrine function.

We then demonstrated that allogeneic ovarian tissue encapsulated in Dual PEG does not sensitize the host immune system. This was tested by consecutively implanting mice with non-encapsulated ovarian allografts followed with ovarian tissue encapsulated in Dual PEG and vice versa. Ovarian tissue in Dual PEG does not sensitization the host, which would allow for consecutive implantations to restore ovarian endocrine function in a physiological manner. Additionally, the capsule being able to protect allogeneic ovarian tissue in an already sensitized host, enables us to possibly implant in humans as all humans have previously been exposed to allo-antigens are to some degree sensitized. Furthermore, additional tests and

immunophenotyping is required to investigate the underlying mechanism of tolerance induction by encapsulating ovarian tissue in degradable PEG. This can be done by conducting mixed lymphocyte cultures at different timepoints to assess the kinetics of exposure of allo-antigens to the immune environment and characterizing the surround immune environment by measuring elevated cytokine levels.

Lastly, we tested whether the Dual PEG capsule can support non-human primate ovarian tissue in a syngeneic and allogeneic non-human primate model of POI. Non-human primates are the most appropriate model for female reproduction and puberty induction. We demonstrated that in both a syngeneic and allogeneic setting, monkeys implanted with ovarian tissue encapsulated in Dual PEG showed evidence of ovarian endocrine restoration with pulsatile levels of estradiol and progesterone and healthy developed follicles in the grafts post-implantation. Additionally, in the allogeneic model, monkeys implanted with encapsulated ovarian allografts demonstrated no increase in circulating CD4+ and CD8+ activity indicating the encapsulated tissue did not evoke an immune response. A challenge moving forward is to allow for maximum diffusion without compromising the immuno-isolating capabilities of the capsule. To do this the tissue must be in close proximity with vascular without being directly exposed to that blood flow which is where immune cells are transported from. A possible course of action is to promote vascular formation via the addition of a biological motif, such as RGD, on the outer shell of the capsule to minimize the distance of nutrient exchange. Additionally, the ability for the capsule to support corpus luteum formation must be investigated as this is essential to knowing whether ovulation is supported. The fact that there was cyclic progesterone in the NHP study indicates corpus luteum was supported, however, no evidence was observed via histological analysis.

The work presented in this dissertation addresses a clinical need to restore reproductive endocrine function in female cancer survivors who experience POI. Particularly for young female cancer survivors who experience POI prior to puberty, physiological puberty induction is vital for post-treatment quality of life as this process affects a multitude of factors including bone health, metabolism, cognition, cardiovascular health, and cognition. Non-physiological pubertal development may cause life-long comorbidities such as poor bone health, abnormal fat deposition, high risk of cardiovascular events, and impaired immune system and cognition. The development of an immuno-isolating capsule for donor ovarian tissue implantation fills a clinical gap in treatment for POI patients as the current options such as HRT and allo-transplantation are associated with limitations such as non-physiological and incomplete delivery of ovarian hormones and re-introduction of cancerous cells. By making allo-transplantation of ovarian tissue possible, females experiencing POI can possibly have their hormonal balance restored through transplantation of donor ovarian tissue; and the use of an immuno-isolating capsule allows implantation of donor ovarian tissue without the need for immunosuppressive therapies. Collectively, this work aims to close the gap to meet a clinical need for girls and women that experience POI due to anticancer treatments; allowing for allo-transplantation of donor ovarian tissue, which will lead to physiological restoration of ovarian endocrine function and a higher quality of life post-treatment.

8.2 Future Directions

To this point, we have tested the capability of the Dual PEG capsule to support and protect allogeneic ovarian tissue in murine and NHP models. Translation of this technology into the clinic

would require proven efficacy and safety with human tissue. In the near future we will test whether the Dual PEG capsule can support human ovarian tissue survival and development. Other groups have utilized biomaterials to promote growth and development of human ovarian follicles implanted in immune deficient mice [204,205]. Yet the application of immunoisolating capsule to support allogeneic applications has not been explored. The volumetric expansion during human folliculogenesis is massive with follicles reaching 2 centimeters in diameter. The first step is to test whether the capsule, as it exists right now, can withstand that large expansion without being mechanically compromised, which would impact its immuno-isolating capabilities. To do this, either fresh or frozen-thawed ovarian tissue will be encapsulated in the Dual PEG capsule and implanted subcutaneously in an immune compromised SCID mouse. To induce folliculogenesis, mice will be stimulated with FSH and hCG and the explant will be extracted and evaluated to see if the capsule can support tissue health and development. Preliminary studies have been conducted with promising results showing the presence of healthy human ovarian follicles present in the graft after 1 and 4 months transplantation in SCID mice. Further improvements in the capsule design will allow facilitated diffusion of the nutrients to improve follicle health, accommodation of larger fragments to extend the duration of the graft function, improved immunoisolating and stealth properties to allow xenograft transplantation without evoking the innate immune response and the possibly to load and reconstitute the capsule multiple time without compromising its integrity and immunoisolating action.

Additionally, capsule modification and mass manufacturing may be conducted by using 3D printing, which can possibly minimize the thickness of the immuno-isolating barrier, decreasing the distance of diffusion for nutrients and metabolites, without compromising immuno-isolation.

Additionally, by decreasing the distance to vasculature, corpus luteum formation may be enhanced which is essential for production of progesterone. The use of 3D printers to manufacture the capsule and streamline the process will help in clinical translation of this technology and mass production. To this end, we are preparing a pre-IND packet for the Food and Drug Administration, including standards and protocols, such as materials used, quality control of tissue, and manufacturing processes. If accepted, this clinical trial encapsulating human ovarian tissue in Dual PEG would be the first to attempt to restore ovarian endocrine function using allo-transplantation and would be a crucial step for allowing female cancer survivors with POI to receive donor ovarian tissue to either induce puberty or restore physiological hormonal balance, addressing the limitations of current treatments.

APPENDIX

Customer Discovery and Development of a Business Plan for the Technology that Aims to Restore Ovarian Endocrine Function in Adolescent Girls with Premature Ovarian Insufficiency

The National Science Foundation (NSF) I-Corps program prepares scientists and engineers to extend their focus beyond the university laboratory and accelerates the economic and societal benefits of NSF-funded, basic-research projects that are ready to move toward commercialization. Through I-Corps, NSF grantees learn to identify valuable product opportunities that can emerge from academic research, and gain skills in entrepreneurship through training in customer discovery and guidance from established entrepreneurs. **As a part of translating our technology to the clinic** our team participated in a 3-month long national I-CORPs course.

Currently young girls suffering from premature ovarian insufficiency (POI) as a result of anticancer treatments have limited and inadequate options to undergo puberty and start their transition into adult life. The existing hormone replacement therapy (HRT) applied to induce puberty in girls with POI leads to long-term morbidities, such as decreased bone density, predisposition to obesity and diabetes. We developed a technology that allows the restoration

of ovarian endocrine function in prepubescent girls and has the potential to become a central mainstream treatment for POI, which would result in significant improvement of the short and long-term health and eliminate long-term morbidities associated with premature ovarian failure. The proposed treatment will significantly lower health costs associated with obesity, diabetes and osteoporosis and translate to positive health economics.

The pre-clinical work in the past 4 years demonstrated that an immuno-isolating capsule can protect encapsulated allogeneic ovarian tissue from an immune response, allowing the allograft to produce ovarian hormones in a physiological regulated manner, restoring ovarian endocrine function. To date, we have demonstrated the feasibility of this application in murine and non-human primate models. The next step is to translate the developed technology towards the clinic, which requires a clear understanding of the existing clinical gap. Many of the academic entrepreneurs assume what they perceive as true about the market and never learn what the customers care about. To avoid making false assumptions, we applied for the National Science Foundation Innovation Corps (NSF I-Corps) to perform customer discovery, determine the customer segments and investigate the current clinical treatments available and how the proposed technology might fill the clinical need. NFS I-Corps entailed a 7-week program, where our team of three, called OvaArt, were tasked to interview more than 100 potential customers and stakeholders to create a business plan using the Business Model Canvas (BMC) from "Business Model Generation" by Alexander Osterwalder and Yves Pigneur (**Figure A1**).

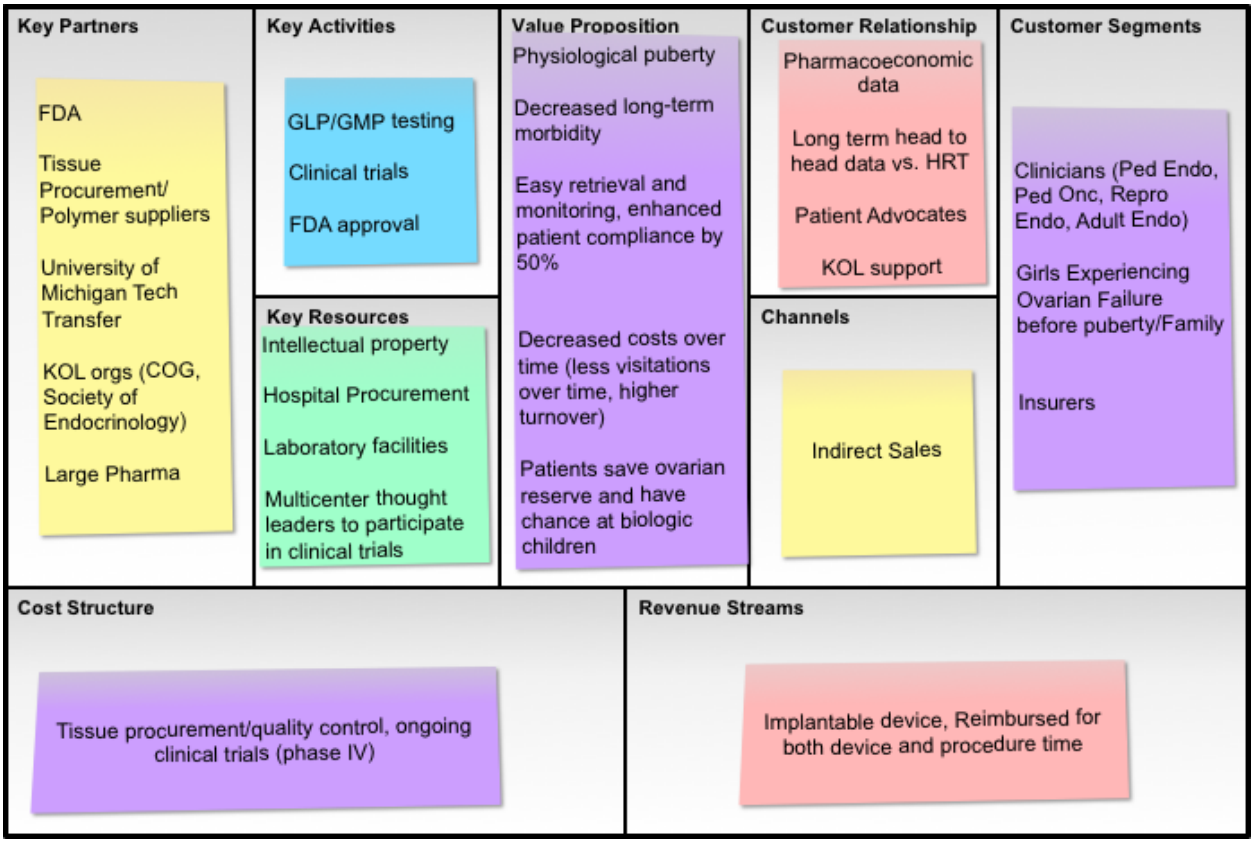

Figure A1: Final iteration of business model canvas after 7-week NSF I-Corps program and interviewing 118 customers.

We reached out and interviewed potential users, payers, and influencers regarding our technology and learned what they value and what the current weaknesses and gaps in the field were; As a result we developed a business plan, value proposition, customer segments, channels, customer relationships, revenue streams, key activities, key resources, key partners, and cost structure after talking to over 100 potential customers about these pillars.

An important aspect of our target patient population is the ecosystem and customer segments surrounding the girls and women that experience POI due to anti-cancer treatments. We hypothesized that pediatric oncologists diagnose and treat the disease, , and years later pediatric

endocrinologists treat the adolescent girls if they experience POI with hormone replacement therapy (HRT). We assumed that the ecosystem for these patients was linear with only 3 main segments. Within the first week of "getting out of the building" and talking to pediatric clinicians, patients and their families, we learned that the ecosystem was more complex, disorganized, disconnected and convoluted than previously hypothesized. We learned that additional segments of the ecosystem would be impacted by OvaArt and the potential application, such as the patient, family of the patient, pediatric oncologists, pediatric endocrinologists, directors of survivorship clinics, nurse case manager, OBGYN and reproduction specialists. We investigated what was important for each segment in terms of ease of use, safety, and advantages over current treatments, and after combining our findings we develops a new value proposition. *The value proposition for OvaArt, is that it would provide an implantable capsule that delivers a constant source of ovarian hormones in a physiological controlled manner, restoring ovarian endocrine function in pediatric patients experiencing POI and allowing them to go through puberty correctly.* The pediatric endocrinologists we interviewed confirmed our value proposition regarding the limitations of HRT treatments. While most pediatric endocrinologists stated that certain milestones such as secondary sexual characteristics could be achieved with HRT, they also recognized limitations of HRT. Namely, compliance was a huge concern as multiple endocrinologists estimated "50-75% of patients don't use HRT as prescribed". This is due to the mode of administration and application being complicated, as patients often have to divide estrogen patches (which originally were developed for post-menopausal women) into eighths to deliver an appropriate dose, the patches would often fall off, children are self-conscious about looking different than peers, and patches would often cause irritation and rashes. Additionally,

we found that fear was a factor in parents avoiding HRT, mostly because of the side effects and increased long term risks for developing cancer. We heard testaments regarding the limitations of HRT as "a one size fits all system" when in reality, treatment and hormone production should be tailored for each patient for appropriate development and regulation. Overall, most endocrinologists from multiple hospital systems (OHSU, Johns Hopkins, UPMC, Childrens Hospital of Pennsylvania, St. Jude's Childrens Hospital) acknowledged the shortcomings of HRT therapy and expressed the importance of appropriate endocrine health during pubertal development and thereafter. When asked whether HRT meets the standards of naturally produced hormones from the ovary, the overwhelming answer was "nature is always better" and HRT does completely mimic the hormonal milieu. By talking to these experts all over the country, we were about to confirm our value proposition of delivering physiological controlled hormones.

Reimbursement for the treatment was another important aspect for us to consider as the technology moves towards the clinic and what needs to be done to maintain a self-sustaining business. We interviewed healthcare consultants, distributors, leaders of biotech companies, insurance companies, and other healthcare providers and determined that an implantable capsule containing a cellular component would be introduced to the clinic through indirect sales and paid for via reimbursement. We learned a common model for an implantable device is the sale of the product to a distributor, in our case a specialty pharmacy company such as Cardinal Health, and the distributor would send the device to the clinic once prescribed by the clinician. The payment for the procedure and capsule would initially be paid for upfront by the family/patient but would then be reimbursed by the respective insurance company (**Figure A2**).

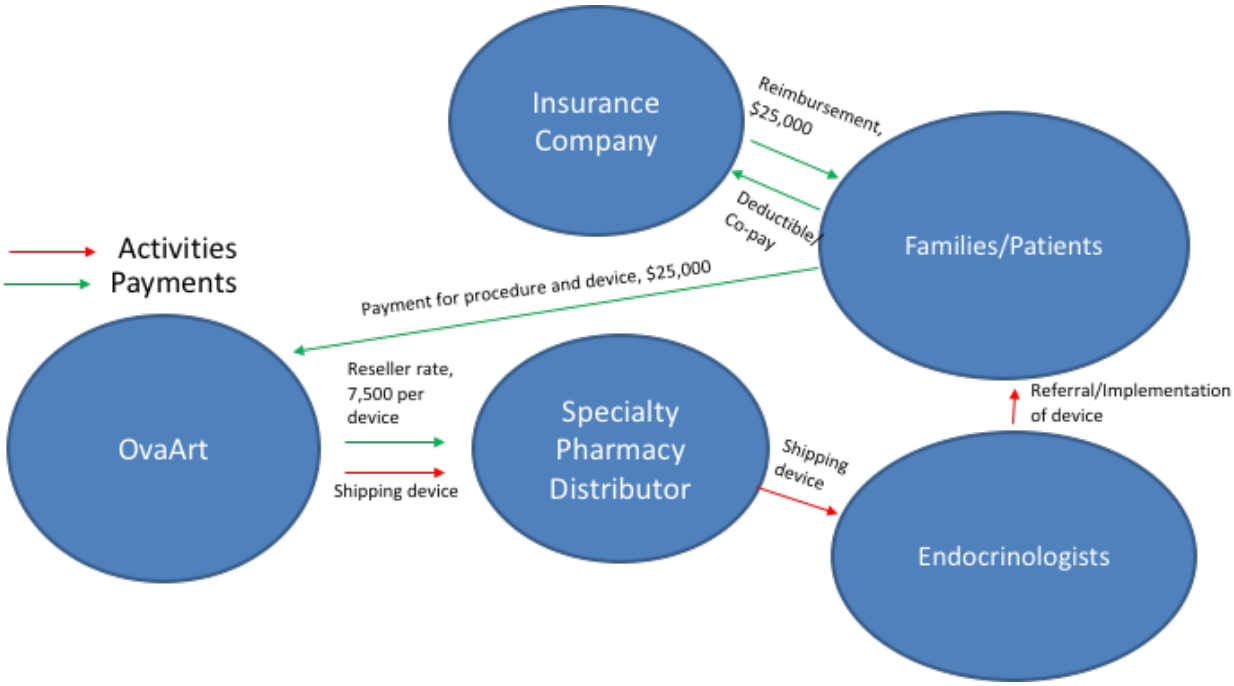

Figure A2: Revenue flow model from manufacturing of the capsule to the patient.

For pricing, consultants and biotech leaders emphasized the importance of value based pricing and "what value we are adding" . This includes potentially decreasing co-morbidities associated with absent puberty and abnormal hormonal balance. From this and comparing to similar spaces such as islet cell transplantation, we initially placed the price of the capsule and procedure at $25,000 for this exercise with the patient having to receive a capsule once per year. Additionally, by setting a price we are able to estimate the market size of our developed technology (**Figure A3**).

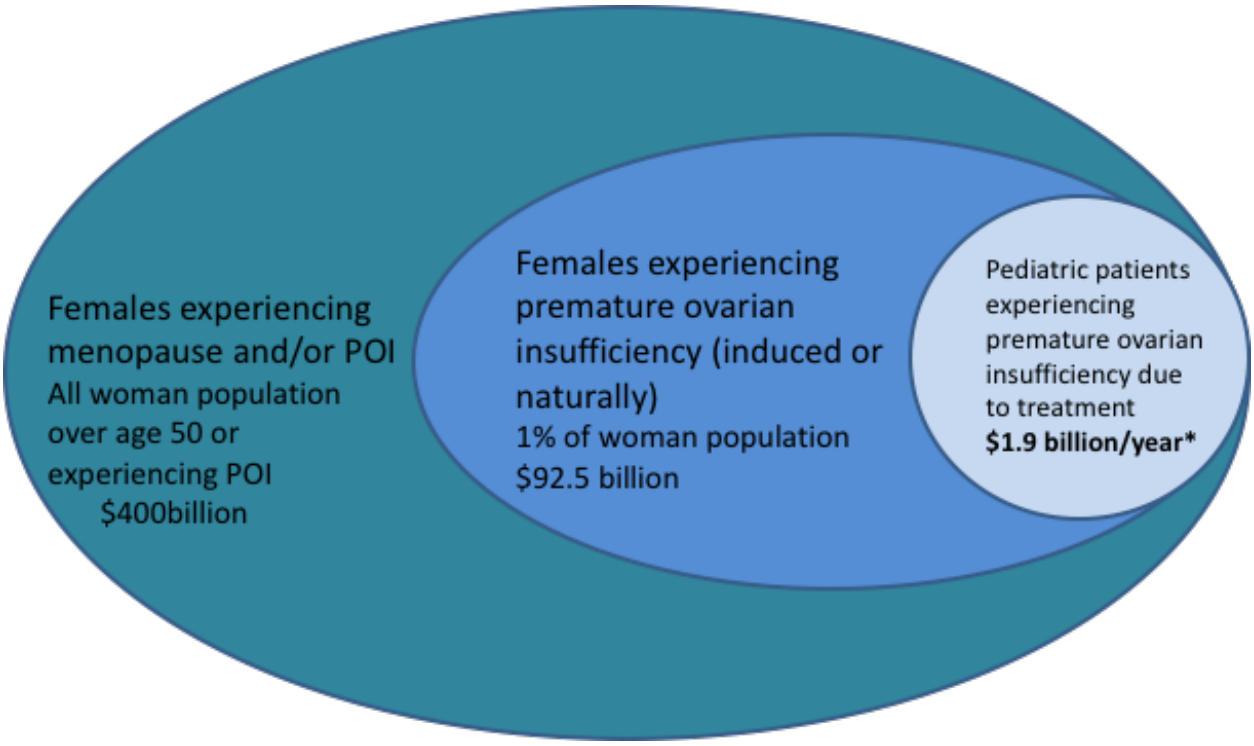

Figure A3: Market size analysis of OvaArt. The target market (smallest circle) consists of 75,000 patients experiencing POI due to anticancer treatments, multiplied by $25,000 per capsule gives a potential market of $1.9 billion.

We estimated that our initial market of pediatric patients who experience POI due to anticancer patients being $1.9 billion/year with potential to apply this technology to larger markets such as all women experiencing POI.

NSF I-Corps program encouraged the team to layout the major steps and milestones that the technology needs to reach the clinic. We have performed pre-clinical studies in murine and non-human primate models and have demonstrated feasibility towards the application of restoring

ovarian endocrine function using ovarian allografts. Through talking to consultants and leaders of biotech companies, we determined that the next key step is to contact the Food and Drug Administration (FDA) (business model canvas) after completing gap analysis and compiling a pre-IND submission package. We anticipate to learn from the FDA what additional tests are needed to move towards a first-in-human clinical trial. Additionally, through mapping out the key milestones that must be made prior to being implemented in humans, we were able to identify certain quality control tests that must be done such as cryopreservation of the capsule and human tissue characterization to make sure the product is within our established tolerances and does not cause harm.

In summary, the NSF I-Corps program was instrumental to bridge the gap between conducting pre-clinical studies and developing a product that will fill a clinical need through talking to potential customers. To gain knowledge about our customer segments, potential business model, and future steps the OvaArt team "got out of the building" and talked to 118 potential customers during a 7-week period (and much more since the program). This entailed talking to experts in multiple hospital systems all over the country including OHSU in Portland, Michigan Medicine in Ann Arbor, St Jude's Children's Hospital in Memphis, UPMC in Pittsburgh, Children's Hospital of Pennsylvania in Philadelphia, and Johns Hopkins Hospital in Baltimore. We confirmed that the current treatment of HRT is associated with limitations, patients care about "feeling normal", and clinicians wish there was a better option than HRT for patients experiencing POI. These findings contributed to our value proposition that the capsule can provide physiological delivery of all ovarian hormones to childhood cancer patients experiencing POI, allowing them to go through puberty correctly and avoid long-term co-morbidities. We were also able to map out the

ecosystem and identify all customer segments that would be influential towards implementing OvaArt into the clinic. Additionally, we were able to develop a minimal viable product and develop a business plan by using the Business Model Canvas. Through the BMC, we mapped out the potential revenue stream of this product, the mode of reimbursement for the patients, what partnerships are vital for the production of this technology, and the major milestones still remaining. From this process we have expanded our knowledge of what it takes to get a product from the bench-side to the clinic. Although the OvaArt team is very early in this process, going through these exercises was crucial to understanding the potential of a developed technology to reach the clinic and what similar companies have done to be successful.

BIBLIOGRAPHY

[1] Byrne J, Fears TR, Gail MH, Pee D, Connelly RR, Austin DF, Holmes GF, Holmes FF, Latourette HB, Meigs JW, et al. Early menopause in long-term survivors of cancer during adolescence. Am J Obstet Gynecol. 1992;166(3):788–793.

[2] Chemaitilly W, Mertens AC, Mitby P, Whitton J, Stovall M, Yasui Y, Robison LL, Sklar CA. Acute ovarian failure in the childhood cancer survivor study. J Clin Endocrinol Metab. 2006;91(5):1723–1728.

[3] Sklar CA, Mertens AC, Mitby P, Whitton J, Stovall M, Kasper C, Mulder J, Green D, Nicholson HS, Yasui Y, Robison LL. Premature menopause in survivors of childhood cancer: a report from the childhood cancer survivor study. J Natl Cancer Inst. 2006;98(13):890–896.

[4] Anderson RA, Mitchell RT, Kelsey TW, Spears N, Telfer EE, Wallace WH. Cancer treatment and gonadal function: experimental and established strategies for fertility preservation in children and young adults. Lancet Diabetes Endocrinol. 2015;3(7):556–567.

[5] Chiarelli AM, Marrett LD, Darlington G. Early menopause and infertility in females after treatment for childhood cancer diagnosed in 1964-1988 in Ontario, Canada. Am J Epidemiol. 1999;150(3):245–254.

[6] Wallace WH, Thomson AB, Saran F, Kelsey TW. Predicting age of ovarian failure after radiation to a field that includes the ovaries. Int J Radiat Oncol Biol Phys. 2005;62(3):738–744.

[7] Thomas-Teinturier C, El Fayech C, Oberlin O, Pacquement H, Haddy N, Labbé M, Veres C, Guibout C, Diallo I, De Vathaire F. Age at menopause and its influencing factors in a cohort of survivors of childhood cancer: earlier but rarely premature. Hum Reprod. 2013;28(2):488–495.

[8] Chemaitilly W, Li Z, Krasin MJ, Brooke RJ, Wilson CL, Green DM, Klosky JL, Barnes N, Clark KL, Farr JB, Fernandez-Pineda I, Bishop MW, Metzger M, Pui CH, Kaste SC, Ness KK, Srivastava DK, Robison LL, Hudson MM, Yasui Y, Sklar CA. Premature Ovarian Insufficiency in Childhood Cancer Survivors: A Report From the St. Jude Lifetime Cohort. J Clin Endocrinol Metab. 2017;102(7):2242-2250. doi: 10.1210/jc.2016-3723. PMID: 28368472; PMCID: PMC5505200.

[9] Jensen AK, Rechnitzer C, Macklon KT, Ifverson MRT, Birkebaek N, Clausen N, Sorenson K, Fedder J, Ernst E, Yding Anderson C. Cyropreservation of ovarian tissue for fertility preservation in a large cohort of young girls: focus on pubertal development. Hum. Reprod. 2016;32(1):154-164.

[10] Zacharin M. Disorders of ovarian function in childhood and adolescence: Evolving needs of the growing child. An endocrine perspective. BJOG An Int. J. Obtet. Gynaecol. 2010;117:156-162.

[11] Beccuti G, Ghizzoni L. Normal and Abnormal Puberty. Endotext. 2015;83-210.

[12] Baily M, Silver R. Sex difference in circadian timing systems: Implications for disease. Frontiers in Neuroendocrinology. 2014;35(1):111-139.

[13] Sellix MT, Menaker M. Circadian clocks in the ovary. Trends Endocrinol Metab. 2010;21(10):628-636.

[14] Miller BH, Takahashi JS. Central Circadian Control of Female Reproductive Function. Front Endocrinol. 2013;4:195

[15] Newell-Fugate AE. The role of sex steroids in white adipose tissue adipocyte function. Reproduction. 2017;153(4):R133-R149.

[16] Guzman C, Hernandez-Bello R, Morales-Montor J. Regulation of Steroidogenesis in Reproduction, Adrenal and Neural Tissues by Cytokines. The Open Neuroendocrinology Journal. 2010;3:161-169

[17] Daan NM, Muka T, Koster MP, Roeters van Lennep JE, Lambalk CB, Laven JS, Fauser CG, Meun C, de Rijke YB, Boersma E, Franco OH, Kavousi M, Fauser BC. Cardiovascular risk in women with premature ovarian insufficiency compared to premenopausal women at middle age. J Clin Endocrinol Metab. 2016;101(9):3306–3315.

[18] Popat VB, Calis KA, Vanderhoof VH, Cizza G, Reynolds JC, Sebring N, Troendle JF, Nelson LM. Bone mineral density in estrogen-deficient young women. J Clin Endocrinol Metab. 2009;94(7):2277–2283.

[19] Green DM, Sklar CA, Boice JD, Mulvihill JJ, Whitton JA, Stovall M, Yasui Y. Ovarian Failure and Reproductive Outcomes After Childhood Cancer Treatment: Results From the Childhood Cancer Survivor Study. J Clin Oncol. 2009;27(14):2374-2381.

[20] Staley K, Scharfman H. A woman's prerogative. Nat Neurosci. 2005;8(6):697-699.

[21] Wallace WH, Kelsey TW, Anderson RA. Fertility preservation in pre-pubertal girls with cancer: the role of ovarian tissue cryopreservation. 2016;105(1):6-12.

[22] Mahajan N. Fertility preservation in female cancer patients: An overview. J Hum Reprod Sci. 2015;8(1):3-13.

[23] Roness H, Kalich-Philosoph L, Meirow D. Prevention of chemotherapy-induced ovarian damage: Possible roles for hormonal and non-hormonal attenuating agents. Hum Reprod Update. 2014;20:759–74.

[24] Woodruff TK. Preserving fertility during cancer treatment. Nat Med. 2009;15:1124–5.

[25] Meirow D, Dor J, Kaufman B, Shrim A, Rabinovici J, Schiff E, et al. Cortical fibrosis and blood-vessels damage in human ovaries exposed to chemotherapy. Potential mechanisms of ovarian injury. Hum Reprod. 2007;22:1626–33.

[26] Blumenfeld Z. How to preserve fertility in young women exposed to chemotherapy. The role of GnRH agonist cotreatment in addition to cryopreservation of embrya, oocytes, or ovaries? Oncologist. 2007;12:1044–54.

[27] Society for Assisted Reproductive Technology. Clinic Summary Report. 2010.

[28] Cardozo ER, Thomson AP, Karmon AE, Dickinson KA, Wright DL, Sabatini ME. Ovarian stimulation and *in-vitro* fertilization outcomes of cancer patients undergoing fertility preservation compared to age matched controls: A 17-year experience. J Assist Reprod Genet. 2015

[29] Donnez J, Jadoul P, Squifflet J, Van Langendonckt A, Donnez O, Van Eyck AS, et al. Ovarian tissue cryopreservation and transplantation in cancer patients. Best Pract Res Clin Obstet Gynaecol. 2010;24:87–100.

[30] Morris SN, Ryley D. Fertility preservation: Nonsurgical and surgical options. Semin Reprod Med. 2011;29:147–54.

[31] Silber S. Ovarian tissue cryopreservation and transplantation: scientific implications. J Assist Reprod Genet. 2016;33(12):1595-1603.

[32] Silber SJ, Lenahan KM, Levine DJ, Pineda JA, Gorman KS, Friez MJ, Crawford EC, Gosden RG. Ovarian transplantation between monozygotic twins discordant for premature ovarian failure. N Engl J Med. 2005;353(1):58-63.

[33] Donnez J, Dolmans MM. Ovarian cortex transplantation: 60 reported live births brings the success and worldwide expansion of the technique towards routine clinical practice. J Assist Reprod Genet. 2015;32(8):1167-1170.

[34]Meirow D, Ra'anani H, Shapira M, Brenghausen M, Derech Chaim S, Aviel-Ronen S, Amariglio N, Schiff E, Orvieto R, Dor J. Transplantations of frozen-thawed ovarian tissue demonstrate high reproductive performance and the need to revise restrictive criteria. Fertil Steril. 2016;106(2):467-474.

[35] Dittrich R, Hackl J, Lotz L, Hoffmann I, Beckmann MW. Pregnancies and live births after 20 transplantation of cryopreserved ovarian tissue in a single center. Fertil Steril. 2015:103(2):462-468.

[36]Fabbri R, Macciocca M, Vicenti R, Paradisi R, Rossi S, Sabattine E, Gazzola A, Seracchioli R. First Italian birth after cryopreserved ovarian tissue transplantation in a patient affected by non-Hodgkin's lymphoma. Int J Hematol Oncol. 2018;7(4):IJH08.

[37] Stern CJ, Gook D, Hale LG, Agresta F, Oldham J, Rozen G, et al. First reported clinical pregnancy following heterotopic grafting of cryopreserved ovarian tissue in a woman after a bilateral oophorectomy. Hum Reprod. 2013;28:2996–9.

[38] Laronda MM, Jakus AE, Whelan KA, Wertheim JA, Shah RN, Woodruff TK. Initiation of puberty in mice following decellularized ovary transplant. Biomaterials. 2015;50:20-9.

[39] Dolmans MM, Luyckx V, Donnez J, Andersen CY, Greve T. Risk of transferring malignant cells with transplanted frozen-thawed ovarian tissue. Fertil Steril. 2013;99(6):1514-22.

[40] Dolmans MM, Marinescu C, Saussoy P, Van Langendonckt A, Amorim C, Donnez J. Reimplantation of cryopreserved ovarian tissue from patients with acute lymphoblastic leukemia is potentially unsafe. Blood. 2010;116(16):2908-14.

[41] Rosendahl M, Anderson MT, Ralfkiaer, Anderson MK, Anderson CY. Evidence of residual disease in cryopreserved ovarian cortex from female patients with leukemia. Fertil Steril. 2010;94(6):2186-90.

[42] Luyckx V, Durant JF, Camboni A, Gilliaux S, Amorim AC, Van Langendonckt L, et al. Is transplantation of cryopreserved ovarian tissue from patients with advanced-stage breast cancers safe: A pilot study. J Assist Reprod Genet. 2013;30(10):1289-99.

[43] Meirow D, Hardan J, Dor J, Fridman E, Elizur S, Ra'anani H, et al. Searching for evidence of disease and malignant contamination in ovarian tissue stored from hematologic cancer patients. Hum Repro. 2008;23(5):1007-13.

[44] Panay N, Hamoda H, Arya R, Savvas M. The 2013 British Menopause Society & Women's Health Concern recommendations on hormone replacement therapy. Menopause Int. 2013;19(2):59-68.

[45] Agarwal S, Alzahrani FA, Ahmed A. Hormone Replacement Therapy: Would it be Possible to Replicate a Functional Ovary? Int J Mol Sci. 2018;19(10). Pii: E3160.

[46] Hershlag A, Rausch ME, Cohen M. Part 2: Ovarian failure in adolescent cancer survivors should be treated. 2011;24(2):101-103.

[47] Sklar CA, Antal Z, Chemaitilly W, Cohen LE, Follin C, Meacham LR, Murad MH. Hypothalamic-Pituitary and Growth Disorders in Survivors of Childhood Cancer: An Endocrine Society Clinical Practice Guideline. J Clin Endocrinol Metab. 2018;103(8):2761-2784.

[48] Sood R, Faubion SS, Kuhle CL, Thielen JM, Shuster LT. Prescribing menopausal hormone therapy: an evidence-based approach. Int J Womens Health. 2014;6:47-57.

[49] Cruise GM, Hegre OD, Scharp DS, Hubbell JA. A sensitivity study of the key parameters in the interfacial photopolymerization of poly(ethylene glycol) diacrylate upon porcine islets. Biotechnol Bioeng 1998; 57: 655–65.

[50] Cruise GM, Hegre OD, Lamberti FV, Hager SR, Hill R, Scharp DS, Hubbell JA. In vitro and in vivo performance of porcine islets encapsulated in interfacially photopolymerized poly (ethylene glycol) diacrylate membranes. Cell Tranplant 1999; 8: 293–306.

[51] Weber LM, Cheung CY, Anseth KS. Multifunctional pancreatic islet encapsulation barriers achieved via multilayer PEG hydrogels. Cell Transplant 2008; 16: 1049–57.

[52] Headen DM, Aubry G, Lu H, García AJ. Microfluidic-based generation of size-controlled, biofunctionalized synthetic polymer microgels for cell encapsulation. Adv Mater 2014; 26: 3003–8.

[53] Gray DW. An overview of the immune system with specific reference to membrane encapsulation and islet transplantation. Ann N Y Acad Sci 2001; 944: 226–39.

[54] Gaur LK. Nonhuman primate models for islet transplantation in type 1 diabetes research. ILAR J. 2004;45(3):324-33.

[55] Liu Z, Hu W, He T, Dai Y, Hara H, Bottino R, Cooper DKC, Cai Z, Mou L. Pig-to-Primate Islet Xenotransplantation: Past, Present, and Future. Cell Transplant. 2017;26(6): 925-947.

[56] Bisceglie V. Ueber die antineoplastische Immunitat; Ueber die Wachstumsfaehigkeit der heterologen Geschwuelste in erwachsenen Tieren nach Einpflanzung in Kollodiumsaeckchen. Ztschr Krebsforsch 1933; 40: 141–141.

[57] Chang TMS. Semipermeable microcapsules. Science 1964; 146: 524–5.

[58] Chick WL, Perna JJ, Lauris V, Low D, Galletti PM, Panol G, Whittemore AD, Like AA, Colton CK, Lysaght MJ. Artificial pancreas using living beta cells: effects on glucose homeostasis in diabetic rats. Science 1977; 197: 780–2.

[59] Lim F, Sun AM. Microencapsulated islets as bioartificial endocrine pancreas. Science 1980; 210: 908–9.

[60] Cieslinski DA, Humes HD. Tissue engineering of a bioartificial kidney. Biotechnol Bioeng 1994; 43: 678–81.

[61] Liu HW, Ofosu FA, Chang PL. Expression of human factor IX by microencapsulated recombinant fibroblasts. Hum Gene Ther 1993; 4: 433–40.

[62] Veiseh O, Doloff JC, Ma M, Vegas AJ, Tam HH, Bader AR, Li J, Langan E, Wyckoff J, Loo WS, Jhunjhunwala S, Chiu A, Siebert S, Tang K, Hollister-Lock J, Aresta-Dasilva S, Bochenek M, Mendoza-Elias J, Wang Y, Qi M, Lavin DM, Chen M, Dholakia N, Thakrar R, Lacík I, Weir GC, Oberholzer J, Greiner DL, Langer R, Anderson DG. Size- and shape-dependent foreign body immune response to materials implanted in rodents and non-human primates. Nat Mater 2015; 14: 643–51.

[63] Boettler T, Schneider D, Cheng Y, Kadoya K, Brandon EP, Martinson L, Herrath von M. Pancreatic tissue transplanted in TheraCyte encapsulation devices are protected and prevent hyperglycemia in a mouse model of immune-mediated diabetes. Cell Transpl. 21 August 2015 Epub ahead of print.

[64] Nabavimanesh MM, Hashemi-Najafabadi S, Vasheqhani-Farahani E. Islets immunoisolation using encapsulation and PEGylation, simultaneously, as a novel design. J Biosci Bioeng 2015; 119: 486–91.

[65] Guiseppi-Elie A. Electroconductive hydrogels: synthesis, characterization and biomedical applications. Biomaterials 2010; 31: 2701–16.

[66] Gehrke SH, Fisher JP, Palasis M, Lund ME. Factors determining hydrogel permeability. Ann N Y Acad Sci 1992; 831: 179–207.

[67] Burczak K, Fujisato T, Hatada M, Ikada Y. Protein permeation through poly(vinyl alcohol) hydrogel membranes. Biomaterials 1994; 15: 231–8.

[68] Cruise GM, Scharp DS, Hubbell JA. Characterization of permeability and network structure of interfacially photopolymerized poly(ethylene glycol) diacrylate hydrogels. Biomaterials 1998; 19: 1287–94.

[69] Dembczynski R, Jankowski T. Determination of pore diameter and molecular weight cut-off of hydrogel-membrane liquid-core capsules for immunoisolation. J Biomater Sci Polym Ed 2001; 12: 1051–8.

[70] Brauker JH, Carr-Brendel VE, Martinson LA, Crudele J, Johnston WD, Johnson RC. Neovascularization of synthetic membranes directed by membrane microarchitecture. J Biomed Mater Res 1995; 29: 1517–24.

[71] D'Amour KA, Bang AG, Eliazer S, Kelly OG, Agulnick AD, Smart NG, Moorman MA, Kroon E, Carpenter MK, Baetge EE. Production of pancreatic hormone-expressing endocrine cells from human embryonic stem cells. Nat Biotechnol 2006; 24: 1392–401.

[72] Kelly OG, Chan MY, Martinson LA, Kadoya K, Ostertag TM, Ross KG, Richardson M, Carpenter MK, D'Amour KA, Kroon E, Moorman M, Baetge EE, Bang AG. Cell-surface markers for the isolation of pancreatic cell types derived from human embryonic stem cells. Nat Biotechnol 2011; 29: 750–6.

[73] Zielinski BA, Aebischer P. Chitosan as a matrix for mammalian cell encapsulation. Biomaterials 1994; 15: 1049–56.

[74] Iwata H, Amemiya H, Matsuda T, Takano H, Hayashi R, Akutsu T. Evaluation of microencapsulated islets in agarose gel as bioartificial pancreas by studies of hormone secretion in culture and by xenotransplantation. Diabetes 1989; 38(Suppl 1): 224–5.

[75] Kuehn C, Fülöp T, Lakey JR, Vermette P. Young porcine endocrine pancreatic islets cultured in fibrin and alginate gels show improved resistance towards human monocytes. Pathol Biol (Paris) 2014; 62: 354–64.

[76] Lin CC, Anseth KS. PEG hydrogels for the controlled release of biomolecules in regenerative medicine. Pharm Res 2009; 26: 631–43.

[77] Wang T, Lacík I, Brissová M, Anilkumar AV, Prokop A, Hunkeler D, Green R, Shahrokhi K, Powers AC. An encapsulation system for the immunoisolation of pancreatic islets. Nat Biotechnol 1997; 15: 358–62.

[78] O'Shea GM, Goosen MF, Sun AM. Prolonged survival of transplanted islets of Langerhans encapsulated in a biocompatible membrane. Biochim Biophys Acta 1984; 804: 133–6.

[79] Clayton HA, London NJ, Colloby PS, Bell PR, James RF. The effect of capsule composition on the biocompatibility of alginate-poly-l-lysine capsules. J Microencapsul 1991; 8: 221–33.

[80] De Vos P, Wolters GH, Fritschy WM, Van Schilfgaarde R. Obstacles in the application of microencapsulation in islet transplantation. Int J Artif Organs 1993; 16: 205–12.

[81] De Vos P, De Haan BJ, Wolters GH, Strubbe JH, Van Schilfgaarde R. Improved biocompatibility but limited graft survival after purification of alginate for microencapsulation of pancreatic islets. Diabetologia 1997; 40: 262–70.

[82] Vandenbossche GM, Van Oostveldt P, Demeester J, Remon JP. The molecular weight cut-off of microcapsules is determined by the reaction between alginate and polylysine. Biotechnol Bioeng 1993; 42: 381–6.

[83] Ponce S, Orive G, Hernandez R, Gascon AR, Pedraz JL, de Haan BJ, Faas MM, Mathieu HJ, de Vos P. Chemistry and biological response against immunoisolating alginate-polycation capsules of different composition. Biomaterials 2006; 27: 4831–9.

[84] Santos E, Zarate J, Orive G, Hernandez RM, Pedraz JL. Biomaterials in cell microencapsulation. *Adv Exp Med Biol* 2010; 670: 5–21.

[85] Tibbitt MW, Anseth KS. Hydrogels as extracellular matrix mimics for 3D cell culture. Biotechnol Bioeng 2009; 103: 655–63.

[86] Vigen M, Ceccarelli J, Putnam AJ. Protease-sensitive peg hydrogels regulate vascularization *in vitro* and *in vivo*. Macromol Biosci 2014; 14: 1368–79.

[87] Engler AJ, Sen S, Sweeney HL, Discher DE. Matrix elasticity directs stem cell lineage specification. Cell 2006; 126: 677–89.

[88] Blakney AK, Swartzlander MD, Bryant SJ. The effects of substrate stiffness on the in vitro activation of macrophages and in vivo host response to poly (ethylene glycol)-based hydrogels. J Biomed Mater Res A 2012; 100: 1375–86.

[89] Hoffman BD, Grashoff C, Schwartz MA. Dynamic molecular processes mediate cellular mechanotransduction. Nature 2011; 475: 316–23.

[90] Elisseeff J, Anseth K, Sims D, McIntosh W, Randolph M, Langer R. Transdermal photopolymerization for minimally invasive implantation. Proc Natl Acad Sci U S A 1999; 96: 3104–7.

[91] Buxton AN, Zhu J, Marchant RE, West JL, Yoo JU, Johnstone B. Design and characterization of poly (ethylene glycol) photopolymerizable semi-interpenetrating networks for chondrogenesis of human mesenchymal stem cells. Tissue Eng 2007; 13: 2549–60.

[92] Hahn MS, McHale MK, Wang E, Schmedlen RH, West JL. Physiologic pulsatile flow bioreactor conditioning of poly (ethylene glycol)-based tissue engineered vascular grafts. A*nn Biomed Eng* 2007; 35: 190–200.

[93] Beamish JA, Zhu J, Kottke-Marchant K, Marchant RE. The effects of monoacrylate poly(ethylene glycol) on the properties of poly(ethylene glycol) diacrylate hydrogels used for tissue engineering. J Biomed Mater Res A 2010; 92: 441–50.

[94] Hubbell JA. Synthetic biodegradable polymers for tissue engineering and drug delivery. Curr Opin Solid State Mater Sci 1998; 3: 246–51.

[95] Metters A, Hubbell J. Network formation and degradation behavior of hydrogels formed by Michael-type addition reactions. Biomacromolecules 2005; 6: 290–301.

[96] Park Y, Lutolf MP, Hubbell JA, Hunziker EB, Wong M. Bovine primary chondrocyte culture in synthetic matrix metalloproteinase-sensitive poly (ethylene glycol)-based hydrogels as a scaffold for cartilage repair. Tissue Eng 2004; 10: 515–22.

[97] Tugba B, Kepsutlu B, Kizilel S. Characterization of protein release from poly (ethylene glycol) hydrogels with crosslink density gradients. J Biomed Mater Res A 2013; 102: 487–95.

[98] Babensee JE, Anderson JM, McIntire LV, Mikos AG. Host response to tissue engineering devices. Adv Drug Deliv Rev 1998; 33: 111–39.

[99] Cheung CY, Anseth KS. Synthesis of immunosiolation barriers that provide localized immunosupression for encapsulated pancreatic islets. Bioconjugate Chem 2006; 17: 1036–42.

[100] Tarantal AF, Lee CC, Itkin-Ansari P. Real-time bioluminescence imaging of macroencapsulated fibroblasts reveals allograft protection in rhesus monkeys (Macaca mulatta). Transplantation 2009; 88: 38–41.

[101] Kumagai-Braesch M, Jacobson S, Mori H, Jia X, Takahashi T, Wernerson A, Flodström-Tullberg M, Tibell A. The TheraCyte™ device protects against islet allograft rejection in immunized hosts. Cell Trans 2013; 22: 1137–46.

[102] Bruin JE, Rezania A, Xu J, Narayan K, Fox JK, O'Neil JJ, Kieffer TJ. Maturation and function of human embryonic stem cell-derived pancreatic progenitors in macroencapsulation devices following transplant into mice. Diabetologia 2013; 56: 1987–98.

[103] Huang SY, Tu CF, Liu SH, Kuo YH. Motility and fertility of alginate encapsulated boar spermatozoa. Anim Reprod Sci 2005; 87: 111–20.

[104] Faustini M, Torre ML, Stacchezzini S, Norberti R, Consiglio AL, Porcelli F, Conte U, Munari E, Russo V, Vigo D. Boar spermatozoa encapsulated in barium alginate membranes: a microdensitometric evaluation of some enzymatic activities during storage at 18. Theriogenology 2004; 61: 173–84.

[105] Lee KY, Mooney DJ. Hydrogels for tissue engineering. 2001, Chem Rev. 2001;101:1869-79.

[106] Bryant SJ, Bender RJ, Durand KL, Anseth KS. Encapsulating chondrocytes in degrading PEG hydrogels with high modulus: engineering gel structural changes to facilitate cartilaginous tissue production. Biotechnol Bioeng. 2004;86:747-755.

[107] Moutos FT, Estes BT, Guilak F. Multifunctional hybrid three-dimensionally woven scaffolds for cartilage tissue engineering. Macromol Biosci. 2010;10:1355-1364.

[108] Roberts JJ, Earnshaw A, Ferguson VL, Bryant SJ. Comparative study of the viscoelastic mechanical behavior of agarose and poly(ethylene glycol) hydrogels. J Biomed Mater Res B Appl Biomater. 2011;99:158-169.

[109] Anderson JM, Rodriguez A, Chang DT. Foreign body reaction to biomaterials. 2008, Semin Immunol. 2008;20:86-100.

[110] Bridges AW, Garcia AJ. Anti-inflammatory polymeric coatings for implantable biomaterials and devices. J Diabetes Sci Technol. 2008;2:984-994.

[111] Kingshott P, Griesser HJ. Surfaces that resist bioadhesion. 1999, Curr Opin Solid State Mater Sci. 1999;4:403-412.

[112] Morra M. On the molecular basis of fouling resistance. J Biomater Sci Polym Ed. 2000;11:547–69.

[113] Szleifer I. Protein adsorption on tethered polymer layers: effect of polymer chain architecture and composition. Physica A. 1997;244:370–388.

[114] Szleifer I. Polymers and proteins: interactions at interfaces. Curr Opin Solid State Mat Sci. 1997;2:337–344.

[115] Lutolf MP, Hubbell JA. Synthesis and physicochemical characterization of end-linked poly(ethylene glycol)-co-peptide hydrogels formed by Michael-type addition. Biomacromolecules. 2003;4:713–22.

[116] Morpurgo M, Veronese FM, Kachensky D, Harris JM. Preparation and Characterization of Poly(ethylene glycol) Vinyl Sulfone. Bioconjugate Chem. 1996;7:363–368.

[117] Milton JM, Zhao X. Degradable heterobifunctional poly(ethylene glycol) acrylates and gels and conjugates derived therefrom. US6362276 B1 USA. 2002 Mar 26;

[118] Harris JM, Sedaghat-Herati MR. Preparation and use of polyethylene glycol propionaldehyde. US 5252714 A USA. 1993 Oct 12

[119] Nhu K, Hyun C, Lee J, Pak Y. Preparation method of peg-maleimide derivatives. US 6828401 B2 USA. 2004 Dec 7

[120] Shih H, Lin CC. Cross-linking and degradation of step-growth hydrogels formed by thiol ene photoclick chemistry. Biomacromolecules. 2012;13:2003–12.

[121] Bowman CN, Nair DP, Podgorski M, Chatani S. Thiol-containing dual cure polymers and methods using same. US9340636 B2 USA. 2016 May 17

[122] Pierschbacher MD, Ruoslahti E. Cell attachment activity of fibronectin can be duplicated by small synthetic fragments of the molecule. Nature. 1984;309:30–33.

[123] Bryant SJ, Nuttelman CR, Anseth KS. Cytocompatibility of UV and visible light photoinitiating systems on cultured NIH/3T3 fibroblasts in vitro. J Biomater Sci Polym Ed. 2000;11:439–457.

[124] Silverman RP, Elisseeff J, Passaretti D, Huang W, Randolph MA, Yaremchuk MJ. Transdermal photopolymerized adhesive for seroma prevention. Plast Reconstr Surg. 1999;103:531–535.

[125] Elisseeff J, McIntosh W, Anseth K, Riley S, Ragan P, Langer R. Photoencapsulation of chondrocytes in poly(ethylene oxide)-based semi-interpenetrating networks. J Biomed Mater Res. 2000;51:164–171.

[126] Burdick JA, Anseth KS. Photoencapsulation of osteoblasts in injectable RGD-modified PEG hydrogels for bone tissue engineering. Biomaterials. 2002;23:4315–4323.

[127] Burdick JA, Anseth KS. Delivery of osteoinductive growth factors from degradable PEG hydrogels influences osteoblast differentiation and mineralization. J Control Release. 2002;83:53.

[128] Bryant SJ, Nuttelman CR, Anseth KS. The effects of crosslinking density on cartilage formation in photocrosslinkable hydrogels. Biomed Sci Instrum. 1999;35:309–314.

[129] Mann BK, Gobin AS, Tsai AT, Schmedlen RH, West JL. Smooth muscle cell growth in photopolymerized hydrogels with cell adhesive and proteolytically degradable domains: synthetic ECM analogs for tissue engineering. Biomaterials. 2001;22:3045–3051.

[130] Williams CG, Malik AN, Kim TK, Manson PN, Elisseeff JH. Variable cytocompatibility of six cell lines with photoinitiators used for polymerizing hydrogels and cell encapsulation. Biomaterials. 2005;26:1211–8.

[131] Nyugen MT, Kryachko ES, Vanquickenborne LG. The chemistry of phenols Part 2. Chichester, England: 2003. p. 140. Chapter 1.

[132] Roberts MJ, Bently MD, Harris JM. Chemistry for peptide and protein PEGylation. Adv Drug Deliv Rev. 2002;54:459–76.

[133] Kim J, Kong YP, Niedzielski SM, Singh RK, Putnam AJ, Shikanov A. Characterization of the crosslinking kinetics of multi-arm poly(ethylene glycol) hydrogels formed via Michael-type addition. Soft Matter. 2016:2076–85.

[134] Sperinde JJ, Griffith LG. Control and Prediction of Gelation Kinetics in Enzymatically Cross-Linked Poly(ethylene glycol) Hydrogels. Macromolecules. 2000;33:5476–5480.

[135] Ma Z, Niu X, Xu Z, Guo J. Synthesis of novel macrophotoinitiator for the photopolymerization of acrylate. J Appl Polym Sci 2014.

[136] Phelps EA, Enemchukwu NO, Fiore VF, Sy JC, Murthy N, Sulchek TA, Barker TH, Garcia AJ. Maleimide cross-linked bioactive PEG hydrogel exhibits improved reaction kinetics and cross-linking for cell encapsulation and in situ delivery. Adv Mater. 2012;24:64–70.

[137] Milašinović N, Čalija B, Vidović B, Sakač MC, Vujić Z, Knežević-Jugović Z. Sustained release of α-lipoic acid from chitosan microbeads synthetized by inverse emulsion method. J Taiwan Inst Chem Eng. 2016;60:106–112.

[138] Bae M, Divan R, Suthar KJ, Macini DC, Gemeinhart RA. Fabrication of Poly(ethylene glycol) Hydrogel Structures for Pharmaceutical Applications using Electron beam and Optical Lithography. J Vac Sci Technol B Microelectron Nanometer Struct Process Meas Phenom. 2010;28:C6P24–C6P29.

[139] Garcia H, Barros AS, Goncalves C, Gama FM, Gil AM. Characterization of dextrin hydrogels by FTIR spectroscopy and solid. Eur Polym J. 2008;44:2318–2329.

[140] Hao Y, Shih H, Munoz Z, Kemp A, Lin CC. Visible light cured thiol-vinyl hydrogels with tunable degradation for 3D cell culture. Acta Biomater. 2014;10:104–14.

[141] Gatica N, Fernandez N, Opazo A, Alegria S, Gargallo L, Radic D. Synthesis and characterization of functionalized vinyl copolymers. Electronegativity and comonomer reactivity in radical copolymerization. Polym Int. 2003;52:1280–1286.

[142] Vijaykumar S, Prasannkumar S, Sherigara BS, Shelke NB, Aminabhavi TM, Reddy BSR. Copolymerization ofN-vinyl pyrrolidone with functionalized vinyl monomers: Synthesis, characterization and reactivity relationships. Macromol Research. 2009;17:1003–1009.

[143] Browning MB, Cereceres SN, Luong PT, Cosgriff-Hernandez EM. Determination of the in vivo degradation mechanism of PEGDA hydrogels. J Biomed Mater Res A. 2014;102:4244–4251.

[144] David A, Day JR, Cichon AL, Lefferts A, Cascalho M, Shikanov A. Restoring Ovarian Endocrine Function with Encapsulated Ovarian Allograft in Immune Competent Mice. Ann Biomed Eng. 2017;45:1685–1696.

[145] Qiu Y, Lim JJ, Scott L, Jr, Adams RC, Bui HT, Temenoff JS. PEG-based hydrogels with tunable degradation characteristics to control delivery of marrow stromal cells for tendon overuse injuries. Acta Biomater. 2011;7:959–66.

[146] Shikanov A, Smith RM, Xu M, Woodruff TK, Shea LD. Hydrogel network design using multifunctional macromers to coordinate tissue maturation in ovarian follicle culture. Biomaterials. 2011;32:2524–2531.

[147] Schechte I, Berger A. On the size of the active size in proteases. I. Papain. Biochem Bioph Res Co. 1967;27:157–162.

[148] Weiss MS, Penalver Bernabe B, Shikanov A, Bluver DA, Mui MD, Shin S, Broadbelt LJ, Shea LD. The impact of adhesion peptides within hydrogels on the phenotype and signaling of normal and cancerous mammary epithelial cells. Biomaterials. 2012;33:3548–3559.

[149] Nguyen KT, West JL. Photopolymerizable hydrogels for tissue engineering applications. Biomaterials. 2002;23:4307–14.

[150] Zaveri TD, Lewis JS, Dolgova NV, Clare-Salzler MJ, Keselowsky BG. Integrin-directed modulation of macrophage responses to biomaterials. Biomaterials. 2014;35:3504–15.

[151] Blakney AK, Swartzlander MD, Bryant SJ. The effects of substrate stiffness on the in vitro activation of macrophages and in vivo host response to poly(ethylene glycol)-based hydrogels. J Biomed Mater Res A. 2012;100:1375–86.

[152] Ginsberg JP. New advances in fertility preservation for pediatric cancer patients. Curr Opin Pediatr. 2011;23:9–13.

[153] Chiarelli AM, Marrett LD, Darlington G. Early menopause and infertility in females after treatment for childhood cancer diagnosed in 1964–1988 in ontario, canada. Am J Epidemiol. 1999;150(3):245–54.

[154] Thibaud E, Rodriguez-Macias K, Trivin C, Esperou H, Michon J, Brauner R. Ovarian function after bone marrow transplantation during childhood. Bone Marrow Transplant. 1998 Feb;21(3):287–90.

[155] Waring AB, Wallace WH. Subfertility following treatment for childhood cancer. Hosp Med. 2000 Aug;61(8):550–7.

[156] Nieman CL, Kinahan KE, Yount SE, Rosenbloom SK, Yost KJ, Hahn EA, Volpe T, Dilley KJ, Zoloth L, Woodruff TK. Fertility preservation and adolescent cancer patients: Lessons from adult survivors of childhood cancer and their parents. Cancer Treat Res. 2007;138:201–17.

[157] Hudson MM, Oeffinger KC, Jones K, Brinkman TM, Krull KR, Mulrooney DA, Mertens A, Castellino SM, Casillas J, Gurney JG, Nathan PC, Leisenring W, Robison LL, Ness KK. Age-

dependent changes in health status in the childhood cancer survivor cohort. J Clin Oncol. 2015;33(5):479–491.

[158] Mariotto AB, Rowland JH, Yabroff KR, Scoppa S, Hachey M, Ries L, Feuer EJ. Long-term survivors of childhood cancers in the united states. Cancer Epidemiol Biomarkers Prev. 2009;18(4):1033–1040.

[159] Phillips SM, Padgett LS, Leisenring WM, Stratton KK, Bishop K, Krull KR, Alfano CM, Gibson TM, de Moor JS, Hartigan DB, Armstrong GT, Robison LL, Rowland JH, Oeffinger KC, Mariotto AB. Survivors of childhood cancer in the united states: Prevalence and burden of morbidity. Cancer Epidemiol Biomarkers Prev. 2015;24(4):653–663.

[160] Robison LL, Hudson MM. Survivors of childhood and adolescent cancer: Life-long risks and responsibilities. Nat Rev Cancer. 2014;14(1):61–70.

[161] Kniazeva E, Hardy AN, Boukaidi SA, Woodruff TK, Jeruss JS, Shea LD. Primordial follicle transplantation within designer biomaterial grafts produce live births in a mouse infertility model. Sci Rep. 2015;5:17709.

[162] Schweicher J, Nyitray C, Desai TA. Membranes to achieve immunoprotection of transplanted islets. Front Biosci (Landmark Ed) 2014;19:49–76.

[163] Rose SR, Horne VE, Howell J, Lawson SA, Rutter MM, Trotman GE, Corathers SD. Late endocrine effects of childhood cancer. Nature Reviews Endocrinology. 2016;12:319-336.

[164] Gargus E, Deans R, Anazoda A, Woodruff TK. Management of Primary Ovarian Insufficiency Symptoms in Survivors of Childhood and Adolescent Cancer. J Natl Compr Canc Netw. 2018;16(9):1137-1149.

[165] Noone AM, Howlader N, Krapcho M, Miller D, Brest A, Yu M, Ruhl J, Tatalovich Z, Mariotta A, Lewis DR, Chen HS, Feuer EJ. Cancer Statistics Review, 1975-2014-SEER Statistics. SEER Cancer Statistics Review. 2017

[166] De Vos M, Smitz J, Woodruff TK. Fertility preservation in women with cancer. Lancet. 2014;384(9950):1302-1310.

[167] Dunkel L, Quinton R. Transition in endocrinology: induction of puberty. Eur J Endocrinol. 2014;170(6);R229-239.

[168] Kim J, Perez AS, Claflin J, David A, Zhou H, Shikanov A. Synthetic hydrogel supports the function and regeneration of artificial ovarian tissue in mice. NPJ Regen Med. 2016;1. Pii:16010.

[169] Sanfins A, Rodrigues P, Albertini DF. GDF-9 and BMP-15 direct the follicle symphony. J Assist Reprod Genet. 2018;35(10):1741-1750.

[170] Shah JS, Sabouni R, Cayton Vaught KC, Owen CM, Albertini DF, Segars JH. Biomechanics and mechanical signaling in the ovary: a systematic review. J Assist Reprod Genet. 2018;35(7):1135-1148.

[171] Suguira K, Pendola FL, Eppig JJ. Oocyte control of metabolic cooperativity between oocytes and companion granulosa cells: energy metabolism. Dev Biol. 2005;279(1):20-30.

[172] Day JR, David A, Cichon AL, Kulkarni T, Cascalho M, Shikanov A. Immunoisolating poly(ethylene glycol) based capsules support ovarian tissue survival to restore endocrine function. J Biomed Mater Res A. 2018;106(5):1381-1389.

[173] Day JR, David A, Kim J, Farkash EA, Cascalho M, Milasinovic N, Shikanov A. The impact of functional groups of poly(ethylene glycol) macromers on the physical properties of photo-polymerized y hydrogels and the local inflammatory response in the host. Acta Biomater. 2018;67:42-52.

[174] Ludwig B, Reichel A, Steffen A, Zimerman B, Schally AV, Block NL, Colton CK, Ludwig S, Kersting S, Bonifacio E, Solimena M, Gendler Z, Rotem A, Barkai U, Bornstein SR. Transplantation of human islets without immunosuppression. Proc Natl Acad Sci USA. 2013;110(47):19054-8.

[175] Sittadjody S, Saul SM, McQuilling, Joo S, Register TC, Yoo JJ, Atala A, Opara EC. In vivo transplantation of 3D encapsulated ovarian constructs in rats corrected abnormalities of ovarian failure. Nature Communications. 2017;8.

[176] Sittadjody S, Saul J, Joo S, Yoo JJ, Atala A, Opara EC. Engineering multilayer ovarian tissue that secretes sex steroids and peptide hormones in response to gonadotropins. Biomaterials. 2013;34(10):2412-2420.

[177] Pradhan KR, Chen Y, Moustoufi-Moab S, Krull K, Oeffinger KC, Sklar C, et al. Endocrine and metabolic disorders in survivors of childhood cancers and health-related quality of life and physical activity. J Clin Endocrinonol Metab. 2019.

[178] Johnson EK, Finlayson C, Rowell EE, Gosiengfiao Y, Pavone ME, Lockart B, et al. Fertility Preservation for Pediatric Patients: Current State and Future Possibilities. J Urol. 2017;198(1):186-94.

[179] Santoro NF, Cooper AR, editors. Primary Ovarian Insufficiency: A Clinical Guide to Early Menopause. Cham (Switzerland): Springer Nature Switzerland AG; 2016. doi: 10.1007/978-3-319-22491-6

[180] Moravek MB, Appiah LC, Anazodo A, Burns KC, Gomez-Lobo V, Hoefgen HR, et al. Development of a Pediatric Fertility Preservation Program: A Report from the Pediatric Initiative Network of the Oncofertility Consortium. J Adolesc Health. 2019;64(5):563-473.

[181] Wallace WHB, Kelsey TW, Anderson RA. Fertility preservation in pre-pubertal girls with cancer: The role of ovarian tissue cryopreservation. Fertil Steril. 2016;105(1):6-12.

[182] Jadoul P, Guilmain A, Squifflet J, Luyckx M, Votino R, Wyns C, *et al.* Efficacy of ovarian tissue cryopreservation for fertility preservation: Lessons learned from 545 cases. Hum Reprod. 2017;32:1046-54.

[183] Armstrong AG, Kimler BF, Smith BM, Woodruff TK, Pavone ME, Duncan FE. Ovarian tissue cryopreservation in young females through the Oncofertility Consurtium's National Physicians Cooperative. Future Oncol. 2018;14(4):363-78.

[184] Shea LD, Woodruff TK, Shikanov A. Bioengineering the ovarian follicle microenvironment. Annu Rev Biomed Eng. 2014;16:29-52.

[185] Duncan FE, Zelinski M, Gunn AH, Pahnke JE, O'Neill CL, Songsasen N, *et al.* Ovarian tissue transport to expand access to fertility preservation: from animals to clinical practice. Reproduction. 2016;152(6):R201-10.

[186] Duncan FE, Pavone ME, Gunn AH, Badawy S, Gracia C, Ginsberg JP, *et al.* Pediatric and Teen Ovarian Tissue Removed for Cryopreservation Contains Follicles Irrespective of Age, Disease Diagnosis, Treatment History, and Specimen Processing Methods. J Adolesc Young Adult Oncol. 2015;4(4):174-83.

[187] Xiao S, Zhang J, Romero MM, Smith KN, Shea LD, Woodruff TK. *in vitro* follicle growth supports human oocyte meiotic maturation. Sci Rep. 2015;5:17323.

[188] Laronda MM, Duncan FE, Hornick JE, Xu M, Pahnke JE, Whelan KA, *et al.* Alginate encapsulation supports the growth and differentiation of human primordial follicles within ovarian cortical tissue. J Assist Repro Genet. 2014;31(8):1013-28.

[189] Jeruss JS, Woodruff TK. Preservation of fertility in patients with cancer. N Engl J Med. 2009;360(9):902-11.

[190] Jenssen AK, Macklon KT, Fedder J, Ernst E, Humaidan P, Andersen CY. 86 successful births and 9 ongoing pregnancies worldwide in women transplanted with frozen thawed ovarian tissue: focus on birth and perinatal outcome in 40 of these children. J Assist Reprod Genet. 2017;34(3):325-36.

[191] Pavone ME, Hirschfield-Cytron J, Tingen C, Thomas C, Thomas J, Lowe MP, *et al.* Human ovarian tissue cortex surrounding benign and malignant lesions. Repro Sci. 2014;21(5):582-9.

[192] Soares M, Saussoy P, Sahrari K, Amorim CA, Donnez J, Dolmans MM. Is transplantation of a few leukemic cells inside an artificial ovary able to induce leukemia in an experimental model? J Assist Reprod Genet. 2015;32(4):597-606.

[193] Rios PD, Kniazeva E, Lee HC, Xiao S, Oakes RS, Saito E, *et al.* Retrievable hydrogels for ovarian follicle transplantation and oocyte collection. Biotechnol Bioeng. 2018;115(8):2075-86.

[194] Colvin MM, Cook JH. Chang PP, Hsu DT, Kiernan MS, Kobashigawa JA, Lindenfeld J, Masri SC, Miller DV, Rodriguez ER, Tyan DB, Zeevi A. Sensitization in Heart Transplantation: Emerging Knowledge: A Scientific Statement from the American Heart Association. Circulation. 2019;139:553-578

[195] Steinman RM, Hawiger D, Lui K, Bonifaz L, Bonnyay D, Mahnke K, Iyoda T, Ravetch J, Dhodapkar M, Inaba K, Nussenzweig M. Dendritic cell function in vivo during the steady state: a role in peripheral tolerance. Ann N Y Acad Sci. 2003;987:15-25.

[196] Antigen Presentation. Immunology Guidebook 2004:267-276.

[197]Bastings L, Beerendonk CC, Westphal JR, Massuger LF, Kaal SE, van Leeuwen FE, Braat DD, Peek R. Autotransplantation of cryopreserved ovarian tissue in cancer survivors and the risk of reintroducing malignancy: a systematic review. Hum Reprod Update. 2013;19(5):483-506.

[198] Grogan JB. Antigen nonspecific rejection of allogeneic skin implants in the anterior chamber of sensitized rats. Invest Ophthalmol Vis Sci. 1985;26(4):501-510.

[199] Garcia de Mattos Barbosa M,Cascalho M, Platt JL. Accommodation in ABO-Incompatible Organ Transplants. Xenotransplantation. 2018;25(3):e121418.

[200] Lee DM, Yeoman RR, Battiglia DE, Stouffer RL, Zelinski-Wooten BM, Fanton JW, Wolf DP. Live birth after ovarian tissue transplant. Nature. 2004;428(6979)137-138.

[201] Lee DM, Thomas CM, Xu F, Yeoman RR, Xu J, Stouffer RL, Wolf DP, Zelinski MB. Subcutaneous ovarian tissue transplantation in nonhuman primates:duration of endocrine function and normalcy of subsequent offspring as demonstrated by reproductive competence, oocyte production, and telomere length. J Assist Repord Genet. 2017;34(11):1427-1434.

[202] Shideler SE, Gee, N, Laughlin LS, Lasley BL. Estorgen and progesterone metabolities and follicle-stimulating hormone in the aged macaque female. Biol. Reprod. 2001;65:1718-1725.

[203] Shideler SE, Gee NA, Chen J, Laughlin LS, Rapp PR, Morrison JH, Roberts JA, Moran FM, Lasley BL. Contribution of ovarian steroid production to urinary estrone conjugate concentrations in macacu mulatta. Am J Primatol. 2003;61:111-121.

[204] Chiti MM, Dolmans MM, Mortiaux L, Zhuge F, Ouni E, Shahri PAK, Van Ruymbeke E, Champagne SD, Donnez J, Amorim CA. A novel fibrin-based artificial ovary prototype resembling human ovarian tissue in terms of architecture and rigidity. J Assist Reprod Genet. 2018;35(1):41-48.

[205] Luckyx V, Dolmans MM, Vanacker J, Scalercio SR, Donnez J, Amorim CA. First step in developing a 3D biodegradable fibrin scaffold ifor an artificial ovary. Journal of Ovarian Research. 2013;6.